ABSTRACT

Title of dissertation: QUASIPERIODICITY AND CHAOS

Suddhasattwa Das, Doctor of Philosophy, 2015

Dissertation directed by: Professor James A. Yorke
Department of Mathematics

In this work, we investigate a property called "multi-chaos" is which a chaotic set has densely many hyperbolic periodic points of unstable dimension k embedded in it, for at least 2 different values of k. We construct a family of maps on the torus having this property. They serve as a paradigm for multi-chaos occurring in higher dimensional systems. One of the factors that leads to this strong form of chaos is the occurrence of a quasiperiodic orbit transverse to an expanding sub-bundle of the tangent bundle. Hence, a key step towards identifying multi-chaos numerically is finding quasiperiodic orbits in high dimensional systems. To analyze quasiperiodic orbits, we develop a method of weighted ergodic averages and prove that these averages have super-polynomial convergence to the Birkhoff average. We also show how this accelerated convergence of the ergodic averages over quasiperiodic trajectories enable us to compute the rotation number, Fourier series and Lyapunov exponents of quasiperiodic orbits with a high degree of precision ($\approx 10^{-30}$).

CHAOS AND QUASIPERIODICITY

by

Suddhasattwa Das

Dissertation submitted to the Faculty of the Graduate School of the
University of Maryland, College Park in partial fulfillment
of the requirements for the degree of
Doctor of Philosophy
2015

Advisory Committee:
Professor James A. Yorke, Chair/Advisor
Professor Mike Boyle
Professor Dmitry Dolgopyat
Professor Brian Hunt
Professor Edward Ott

Preface

Many high dimensional chaotic systems have periodic saddles of different unstable dimensions embedded within the chaotic set. To study dynamical systems with this kind of unstable dimension variability, a property called "multi-chaos" is introduced and investigated, where a chaotic set has densely many periodic saddles of unstable dimension k embedded in it, for at least 2 different values of k. Our studies involve the dynamics on quasiperiodic subsets of the chaotic system. We begin by defining a method of weighted Birkhoff averages in Chapter 1, and we show that in quasiperiodic dynamical systems, our weighted averages converge far faster than the unweighted ergodic averages proposed by Birkhoff, provided the functional f is sufficiently differentiable. In Chapter 2, this weighted Birkhoff average is used as a computational tool, and is used for numerically identifying one or two period quasiperiodic sets. In particular, the method is used to compute rotation numbers and conjugacies (i.e. changes of variables) and their Fourier series, often with 30-digit precision.

In Chapter 3, the focus is on skew-product maps on the torus of the form $(x_{n+1}, y_{n+1}) = (mx_n, g(x_n, y_n)) \mod 1$ Sufficient conditions for a torus map to be conjugate to a skew-product map are presented, with these conditions being open in the C^1 topology.

In Chapter 4, we finally construct a family of toral maps which happen to be the first examples of multi-chaos. The conjugacy theorem established in Chapter 3 is used, along with the assumption of a quasiperiodic curve being present, to prove the occurrence of multi-chaos.

In Appendix A, we conclude the investigation of toral skew-product map by proving that if there is a dense set of periodic saddles, then the torus splits into a finite number of invariant cylinders with disjoint interiors, with the map being transitive on each cylinder.

I am specially thankful to my co-authors other than my advisor Jim Yorke, who are Evelyn Sander from the Department of Mathematics, George Mason University and Yoshitaka Saiki from the Graduate School of Commerce and Management, Hitotsubashi University for their cooperation and contributions. I have listed below the authors for the various chapters of my thesis.

1. Chapter 1. S Das, J Yorke, *submitted*.

2. Chapter 2. S Das, E Sander, Y Saiki, J Yorke *submitted*.

3. Chapter 3. S Das, J Yorke.

4. Chapter 4. S Das, Y Saiki, J Yorke.

5. Appendix A. S Das, published in *Topology Proceedings* **(47)**, 2015.

Dedication

I humbly dedicate my work to the memory of the two patriarchs of my family, my grandfathers Brojendra Kumar Mondal and Dharmabrata Das. The story of their struggle, determination, sacrifices and meritorious lives will always inspire us.

Acknowledgments

My graduate experience has been one that I will cherish forever and I am grateful to all those people who have been with me during this journey.

First of all, I want to thank my advisor, Professor James A Yorke, for exposing me to challenging and interesting questions in dynamics over the past four years. He is a never ending source of ideas for me and has taught me to think differently and originally. I have received his continual support and encouragement, especially when we were present together at academic meetings. He has always been available for me and he is the perfect mixture of mathematician, coach and humorist.

I am grateful to Evelyn Sander and Y Saiki, my collaborators in some of my investigations, for their contributions and the knowledge and experience I gained from them. I look forward to work with them more in the future.

I would also like to thank Professors Brian Hunt and Edward Ott. I have spent many an hour with them, getting their ideas about progressing with my work. They are authorities on the field that I work in and I have found their second opinions and suggestions indispensible. I have also found my occasional discussions with Professors Dima Dolgopyat and Vadim Kaloshin very useful.

I will always be grateful to my co student, Madhura Joglekar, who was my senior and helped me settle into graduate school. She has been a constant friend and help me navigate the initial obstacles of research and student life.

I would also like to acknowledge help and support that I have from other members of the Math department. My life in graduate school would have been less

easier, if I did not have supporting and friendly people like Dr. Larry Washington, Sandy Allen, Celeste Regalado, Linette Berry and Haydee Hidalgo, and their constant support to graduate students. I have depended on them heavily to stay on course with my graduate school requirements.

As from childhood, I find myself indebted to my parents for being continuously supportive over the past four years, and often the voice of sanity for me. Their support and patience, which I have come to take for granted, has been like a protective bubble around me.

I am grateful to my brother, who I have found to be both a family member and a wiser friend. It gave me great comfort sharing my experiences with him.

I would also like to thank Dr. Soumitro Banerjee and Dr. Shyamol Dana, also great experts in my field. They have always cared for me and I have without fail got good advice in some form or the other, when I have spoken to them.

My journey would not have been smooth without the help of my housemates at my place of residence. I am especially grateful to Dena Crosson for providing the perfect homely environment to live and work in.

Table of Contents

List of Figures

Chapter 1: Super-convergence of ergodic averages on quasiperiodic orbits

Abstract. The Birkhoff Ergodic Theorem asserts that time averages of a function evaluated along a trajectory of length N converge to the space average, the integral of f, as $N \to \infty$, for ergodic dynamical systems. But that convergence can be slow. Instead of uniform averages that assign equal weights to points along the trajectory, we consider averages with a non-uniform distribution of weights, weighing the early and late points of the trajectory much less than those near the midpoint $N/2$. We show that in typical quasiperiodic dynamical systems, our weighted averages converge far faster provided f is sufficiently differentiable. This result can be applied to obtain efficient numerical computation of rotation numbers, invariant densities and conjugacies of quasiperiodic systems.

1.1 Introduction

Let $T : X \to X$ be a map on a topological space X with a probability measure μ for which T is invariant. Given a point x in X and a real- or vector-valued function

f on X, we will refer to a long-time average of the form

$$B_N(f) := \frac{1}{N}\sum_{n=0}^{N-1} f(T^n(x)), \tag{1.1}$$

as a **Birkhoff average**. Throughout this paper, $f : X \to E$ where E is a finite-dimensional real vector space. The limits of such sequences frequently occur in dynamical systems. If μ is a probability measure on X and T preserves the probability measure μ and is ergodic, then the von Neumann Ergodic Theorem (e.g. see Theorem 4.5.2. in [1]) states that for $f \in L^2(X, \mu)$, the Birkhoff average (1.1) converges in the L^2 norm to the integral $\int_X f d\mu$. The Birkhoff Ergodic Theorem (see Theorem 4.5.5. in [1]) strengthens von Neumann's theorem and concludes that if $f \in L^1(X, \mu)$, then (1.1) converges to the integral $\int_X f d\mu$ for μ-a.e. point $x \in X$. The Birkhoff average (1.1) can be interpreted as an approximation to an integral, but convergence is very slow, such as for some constant C,

$$\left| \frac{1}{N}\Sigma_{n=1}^{N} f(T^n(x)) - \int_X f d\mu \right| \leq CN^{-1},$$

For general ergodic dynamical systems, the rate of convergence of these sums can be arbitrarily slow, as shown in [2]. For many purposes the speed of convergence is irrelevant but it is important for numerical computations.

Definitions. Let $(a_N)_{N=0}^{\infty}$ be a sequence in a normed vector space such that $a_N \to b$ as $N \to \infty$. We say (a_N) has **super-polynomial convergence** to b or **super converges** to b if for each integer $m > 0$ there is a constant $C_m > 0$ such that

$$|a_N - b| \leq C_m N^{-m} \text{ for all } m \in \mathbb{N}.$$

Instead of weighting the terms $f(T^n(x))$ in the average equally, we weight the early and late terms of the set $1, \cdots, N$ much less than the terms with $n \sim N/2$ in the middle . We insert a weighting function w into the Birkhoff average, which will primarily be the following well known C^∞ function that we will call the **exponential weighting**,

$$w(t) = \begin{cases} \exp\left(\frac{1}{t(t-1)}\right), & \text{for } t \in (0,1) \\ 0, & \text{for } t \notin (0,1) \end{cases} \tag{1.2}$$

Let $\mathbb{T}^{\boldsymbol{d}}$ denote a d-dimensional torus. For $X = \mathbb{T}^d$ and a continuous f and for $\phi \in \mathbb{T}^d$, we define what we call a **Weighted Birkhoff ($\mathbf{WB}_N$) average**

$$\mathrm{WB}_N(f)(x) := \frac{1}{A_N} \sum_{n=0}^{N-1} w\left(\frac{n}{N}\right) f(T^n x), \text{ where } A_N := \sum_{n=0}^{N-1} w\left(\frac{n}{N}\right). \tag{1.3}$$

Of course the sum of the terms $w\left(\frac{n}{N}\right)/A_N$ is 1. Continuity of w guarantees

$$\lim_{N\to\infty} \frac{A_N}{N} = \int_0^1 w(t)dt. \tag{1.4}$$

We introduced the **exponentially weighted Birkhoff average** of Eqns. (1.3,1.4) for numerical investigations of quasiperiodic systems in [3]. Motivated by finding how effective our method was numerically, we discovered the theorem and proof in this paper.

Quasiperiodicity. Each $\vec{\rho} \in (0,1)^d$ defines a **rotation**, i.e. a map $T_{\vec{\rho}}$ on the d-dimensional torus $\mathbb{T}^d$, defined as

$$T_{\vec{\rho}} : \theta \mapsto \theta + \vec{\rho} \mod 1 \text{ in each coordinate.} \tag{1.5}$$

This map acts on each coordinate θ_j by rotating it by some angle ρ_j. We call the ρ_js **"rotation numbers"**.

A vector $\vec{\rho} = (\rho_1, \ldots, \rho_d) \in \mathbb{R}^d$ is said to be **irrational** if there are no integers k_j for which $k_1\rho_1 + \cdots + k_n\rho_n \in \mathbb{Z}$, except when all k_j are zero. In particular, this implies that each ρ_j must be irrational.

The simplest example of d-dimensional quasiperiodicity is a (pure) **irrational rotation**, that is, a rotation by an irrational vector ρ. A continuous but not necessarily invertible map $T : X \to X$ is said to be **d-dimensionally C^m quasiperiodic** on a set $X_0 \subseteq X$ for some $d \in \mathbb{N}$ iff there is a C^m-diffeomorphism $h : \mathbb{T}^d \to X_0$, such that,

$$T(h(\theta)) = h(T_{\vec{\rho}}(\theta)). \tag{1.6}$$

where $T_{\vec{\rho}}$ is an irrational rotation. In this case, h is a conjugacy of $T|_{X_0}$ to $T_{\vec{\rho}}$.

Unique invariant probability measure. Lebesgue probability measure $\boldsymbol{\lambda}$ on $\mathbb{T}^d$ is the unique invariant probability measure for any irrational rotation $T_{\vec{\rho}}$. A map $T : X_0 \to X_0$ therefore has a unique invariant probability measure μ which is defined as

$$\mu(U) := \lambda(h^{-1}(U)), \text{ for every Borel set } U \subseteq X_0.$$

Diophantine rotations. An irrational vector $\vec{\rho} \in \mathbb{R}^d$ is said to be **Diophantine** if for some $\beta > 0$ it is **Diophantine of class** β (see [4], Definition 3.1), which means there exists $C_\rho > 0$ such that for every $\vec{k} \in \mathbb{Z}^d$, $\vec{k} \neq 0$ and every $p \in \mathbb{Z}$,

$$|\vec{k} \cdot \vec{\rho} - p| \geq \frac{C_\rho}{\|k\|^{d+\beta}}. \tag{1.7}$$

For every $\beta > 0$ the set of Diophantine vectors of class β have full Lebesgue measure in $\mathbb{R}^d$ (see [4], 4.1). The Diophantine class is crucial in the study of quasiperiodic behavior, for example in [5] and [6].

Theorem 1.1.1 *Let X be a C^∞ manifold and $T : X \to X$ be a d-dimensional C^∞ quasiperiodic map on $X_0 \subseteq X$, with invariant probability measure μ. Assume T has a Diophantine rotation vector. Let $f : X \to E$ be C^∞, where E is a finite-dimensional, real vector space. Assume w is the exponential weighting (see Eqn. (1.2)). Then for each $x_0 \in X_0$, the weighted Birkhoff average $WB_N f(x_0)$ has super convergence to $\lim_{N\to\infty} B_N(f) = \int_{X_0} f d\mu$.*

In particular $\mathrm{WB}_N f(x_0)$ and $B_N(f)(x_0)$ have the same limit as $N \to \infty$, so the weighted Birkhoff average provides a fast way of computing the limit of a Birkhoff average.

In [7], A. Luque and J. Villanueva develop methods for obtaining rotation numbers by taking repeated averages of averages of a quasiperiodic signal. By taking p nested averages, their method obtains the rotation number with an error bounded by $C_p N^{-p}$, where C_p is a constant. The method of computation depends on p and as p increases the computational complexity increases for fixed N. Also, their computation time $T(p, N)$ obeys $T(p, N)/N \to \infty$ as $p \to \infty$. In comparison, computation time for our weighted Birkhoff average is simply proportional to N since it requires a sum of N numbers.

The convergence of weighted ergodic sums have been discussed in [8] , [9] and [10], but without any conclusions on the rate of convergence. In [11], a convergence rate of $O(N^{-\alpha})$, $(0 < \alpha < 1)$, was obtained for functions in $L^{2+\epsilon}$ for a certain choice of weights.

If the ergodic process T is chaotic instead of quasiperiodic, (for example,

Bernoulli shifts), then weighted Birkhoff averages provide no advantage over Birkhoff averages.

The exponential weighting function's properties needed in our proof of the above result are that $w \in C^\infty([0,1])$, that w and all of its derivatives are 0 at both 0 and 1, and that $\int_0^1 w(x)dx \neq 0$.

1.2 Applications of Theorem 1.1.1

Why are we interested in quasiperiodic subsets of dynamical systems? There are a variety of "basic sets" that can be seen in dynamical systems, where by **basic set** we mean a set that has a dense trajectory and is not in a strictly larger set having that property. But for typical dynamical systems (typical in some measure-theoretic sense), it is conjectured in [12] that only three kinds can be found, namely, periodic orbits, chaotic sets, and quasiperiodic sets. A typical Hamiltonian system corresponds not to a single dynamical system but rather to a one-parameter family of dynamical systems, so for Hamiltonian systems it is possible that one could only find those three kind of basic sets when studying a typical energy surface of a typical Hamiltonian. Tools have been lacking to determine if a set is quasiperiodic, and so our effort here is to provide such a tool.

Why do we care about trajectory averages of smooth functions? Suppose the map $T : X \to X$ has an (invariant) d-dimensional quasiperiodic subset X_0 with rotation vector $\vec{\rho}$, so $T_\rho : \mathbb{T}^d \to \mathbb{T}^d$ is the rotation map in (1.5). Let $h : \mathbb{T}^d \to X_0$ be a conjugacy map that embeds $\mathbb{T}^d$ into X. Given some point

$x_0 \in X_0$, we can choose the conjugacy map h uniquely by requiring $h(\vec{0}) = x_0$. If the map T on the larger space X is C^∞ or analytic, do we know anything about the smoothness of X_0 or the smoothness of T restricted to X_0? Do we know how typical $\vec{\rho}$ is likely to be? While almost every $\vec{\rho} \in \mathbb{T}^d$ is Diophantine, it is not obvious that our $\vec{\rho}$ is similarly typical. Our result here allows us to compute $\vec{\rho}$ to 30-digit (quadruple) precision in [3] and we can evaluate the smoothness of h, which generally appears to be real-analytic in [3], in the sense that the Fourier coefficients a_k of h converge to 0 exponentially fast as $k \to \infty$ – in the examples investigated. If T is analytic in a complex neighborhood X_0 and g is analytic in a complex neighborhood of its domain, then we expect to see the Fourier coefficients of g converge exponentially fast to 0. The ability to resolve such behavior depends on fast computation of Fourier coefficients, as is possible with WB_N. Also, see our examples 1 and 2 below.

We will look at a few useful applications of Theorem 1.1.1 in the following applications or "examples".

1.2.1 Rotation vectors

Rotation numbers and vectors play a key role in quasiperiodicity, so we begin by providing some elementary and entertaining facts. Dimension 2 is adequate for conveying these ideas which extend to dimension $d \geq 2$ as well.

Dependence of rotation vector on coordinates. We have defined $\vec{\rho}$ in Eqn. 1.5 in terms of a given coordinate system. We can say the coordinate system has **quasiperiodic coordinates** when Eqn. 1.5 holds for some (ρ_1, ρ_2). Conversely,

we call the vector (ρ_1, ρ_2) a **representation** of $\vec{\rho}$ if there exists a basis (v_1, v_2) of $\mathbb{R}^2$ such that $\vec{\rho} = \rho_1 v_1 + \rho_2 v_2 \mod 1$. Any change of quasiperiodic coordinates to quasiperiodic coordinates is linear on the lift to $\mathbb{R}^2$. Le S denote this set of linear maps. Then S is also the set of integer-entried matrices with determinant ± 1. (For simplicity, we assume that the origin is fixed.) Define $\mathbf{\Gamma(\vec{\rho})}$ be the set of all representations.

Proposition A *Given a representation (ρ_1, ρ_2) of $\vec{\rho}$, $A(\rho_1, \rho_2)$ is a representation of $\vec{\rho}$ for each $A \in S$.*

To see this, let $A = \begin{pmatrix} a & b \\ c & d \end{pmatrix} \in S$ and (ρ_1, ρ_2) be a representation of $\vec{\rho}$ in terms of basis vectors u_1, u_2 in R^2 viewed as the lift of $\mathbb{T}^2$. Since A is invertible, there is a basis v_1, v_2 such that $v_i = A^{-1}u_i$, for $i = 1, 2$. Then $\vec{\rho} = \Sigma \rho_i u_i = \Sigma \rho_i A v_i = \rho_1(av_1 + bv_2) + \rho_2(cv_1 + dv_2) = (a\rho_1 + c\rho_2)v_1 + (b\rho_1 + d\rho_2)v_2 = \rho_1' v_1 + \rho_2' v_2$, where $(\rho_1', \rho_2') = A(\rho_1, \rho_2)$. ∎

Proposition B *Given a representation $\rho = (\rho_1, \rho_2)$ of $\vec{\rho}$, every representation $\rho' = (\rho_1', \rho_2')$ of $\vec{\rho}$ is of the form $A(\rho_1, \rho_2)$ for some $A \in S$.*

To see this, let $\vec{\rho} = \sum \rho_i u_i = \sum \rho_i' v_i$, where u_1, u_2 and v_1, v_2 are bases. Choose $A \in S$ such that $Av_i = u_i$. Then as above, $A\rho = \rho'$. ∎

Proposition C *For each $A \in S$, $A\Gamma(\vec{\rho}) = \Gamma(\vec{\rho})$.*

From Proposition A, for each $A \in S$, $A\Gamma(\vec{\rho}) \subseteq \Gamma(\vec{\rho})$. Furthermore, since A^{-1} is also in S, we must have that

$$\Gamma(\vec{\rho}) = AA^{-1}\Gamma(\vec{\rho}) \subseteq A\Gamma(\vec{\rho}) \subseteq \Gamma(\vec{\rho}). \quad ∎$$

Proposition D *For $\vec{\rho}$ Diophantine, the set of pairs $\Gamma(\vec{\rho}) \mod 1$ is dense in*

$\mathbb{T}^2$.

To see this, note that the matrices $B_m := \begin{pmatrix} 1 & m \\ 0 & 1 \end{pmatrix}$ and $C_k = \begin{pmatrix} 1 & 0 \\ k & 1 \end{pmatrix}$ are in S for all integers m and k, as is $A := B_m C_k$. Then the vectors $(\rho_1, y_k) = C_k(\rho_1, \rho_2)$ mod 1 are "vertical" translates (translates in the direction $(0,1)$) of (ρ_1, ρ_2) mod 1. where $\{y_k\}$ is a dense set in S^1. When we similarly apply B_m for all m to each (ρ_1, y_k) we obtain a dense set of "horizontal" translates of (ρ_1, y_k) and thereby obtain a dense set in $\mathbb{T}^2$. Of course every coordinate of every point in that dense set is of the form $k_1\rho_1 + k_2\rho_2$ mod 1 where k_1 and k_2 are integers. ∎

Example 1, Determining the Rotation Vector. The spirit of the Birkhoff ergodic theorem is that knowing a function's values only along a typical trajectory, one can determine, in the limit, the function's spatial average. We do not need to know the points on the trajectory or even where the invariant set is. Given a map $T : X \to X$ with a quasiperiodic set X_0 and a trajectory $(x_n) \subset X_0$, an investigator must convert each x_n into a set of d-dimensional angles ϕ_n, as shown for a 1D-case in Fig. 1.1. Our goal is to determine the rotation vector $\vec{\rho} \in \mathbb{T}^d$, purely from $(\phi_n) \in \mathbb{T}^d$. There are some hidden subtelities. The standard approach towards computing $\vec{\rho}$ is as the limit $\vec{\rho} = \lim_{N\to\infty} N^{-1}(\bar{\phi}_N - \bar{\phi}_0)$, where the quantity $\bar{\phi}_N - \bar{\phi}_0$ is computed as $\sum_{n=0}^{N-1} \Delta\phi_n$, where $\Delta\phi_n := \angle(\phi_{n+1}, \phi_n)$ is some measure of the angle from ϕ_n to ϕ_{n+1}. Even in the 1D-case, there are two ways to measure the angle between ϕ_n and ϕ_{n+1}. In general, it can be difficult to define such a $\Delta\phi : X_0 \to \mathbb{R}^d$ which is continuous. In some 1D cases, $\Delta\phi$ can be chosen to be the positive angle from ϕ_n to ϕ_{n+1}. That would not work however in Fig. 1.1, where $\Delta\phi$ must be the

shortest angular difference from ϕ_n to ϕ_{n+1}. In another example, if an astronomer measures the angular position of Mars from the earth, the angle sometimes makes small positive changes and sometimes negative, exhibiting "retrograde motion". In such a case, it is appropriate to choose $\Delta\phi$ so as to minimize the absolute value of the angular change.

To avoid these problems, we will make two assumptions on ϕ and $\Delta\phi$. We begin with a definition.

Definition. Let $\phi : X_0 \to \mathbb{T}^d$ be a C^∞ map. Then the lift $\bar{\phi} : \bar{X}_0 \equiv \mathbb{R}^d \to \mathbb{R}^d$ can be written in the form $\bar{\phi}(\theta) = A\bar{\theta} + g(\theta)$, where $g : \mathbb{R}^d \to \mathbb{R}^d$ is bounded (and periodic with period 1 in each coordinate), and A is a matrix called the **homology matrix** of ϕ, so that

$$A = \phi_* : H_1(X_0) \to H_1(\mathbb{T}^d).$$

Note that while this matrix A has a slightly different meaning from the A in the above proposition, the entries of A are again integers. We say ϕ is a **unit degree map** if the determinant of A is ± 1. In that case, A^{-1} is also an integer valued matrix with determinant ± 1. Note that, if ϕ is unit-degree, then there is a choice of coordinates for θ under which A is the identity, and henceforth, we will assume that A is the identity.

(A1) ϕ is a unit degree map.

(A2) $\Delta\phi : X_0 \to \mathbb{R}^d$ is a continuous map such that for each $x \in X_0$, each lift $\bar{\phi(x)}$ of $\phi(x)$, $\Delta\phi(x) + \bar{\phi(x)}$ is a lift of $\phi(T(x)$. Let ϕ_n be the point $\phi(x_n)$. Then note that $\Delta\phi(x_n)$ is a lift of $\phi_{n+1} - \phi_n$. Fix any lift $\bar{\phi}_0$ of ϕ_0 and inductively define $\bar{\boldsymbol{\phi}}_{\boldsymbol{n}}$

$:= \bar{\phi}_{n-1} + \Delta\phi(\theta_{n-1})$. Note that by virtue of $\Delta\phi$, $\bar{\phi}_n$ is always a lift of ϕ_n.

Corollary 1.2.1 *Let X, X_0, T, and w be as in Theorem 1.1.1. Let $\phi : X_0 \to \mathbb{T}^d$ and $\Delta\phi : X_0 \to \mathbb{R}^d$ satisfy assumptions (A1) and (A2). Then for every initial point $x_0 \in X_0$,*

$$WB_N(\Delta\phi) := \frac{1}{A_N} \sum_{n=0}^{N-1} w\left(\frac{n}{N}\right) \Delta\phi_n$$

has super convergence to a vector $\bar{\vec{\rho}}$, which is a lift of the rotation vector $\vec{\rho}$, uniformly in x_0 as $N \to \infty$.

In other words, $\vec{\rho} = \bar{\vec{\rho}} \mod 1$, (i.e., mod 1 in each coordinate).

Proof By Theorem 1.1.1, the sum has super convergence to the integral $\int_{X_0} \Delta\phi d\mu$. By the Birkhoff Ergodic Theorem, $\int_{X_0} \Delta\phi d\mu$ is also the limit of the unweighted Birkhoff sum $\frac{1}{N} \sum_{n=0}^{N-1} \Delta\Phi_n$, which is equal to $\frac{1}{N} \sum_{n=0}^{N-1} [\bar{\phi}_{n+1} - \bar{\phi}_n]$, which is equal to $(\bar{\phi}_N - \bar{\phi}_0)/N$. Therefore, the sum in the claim has super convergence to the limit $\lim_{N\to\infty} \frac{\bar{\phi}_N - \bar{\phi}_0}{N}$. We will now show that this limit is the rotation number $\vec{\rho}$.

Note that since (x_n) is a quasiperiodic trajectory, there exists an unknown rotation vector $\vec{\rho}$ and an unknown continuous, periodic function $h : \mathbb{R}^d \to \mathbb{R}^d$ so that for each n, $\bar{x}_n = n\vec{\rho} + h(n\vec{\rho})$ is a lift of x_n.

Therefore $\bar{\phi}_n = A\bar{x}_n + g(\bar{x}_n) = nA\vec{\rho} + Ah(n\vec{\rho}) + g(n\vec{\rho} + h(n\vec{\rho}))$.

Therefore $\frac{\bar{\phi}_N}{N} = A\vec{\rho} + \frac{Ah(n\vec{\rho})}{N} + \frac{g(n\rho + h(n\vec{\rho}))}{N}$, which tends to $A\vec{\rho}$ as $N \to \infty$.

Therefore, $\lim_{N\to\infty} \frac{\bar{\phi}_{N-1} - \bar{\phi}_0}{N} = A\vec{\rho}$. ∎

Remark. Here we give one way of constructing the map $\Delta\phi$. Suppose there exists a vector $\vec{p} \in [0,1)^d$ such that the set $\{T(\theta) - \theta + \vec{p} : \theta \in (0,1)^d\}$ lies in the

open box interior $(0,1)^d$ in $\mathbb{R}^d$. Given a point $\theta \in X_0$, let $\bar{\theta}$ be any lift of θ to $\mathbb{R}^d$. Let $\bar{T}\theta$ be that unique lift of $T\theta$ to $\mathbb{R}^d$ which satisfies $\bar{T}\theta - \bar{\theta} + \vec{p} \in [0,1)^d$. Then the following function $\boldsymbol{\Delta\phi} : X_0 \to \mathbb{R}^d$ is smooth and independent of the choice of the lift.

$$\Delta\phi(\theta) := \bar{\phi}(\bar{T}\theta) - \bar{\phi}(\bar{\theta}).$$

Remark. Consider the case of a 1-dimensional quasiperiodic set X_0 embedded in $X = \mathbb{R}^2$. Let $C := C_B \cup C_U$ be the complement of X_0 in $\mathbb{R}^2$, where C_B and C_U are the bounded and unbounded components of C respectively. For $p \in \mathbb{R}^2 \setminus X_0$, define

$$\phi(x) = (x-p)/\|x-p\|. \tag{1.8}$$

Hence $\phi(\theta) \in \mathbb{T}^d$ where $d = 1$. If $p \in C_B$, then ϕ is a unit degree map. Suppose that the range of values of $\phi(Tx) - \phi(x) \mod 1$ does not include an angle θ_0. Then $\Delta\phi$ can be taken to be the difference

$$\Delta\phi(x) : \phi(T(x)) - \phi(x) - \theta_0 \mod 1 \tag{1.9}$$

So $\Delta\phi_n$ is the length of the arc joining ϕ_n to ϕ_{n+1} and avoiding the angle θ_0. We have illustrated this in Fig. 1.1.

1.2.2 Computing Fourier series.

Example 2, Fourier Series of the embedding. Assume $X_0 \subset \mathbb{R}^D$. If a map T is quasiperiodic on X_0, then there is a homeomorphism $h : \mathbb{T}^d \to X_0 \subset \mathbb{R}^D$ such that for every $theta \in \mathbb{T}^d$, $T(h(\theta)) = h(\theta + \vec{\rho})$.

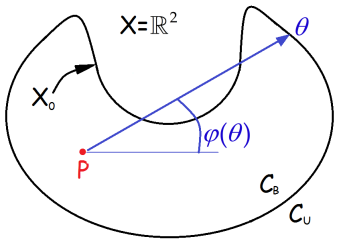

Figure 1.1: **Rotation number on a quasiperiodic curve.** Given a quasiperiodic curve X_0 embedded in $X = \mathbb{R}^2$, one can define ϕ as in Eq. 1.8. Let $\rho_\phi := \lim_{N\to\infty} \frac{1}{N} \sum_{n=0}^{N-1} w\left(\frac{n}{N}\right) [\bar{\phi}_{n+1} - \bar{\phi}_n]$. If p lies outside the curve X_0, then $\rho_\phi = 0$. If p lies in the interior of X_0, then ρ_ϕ is ρ or $1-\rho$, both being legitimate representations of ρ.

We can compute a Fourier series for $h(\theta)$ provided the rotation number $\vec{\rho}$ for the map is known, but that can be calculated as a weighted average, as explained above in Corollary 1.2.1. The map h is not known explicitly, but its values $(x_n := h(n\vec{\rho} \mod 1))_{n=0,1,2,\ldots}$ are known. For every $\vec{k} \in \mathbb{Z}^d$, the $\vec{k}$-th Fourier coefficient of h is described below.

$$a_{\vec{k}}(h) := \int_{\mathbb{T}^d} h(\theta) e^{-i2\pi\vec{k}\cdot\theta} d\theta.$$

Now h can be represented by its Fourier series. For every $\theta \in \mathbb{T}^d$,

$$h(\theta) = \sum_{\vec{k}\in\mathbb{Z}^d} a_{\vec{k}} e^{i2\pi\vec{k}\cdot\theta}.$$

The smoothness of h is not known apriori, but once the computation of the fourier coefficients have converged, the smoothness can be non-rigorously deduced from the decay rate of the coefficients $a_{\vec{k}}$ with $\|\vec{k}\|$. Therefore, the crucial step in this estimation is an accurate calculation of each $a_{\vec{k}}$, which can be obtained as the limit of a weighted Birkhoff average, as stated in the following Corollary.

Corollary 1.2.2 *Under the assumptions of Corollary 1.2.1, the quantity*

$$\lim_{N\to\infty} WB_N[h(\theta)e^{-i2\pi\vec{k}\cdot\theta}] = \lim_{N\to\infty}\frac{1}{A_N}\sum_{n=0}^{N-1} w\left(\frac{n}{N}\right) x_n e^{-i2\pi n\vec{k}\cdot\vec{\rho}}$$

has super-convergence as $N\to\infty$ to $a_{\vec{k}}(h)$, the $\vec{k}$-th Fourier coefficient of h

Proof By Theorem 1.1.1, the limit of the weighted Birkhoff average of the smooth function $h(\theta)e^{-i2\pi\vec{k}\cdot\theta}$ has super convergence to the integral $\int_{\mathbb{T}^d} h(\theta)e^{-i2\pi\vec{k}\cdot\theta}d\theta$, which is precisely $a_{\vec{k}}(h)$, the $\vec{k}$-th Fourier coefficient of h. ∎

The question of *smoothness of conjugacy to a pure rotation* is an old problem. While we can only determine the degree of differentiability of the conjugacy function h computationally (non-rigorously) by observing how quickly its Fourier series coefficients a_k go to 0 as $\|k\|\to\infty$, the papers [4], [13], [14] and [15] arrive at rigorous conclusions on the differentiability of h by making various assumptions on the smoothness of the quasiperiodic map T and the Diophantine class of its rotation number ρ. In our case, we conclude that h is real-analytic if $\|a_k\|$ decreases exponentially fast, i.e., $\log\|a_{\vec{k}}\| \le A + B|\vec{k}|$ for some A and B, to the extent checkable with a given computer precision. Also see [3] for a discussion on computing Fourier coefficients of maps between tori instead of maps from the torus to $\mathbb{R}^D$. For example, for the circle map $\theta\mapsto\theta+g(\theta) \mod 1$, it is appropriate to compute the Fourier series of the *periodic part* $g(\theta)$ of the map.

Example 3, computing the integral of a periodic C^∞ function. We designed the above theorem as a tool for investigating quasiperiodic sets, but sometimes we can artificially create the quasiperiodic dynamics. To integrate a C^∞ map

with respect to the Lebesgue measure when the map is periodic in each of its d variables, we can rescale its domain to a d-dimensional torus $\mathbb{T}^d = [0,1]^d \mod 1$ in each coordinate. Choose $\vec{\rho} = (\rho_1, \cdots, \rho_d) \in (0,1)^d$ of Diophantine class $\beta > 0$. Let $T = T_{\vec{\rho}}$ be the rotation by the Diophantine vector ρ on $\mathbb{T}^d$. Let w be the exponential weighting function Eq. (1.2). Then by Theorem 1.1.1, for every $\theta \in \mathbb{T}^d$, $\mathrm{WB}_N(f)(\theta)$ *has super convergence to* $\int_{\mathbb{T}^d} f d\mu$ *and convergence is uniform in* θ.

1.3 A C^m version of our Theorem

Theorem 1.1.1 is a special case of the technically more detailed Theorem 1.3.1 which we shall state and prove in this section. We have formulated Prop. 1.3.3 to show the source of the N^{-m} term that guarantees the rapid convergence of weighted Birkhoff averages.

Window functions. We will say that a function $w : \mathbb{R} \to \mathbb{R}$ is a **window function** if w is 0 outside $[0,1]$ and is positive in $(0,1)$. For $m \in \mathbb{N}$, we will say that the window function is of **order** m if w is C^m. Hence for $m \geq 1$, w and its first m derivatives are 0 at 0 and 1. We will say that a window function has **order 0** if it is continuous, for example, the window function which is $x(1-x)$ on $[0,1]$ is order-0, while $\sin^2(\pi t)$ is order-1. In order to include the situation in (1.1), we say that the window function which is 1 on $[0,1]$ (and 0 outside) is of **order -1**. We say that w is of **order ∞** if it is of order m for every $m \in \mathbb{N}$, for example, the exponential weighting function in Eq. (1.2).

Theorem 1.3.1 *For some* $m, M \in \mathbb{N}$, *let* X *be a* C^M *manifold and* $T : X \to X$

be a C^M d-dimensional quasiperiodic map on $X_0 \subseteq X$, with invariant probability measure μ and a rotation vector of Diophantine class β. Let $f : X \to E$ be C^M, where E is a finite-dimensional, real vector space. Assume w is an order-m window function. Assume

$$m < \frac{M-d}{d+\beta} \tag{1.10}$$

Then

$$(WB_N f)(x_0) = \int_{X_0} f \, d\mu + O\left(\frac{1}{N^m}\right) \text{ uniformly in } x_0 \in X_0, \text{ as } N \to \infty. \tag{1.11}$$

We note again that $\mathrm{WB}_N(f)(x_0)$ converges to $\int_{X_0} f \, d\mu$, which is also the limit of the corresponding Birkhoff averages. Hence WB_N provides an efficient way of computing the limit of Birkhoff averages.

Are the estimates sharp? The estimates used in the proof may be able to be improved and hence, Eq. 1.11 might be sharpened. For the case where X and T are C^∞ and w is order-∞ and the dimension d of X_0 is 1, we have made a couple of heuristic numerical experiments using examples of f that are C^1 and C^3 ($M = 1$ and 3, respectively) using the golden mean $\frac{\sqrt{5}-1}{2}$ and $\frac{1}{e}$ as values for ρ. For the golden mean, $\beta = 0$. Our experiments were in quadruple precision (32-digit precision).

If f is C^3, then m is 1 by Eq. 1.10, so Eq. 1.11 predicts a convergence rate of $O(N^{-1})$. But in numerical experiments we observe convergence rates of approximately $O(N^{-5.7})$ and $O(N^{-4.9})$ for ρ equal to the golden mean and $\frac{1}{e}$ respectively. For the examples where f is C^1, the corresponding rates were approximately $O(N^{-3.1})$ and $O(N^{-3.1})$, even though Eq. 1.11 does not make any predictions about

this case.

1.3.1 Proof of Theorem 1.3.1

To prove Theorem 1.3.1, we use the coordinates θ on X_0 for which Eq. (1.6) holds. So for the rest of this section, $X_0 = \mathbb{T}^d$ and T is an irrational rotation $T_{\vec{\rho}}$, as described in Eq. (1.5). Of course $T^n_{\vec{\rho}} = T_{n\vec{\rho}} : \theta \mapsto \theta + n\vec{\rho} \mod \mathbb{Z}^d$. As a result, $f(T^n_{\vec{\rho}}(\theta)) = f(\theta + n\vec{\rho})$. Therefore, in this dynamical system, (1.3) takes the form

$$\mathrm{WB}_N f = \frac{1}{A_N} \Sigma_n w\left(\frac{n}{N}\right) f(\theta + n\vec{\rho}). \tag{1.12}$$

Our first lemma gives an upper bound on the decay rate of the quantity $|e^{i2\pi\vec{k}\cdot\vec{\rho}} - 1|$ for a vector $\vec{\rho}$ of Diophantine class β, and for each $\vec{k} \in \mathbb{Z}^d$. This inequality is suggested by Arnold's study of small denominators in [16].

Lemma 1.3.2 (A Diophantine Inequality.) *For a vector $\vec{\rho}$ of Diophantine class $\beta > 0$, there exists $C_\rho > 0$ such that*

$$\frac{1}{|e^{i2\pi\vec{k}\cdot\vec{\rho}} - 1|} \leq (4C_\rho)^{-1}\|\vec{k}\|^{d+\beta} \text{ for each } \vec{k} \in \mathbb{Z}^d.$$

Proof A little trigonometry reveals $|e^{i2\pi\vec{k}\cdot\vec{\rho}} - 1| = 2|\sin(\pi\vec{k}\cdot\vec{\rho})|$ which equals $2|\sin(\vec{k}\cdot\vec{\rho} - p)\pi)|$ for every integer p. Choose p so that $(\vec{k}\cdot\vec{\rho} - p)\pi \in [-\pi/2, +\pi/2]$. But $|\sin(x)| \geq 2|x|\pi$ for $x \in [-\pi/2, \pi/2]$. Therefore, $|e^{i2\pi\vec{k}\cdot\vec{\rho}} - 1| \geq 2|\vec{k}\cdot\vec{\rho} - p|\pi)\frac{2}{\pi} = 4|\vec{k}\cdot\vec{\rho} - p| \geq 4C_\rho\|k\|^{-d-\beta}$ from Ineq. (1.7). Taking reciprocals, we get the inequality claimed by the lemma. ∎

A convention for summation notation. Since $w\left(\frac{n}{N}\right)$ is 0 for $n \leq 0$ or $n \geq N$, we can adopt the convention of writing $\boldsymbol{\Sigma}_{\boldsymbol{n}}$ denote the sum over all integers.

For any map $h : \mathbb{Z} \to \mathbb{C}$, note that

$$\sum_n w\left(\frac{n}{N}\right) h(n) = \sum_{n=-\infty}^{\infty} w\left(\frac{n}{N}\right) h(n) = \sum_{n=1}^{N-1} w\left(\frac{n}{N}\right) h(n).$$

Some operators. Let for each $N \in \mathbb{N}$, let $\boldsymbol{\sigma_{1/N}}$ denote the operator on functions on $\mathbb{R}$ which is defined as $(\sigma_{1/N} w)(t) = w(t - \frac{1}{N})$. Note that $\sigma_{1/N} w\left(\frac{n}{N}\right) = w(\frac{n-1}{N})$. Let $\boldsymbol{I}$ denote the identity operator. Given a transformation T, the **Koopman operator** $\boldsymbol{U}$ operates on functions and is defined as

$$Uf := f \circ T.$$

In our case, since $T \equiv T_{\vec{\rho}}$,

$$(Uf)(\theta) = f \circ T_{\vec{\rho}} = f(\theta + \rho).$$

Proposition 1.3.3 (Polynomial Decay) *For every positive integer m and every C^m function $w : \mathbb{R} \to \mathbb{R}$ with support in $[0, 1]$,*

$$\sum_n w\left(\frac{n}{N}\right) U^n (U - I)^m = \sum_n (\sigma_{1/N} - I)^m w\left(\frac{n}{N}\right) U^n = \sum_n w^{(m)}(\frac{n}{N})[N^{-m} + o(N^{-m})]U^n.$$

Proof We will first prove the first equality for $m = 1$. We will use the fact that $\sum_n w\left(\frac{n}{N}\right) U^{n+1} = \sum_n w(\frac{n-1}{N})U^n$, which follows from the fact that the index n runs over all integers.

$$\begin{aligned}
\sum_n w\left(\frac{n}{N}\right) U^n (U - I) &= \sum_n w\left(\frac{n}{N}\right) U^{n+1} - \sum_n w\left(\frac{n}{N}\right) U^n. \\
&= \sum_n w(\frac{n-1}{N})U^n - \sum_n w\left(\frac{n}{N}\right) U^n. \\
&= \sum_n (\sigma_{1/N} - I) w\left(\frac{n}{N}\right) U^n.
\end{aligned}$$

Apply the above operation m times to obtain the first inequality.

Since w is a C^m function, its m-th derivative $w^{(m)}$ is continuous and an application of Taylor's theorem yields the following equation for each $t \in \mathbb{R}$. See [17], Chapter VII for more details.

$$(\sigma_{1/N} - I)^m w(t) = N^{-m} w^{(m)}(t) + o(N^{-m}).$$

Making this substitution completes the proof. ∎

For each $f \in L^2(\mathbb{T}^d, \lambda)$ we can write its Fourier series representation

$$f(\theta) = \sum_{k \in \mathbb{Z}^d} a_k e^{i2\pi k \cdot \theta}, \text{ where } \theta \in \mathbb{T}^d.$$

Let $\mathbb{Z}_{\mathbf{0}}^{\boldsymbol{d}}$ denote the set of integer-valued vectors excluding the zero vector, i.e., $\mathbb{Z}^d \backslash \{0\}$.

Proposition 1.3.4 *Let $T : \mathbb{T}^d \to \mathbb{T}^d$ be a rotation by the irrational vector ρ. (see (1.5)). There is a constant $C_{w,m} > 0$ such that for every $f \in L^2(\mathbb{T}^d, \lambda)$, every $\theta \in \mathbb{T}^d$,*

$$\left| (WB_N)(f)(\theta) - \int_{\mathbb{T}^d} f d\lambda \right| \leq \frac{C_{w,m}}{N^m} \sum_{k \in \mathbb{Z}_0^d} \left| \frac{a_k}{(e^{i2\pi k \cdot \rho} - 1)^m} \right|.$$

Proof For each $k \in \mathbb{Z}^d$, let $\boldsymbol{f_k}$ denote the function $f_k(\theta) = e^{i2\pi k \cdot \theta}$ on $\mathbb{T}^d$. Then f_k is an eigenvector for the operator U with eigenvalue $e^{i2\pi k \cdot \rho}$, because of the following relation.

$$U^n f_k = U^n e^{i2\pi k \cdot \theta} = U^{n-1} e^{i2\pi k \cdot (\theta + \rho)} = e^{i2\pi k \cdot (\theta + n\rho)}. \tag{1.13}$$

Therefore, $\mathrm{WB}_N (U - I)^m f_k = \mathrm{WB}_N (e^{i2\pi k \cdot \rho} - 1)^m f_k = (e^{i2\pi k \cdot \rho} - 1)^m \mathrm{WB}_N e^{i2\pi k \cdot \theta}$, i.e.,

$$\begin{aligned}
(e^{i2\pi k\rho} - 1)^m (\mathrm{WB}_N f_k)(\theta) &= \mathrm{WB}_N (U - I)^m f_k(\theta) \\
&= \frac{1}{A_N} \sum_n w\left(\frac{n}{N}\right) U^n (U - I)^m e^{i2\pi k \cdot \theta} \\
&= \frac{1}{A_N} \sum_n w^{(m)}(\frac{n}{N}) [N^{-m} + o(N^{-m})] U^n e^{i2\pi k \cdot \theta} \text{ by Prop. 1.3.3.}
\end{aligned}$$

There exists some constant $C'_{w,m} \geq 1$ such that $N^{-m} + o(N^{-m}) \leq C'_{w,m} N^{-m}$. Also note that for $\forall \theta$,

$|U^n f_k(\theta)| = |e^{i2\pi k\cdot(n\rho+\theta)}| = 1$. Therefore,

$$\begin{aligned}
|(\mathrm{WB}_N f_k)(\theta)| &\leq \frac{1}{|e^{i2\pi k\rho} - 1|^m} \frac{1}{A_N} C'_{w,m} N^{-m} \sum_n |w^{(m)}(\frac{n}{N})| \\
&\leq \frac{1}{|e^{i2\pi k\rho} - 1|^m} \frac{N}{A_N} C'_{w,m} N^{-m} \|w^{(m)}\|_{C^0} \\
&\leq \frac{1}{|e^{i2\pi k\rho} - 1|^m} \frac{C''_w}{\int_0^1 w(t)dt} C'_{w,m} N^{-m} \|w^{(m)}\|_{C^0} \text{ from Eq.(1.4)}
\end{aligned}$$

for some constant $C''_w > 0$. In summary, there exists a constant $C_{w,m} = C''_w C'_{w,m} \frac{\|w^{(m)}\|_{C^0}}{\int_0^1 w(t)dt} > 0$ such that for every $\theta \in \mathbb{T}^d$,

$$|(\mathrm{WB}_N f_k)(\theta)| \leq C_{w,m} N^{-m} |e^{i2\pi k\rho} - 1|^{-m}. \tag{1.14}$$

Note that the Fourier coefficient a_0 of f is the integral $\int_{\mathbb{T}^d} f d\lambda$ and is also $\mathrm{WB}(a_0 f_0)(\theta)$ for every N since $f_0 \equiv 1$. Therefore, by (1.14)

$$\begin{aligned}
\left|(\mathrm{WB}_N)(f)(\theta) - \int_{\mathbb{T}^d} f d\lambda\right| &= \left|\sum_{k\in\mathbb{Z}_0^d} a_k (\mathrm{WB}_N f_k)(\theta)\right| \\
&\leq \sum_{k\in\mathbb{Z}_0^d} |a_k (\mathrm{WB}_N f_k)(\theta)| \\
&\leq \frac{C_{w,m}}{N^m} \sum_{k\in\mathbb{Z}_0^d} \frac{|a_k|}{|e^{i2\pi k\rho} - 1|^m}. \qquad \blacksquare
\end{aligned}$$

Proof of Theorem 1.3.1 Since $f \in C^M$, there exists $C_{f,M} > 0$ depending on f and M such that for each $k \in \mathbb{Z}_0^d$, $|a_k| \leq C_{f,M} \|k\|^{-M}$. This bound on the decay rate of Fourier coefficients can be obtained by differentiating the Fourier series of f, M times. Since f is C^M, $f^{(M)}$ is continuous and hence integrable. By the Riemann Lebesgue lemma (see Chapter II.1, [18]), the Fourier coefficients of $f^{(M)}$ converge to zero and hence the inequality holds. The Diophantine property of ρ allows us to

combine this inequality with the inequality in Lemma 1.3.2 to give

$$\sum_{k\in\mathbb{Z}_0^d}\left|\frac{a_k}{(e^{i2\pi k\rho}-1)^m}\right| \leq \frac{C_{f,m}}{(4C_\rho)^m}\sum_{k\in\mathbb{Z}_0^d}\|k\|^{-(M-m(d+\beta))} \tag{1.15}$$

It is known that the sum $\sum_{k\in\mathbb{Z}_0^d}\|k\|^{-\alpha}$ converges when $\alpha > d$. Therefore, the criteria $M - m(d+\beta) > d$ ensures that $\sum_{k\in\mathbb{Z}_0^d}\|k\|^{-(M-m(d+\beta))} < \infty$. Therefore, by Proposition 1.3.4,

$$\left|(\mathrm{WB}_N)(f)(\theta) - \int_{\mathbb{T}^d} f d\lambda\right| \leq \frac{C_{w,m}}{N^m}\frac{C_{f,m}}{(4C_\rho)^m}\sum_{k\in\mathbb{Z}_0^d}\|k\|^{-(M-(d+\beta)m)} = O(\frac{1}{N^m}).$$

In other words, $(\mathrm{WB}_N)(f)(\theta) = \int_{\mathbb{T}^d} f d\lambda + O(\frac{1}{N^m})$ uniformly in θ. ∎

Chapter 2: Quantitative Quasiperiodicity

Abstract. The Birkhoff Ergodic Theorem concludes that time averages, i.e., Birkhoff averages, $\Sigma_{n=0}^{N-1} f(x_n)/N$ of a function f along a length N ergodic trajectory (x_n) of a function T converge to the space average $\int f d\mu$, where μ is the unique invariant probability measure. Convergence of the time average to the space average is slow. We introduce a modified average of $f(x_n)$ by giving weights to the "end" terms which smoothly vanish to zero as n approaches 0 or $N-1$ (smoothly as a function of $\frac{n}{N}$. When (x_n) is a trajectory on a quasiperiodic torus and f and T are C^∞, we show that our weighted Birkhoff averages converge "super" fast to $\int f d\mu$ with respect to the number of iterates N, *i.e.* with error decaying faster than N^{-m} for every integer m. Our goal is to show that our weighted Birkhoff average is a powerful computational tool, and this paper illustrates its use for several examples where the quasiperiodic set is one or two dimensional. In particular, we compute rotation numbers and conjugacies (i.e. changes of variables) and their Fourier series, often with 30-digit precision.

2.1 Introduction

Quasiperiodicity is a key type of observed dynamical behavior in a diverse set of applications. Tori with quasiperiodic motion persist for small perturbations by the Kolmogorov-Arnold-Moser theory, but such behavior is also observed for non-conservative systems well beyond this restricted regime. We believe that quasiperiodicity is one of only three types of dynamical behaviors occurring in basic sets of typical systems. See [12] for the statement of our formal conjecture of this basic set triumvirate. For example, quasiperiodicity occurs in a system of weakly coupled oscillators, in which there is an invariant smooth attracting torus in phase space with behavior that can be described exclusively by the phase angles of rotation of the system. Indeed, it is the property of the motion being described using only a set of phase angles that always characterizes quasiperiodic behavior. In a now classical set of papers, Newhouse, Ruelle, and Takens demonstrated a route to chaos through a region with quasiperiodic behavior, causing a surge in the study of the motion [19]. There is active current interest in development of a systematic numerical and theoretical approach to bifurcation theory for quasiperiodic systems. Our goal in this paper is to present a fast numerical method for the fast calculation of the limit of Birkhoff averages in quasiperiodic systems, allowing us to compute various key quantities. If f is integrable and the dynamical system is ergodic on the set in which the trajectory lives, then the Birkhoff Ergodic Theorem asserts that the Birkhoff average $\Sigma_{n=0}^{N-1} f(x_n)/N$ of a function f along an ergodic trajectory (x_n) converges to the space average $\int f d\mu$ as $N \to \infty$ for μ-almost every x_0, where μ

is the unique invariant probability measure. In particular, almost all trajectories with initial point in the ergodic set have the same limit of their Birkhoff averages. We develop a numerical method for calculating the limit of such averages, where instead of weighting the terms $f(x_n)$ in the average equally, we weight the early and late terms of the set $\{0, \ldots, N-1\}$ much less than the terms with $n \sim N/2$ in the middle. That is, rather than using the equal weighting $(1/N)$ in the Birkhoff average, we use a weighting function $w(n/N)$, which will primarily be the following well known C^∞ function that we will call the **exponential weighting function**, $w_{\exp}(t) = \exp(1/(t(t-1))$. In a companion paper [20], it is rigorously shown that for C^∞ quasiperiodic systems with a C^∞ function f, this weighting function leads to super convergence with respect to N, meaning faster than any polynomial in N^{-1}. This super convergence arises from the fact that we are taking advantage of the quasiperiodic nature of the map or flow. In particular, our method uses the underlying structure of a quasiperiodic system, and would not give improved convergence results for chaotic systems. We demonstrate the method and its convergence rate by computing rotation numbers, conjugacies, and their Fourier series in dimensions one and two. We will refer to a one-dimensional quasiperiodic curve as a *curve*.

Other authors have considered related numerical methods before, in particular [7, 21], which we will compare to our approach when we introduce our method in Section 2.2. See also [5, 6, 11, 22–28].

We start by describing our results for a key example of quasiperiodicity: the (circular, planar) restricted three-body problem (**R3BP**). This is an idealized model of the motion of the planet, a large moon, and a spacecraft governed by Newtonian

mechanics, in a model studied by Poincaré [29, 30]. In particular, we consider a planar three-body problem consisting of two massive bodies ("planet" and "moon") moving in circles about their center of mass and a third body ("spacecraft") whose mass is infinitesimal, having no effect on the dynamics of the other two.

We assume that the moon has mass μ and the planet mass is $1-\mu$ where $\mu = 0.1$, and writing equations in rotating coordinates around the center of mass. Thus the planet remains fixed at $(-0.1, 0)$, and the moon is fixed at $(0.9, 0)$. In these coordinates, the satellite's location and velocity are given by the *generalized position vector* (q_1, q_2) and *generalized velocity vector* (p_1, p_2). The equations of motion are as follows (see [30]).

$$\begin{aligned} dq_1/dt &= p_1 + q_2, \\ dq_2/dt &= p_2 - q_1, \\ dp_1/dt &= p_2 - \mu(q_1 - 1 + \rho)d_{moon}^{-3} - (1-\mu)(q_1+\mu)d_{planet}^{-3}, \\ dp_2/dt &= -p_1 - \mu q_2 d_{moon}^{-3} - (1-\mu)q_2 d_{planet}^{-3}, \end{aligned} \tag{2.1}$$

where

$$d_{moon} = ((q_1 - 1 + \mu)^2 + q_2^2)^{0.5} \text{ and } d_{planet} = ((q_1+\mu)^2 + q_2^2)^{0.5}.$$

The following function H is a Hamiltonian for this system

$$H = [(p_1^2 + p_2^2)/2] + [q_2 p_1 - q_1 p_2] - [\mu\ d_{planet}^{-1} + (1-\mu)\ d_{moon}^{-1}]. \tag{2.2}$$

The terms in the square brackets are resp. the kinetic energy, angular moment, and the angular potential. For fixed H, Poincaré reduced this problem to the study of the Poincaré return map for a fixed value of H, only considering a discrete trajectory

of the values of (q_1, p_1) on the section $q_2 = 0$ and $dq_2/dt > 0$. Thus we consider a map in two dimensions rather than a flow in four dimensions. Fig. 2.2 shows one possible motion of the spacecraft for the full flow. The orbit is spiraling on a torus. The black curve shows the corresponding trajectory on the Poincaré return map. Fig. 2.1 shows the Poincaré return map for the spacecraft for a variety of starting points. A variety of orbits are shown, most of which are quasiperiodic invariant curves. An exception is A-trajectory in Fig. 2.1(a), which is an invariant recurrent set consisting of 42 curves. Each curve is an invariant quasiperiodic curve under the 42^{nd} iterate of the map.

Using weighted Birkhoff averages, we find that the Fourier series coefficients decrease exponentially fast (see Fig. 2.3(c)), which strongly suggests the conjugacy function is real analytic. The speed of convergence in Fig. 2.3(d) means that we have an effective computational method yielding an accuracy that is close to the limit of numeric precision, provided N is sufficiently large. In particular, we have computed trajectories for the Poincaré return map using an 8^{th} order Runge-Kutta method with time step 10^{-5}, in quadruple precision. Fig. 2.3(d) is consistent with 30-digit accuracy. Section 2.2 formally define the computed values given in this list for the quasiperiodic orbit of the three-body problem labeled B_1 in Fig. 2.1(b). Here is a list of what our numerical methods yield for the restricted three-body problem:

1. The rotation number is given in Table 2.1, computed to 30 digits of accuracy, and Fig. 2.3(d) shows the accuracy plateauing at about 30-digit precision.

2. We can compute the Fourier series of up to 200 terms. There is a conju-

Example	Equation	Rotation number(s)	Rela
R3BP	2.1	0.063961728757453097164077724400302	2.
Standard map	2.3	0.120552721973755133002981643698 39	
Forced van der Pol oscillator, $F = 5$	2.4	0.292061263291995892855775787189 59	
Forced van der Pol oscillator, $F = 15$	2.4	0.375534411131440108849089280833 18	
Forced van der Pol oscillator, $F = 25$	2.4	0.562353700926850566344192213361 54	
Two-dimensional torus	2.5	ρ_1, ρ_2 in Table 2.2	

Table 2.1: **Summary of our numerical calculations.**

gacy map h between the first return map and a pure rotation on the circle. Evaluating the Fourier series allows us to reconstruct the conjugacy map (*cf.* Fig. 2.3(a)).

3. The exponential decay of the coefficients in the Fourier series described in Fig. 2.3(c) is a strong indication of the analyticity of conjugacy function (*cf.* Fig. 2.3(b)).

Our paper proceeds as follows: In Section 2.2, we describe our numerical method in detail. We illustrate our method for a series of four examples, including an example of a two-dimensionally quasiperiodic map. In all cases, we get fast convergence and are in most cases able to give results with about thirty digits of precision. For convenience of the reader, have summarized our numerical findings in Table 2.1. Finally, Section 2.3 contains our concluding remarks.

2.2 The WB_N method and its applications

2.2.1 Three Dynamical Systems

The standard map. The standard map is an area preserving map on the two-dimensional torus, often studied as a typical example of analytic twist maps (see [31]). It is defined as follows*

$$S_1 \begin{pmatrix} x \\ y \end{pmatrix} = \begin{pmatrix} x + y \\ y + \sin(x + y) \end{pmatrix} \pmod{2\pi}. \tag{2.3}$$

Fig. 2.4(a) shows the trajectories starting at a variety of different initial conditions plotted in different colors. The shaded set is a large invariant chaotic set with chaotic behavior, but many other invariant sets consist of one or more topological circles, on which the system has quasiperiodic behavior. For example, initial condition $(\pi, 1.65)$ leads to chaos while $(\pi, 1.5)$ leads to a quasiperiodic trajectory. As is clearly the case here, one-dimensional quasiperiodic sets often occur in families for non-linear processes, structured like the rings of an onion. There are typically narrow bands of chaos between quasiperiodic onion rings. Usually these inner rings are differentiable images of the d-torus. Yamaguchi and Tanikawa [31] and Chow et. al. [32] show that the outermost limit (the onion's skin, to continue the analogy) will still be a torus, but may not be differentiable. We have computed the rotation number for the standard map orbit shown in the Fig. 2.4(b) using quadruple precision. Its value is given in Table 2.1.

*The standard map generally depends on a parameter α, but we only consider the case $\alpha = 1$.

The forced Van der Pol oscillator. Fig. 2.6 shows orbits for the time-$2\pi/0.83$ map of the following periodically forced Van der Pol oscillator with nonlinear damping [33]

$$\frac{d^2x}{dt^2} - 0.2\left(1 - x^2\right)\frac{dx}{dt} + 20x^3 = F\sin\left(0.83t\right), \tag{2.4}$$

for several values of F. While the innermost orbit shown is a chaotic attractor, the outer orbits are topological circles with quasiperiodic behavior[†]. Our computed rotation numbers for the three orbits $F = 15.0, 25.0$, and 35.0 are given in Table 2.1.

A two-dimensional torus map. So far, the quasiperiodic sets studied here are closed curves. We now introduce an example of a two-dimensional quasiperiodic torus map on $\mathbb{T}^2$. This is a two-dimensional version of Arnold's family of one-dimensional maps (see [16]). It was originally introduced in two papers [34,35]. The map is given by (T_1, T_2) where

$$\begin{aligned} T_1(x,y) &= \left[x + \omega_1 + \frac{\epsilon}{2\pi}P_1(x,y))\right] \pmod 1, \\ T_2(x,y) &= \left[y + \omega_2 + \frac{\epsilon}{2\pi}P_2(x,y)\right] \pmod 1, \end{aligned}$$

and $P_i(x,y), i = 1, 2$ are periodic functions with period one in both variables, defined by:

$$P_i(x,y) = \sum_{j=1}^{4} a_{i,j}\sin(2\pi\alpha_{i,j}), \text{ with } \alpha_{i,j} = r_j x + s_j y + b_{i,j}.$$

The values of all coefficients are given in Table 2.2. This choice of this function is based on [34,35]. Both papers use the same form of equation, though the constants are close to but not precisely the same as the ones used previously. This is fitting

[†]As with the standard map, we have specified all non-essential parameters rather than stating the most general form of the Van der Pol equation.

Coefficient	Value
ϵ	0.4234823
ω_1	0.71151134457776362264681206697006238
ω_2	0.87735009811261456100917086672849971
$a_{1,j}$	$(-0.268, -0.9106, 0.3, -0.04)$
$a_{2,j}$	$(0.08, -0.56, 0.947, -0.4003)$
$b_{1,j}$	$(0.985, 0.504, 0.947, 0.2334)$
$b_{2,j}$	$(0.99, 0.33, 0.29, 0.155)$
r_j	$(1, 0, 1, 0)$
s_j	$(0, 1, 1, -1)$
Computed ρ_1	0.71805375998206610709524493611 7
Computed ρ_2	0.88530466659609979211336682415 7

Table 2.2: **Coefficients for the torus map.** All values are used in quadruple precision, but in this table the repeated zeros on the end of the number are suppressed.

with the point of view advocated by these papers: that the constants should be randomly chosen. Since we are using higher precision, we have chosen constants that are irrational to the level of our precision. The forward orbit is dense on the torus, and the map is a nonlinear map which exhibits two-dimensional quasiperiodic behavior.

Fig. 2.7(a) depicts iterates of the orbit, indicating that it is dense in the torus. We use our weighted Birkhoff average to compute the two Lyapunov exponents,

which have super convergence to zero. Fig. 2.7(b) shows one of them. In terms of method, this is just a matter of changing the function f used in WB_N in Eq. (1.3). Likewise, finding rotation numbers in two dimensions uses the same technique as in the one-dimensional case (*cf.* Fig. 2.7(c)). In all of our calculations, the computation is significantly longer than in one dimension in order to get the same accuracy, perhaps because in two dimensions, coverage of dense orbit varies like the square of the side length of the domain.

Convergence rate of $\mathrm{WB}_{\boldsymbol{N}}$. In order to illustrate how fast the convergence of our method is as $N \to \infty$, we introduce four different possible values for the weighting function w, depicted in Fig. 2.8(a), and compare the convergence results for computing the rotation number for each of these choices of w.

$$\begin{aligned} w_{equal}(t) &= 1 \text{ (Birkhoff's choice)} \\ w_{quad}(t) &= t(1-t) \\ w_{(\sin^2)}(t) &= \sin^2(\pi t) \\ w_{\exp}(t) &= \exp\left(-1/(t(1-t))\right). \end{aligned} \tag{2.5}$$

Recall that the last function in the list, $w_{\exp}$, is the function used in our calculations. If we compute with the first choice of w, we recover the truncated sum in the definition of the Birkhoff average. To estimate the error, we expect the difference $f(x_{N+1}) - f(x_N)$ to be of order one, implying that

$$\mathrm{WB}_{w_{equal},N+1} - \mathrm{WB}_{w_{equal},N} \sim 1/N.$$

The choice of a particular starting point also creates a similar uncertainty of order $1/N$. Every function w is always positive between 0 and 1. For all but the first

choice, the function vanishes as t approaches 0 and 1. In addition, going down the list, increasing number of derivatives of w vanish for $t \to 0$ and $t \to 1$, with all derivatives of $w_{\exp}$ vanishing at 0 and 1. We thus expect the effect of the starting and endpoints to decay at the same rate as this number of vanishing derivatives. Indeed, we find that w_{quad} corresponds approximately to order $1/N^2$ convergence, $w_{(\sin^2)}$ to $1/N^3$ convergence, and $w_{\exp}$ to convergence faster than any polynomial in $1/N$, i.e., for every integer m, there is a constant $C > 0$ such that for N sufficiently large, $|\mathrm{WB}_N f - \int f d\mu| \leq CN^{-m}$. Figs. 2.8(b) and 2.7(b,c) show this effect.

Related methods. See [7,21] for references to earlier methods for computing rotation numbers. In [7,21], A. Luque and J. Villanueva develop fast methods for obtaining rotation numbers for analytic functions on a quasiperiodic torus, sometimes with quasiperiodic forcing with several rotation numbers. The paper [7] examines a smooth function f on a quasiperiodic torus. Let f_n denote the value of f at the n^{th} trajectory point. From this sequence they can obtain the rotation number with error satisfying $|error| \leq C_p N^{-p}$ for any p where C_p is a constant. The method of computation depends on p and as p increases the computational complexity increases for fixed N. If $T(p, N)$ is their computation time, it appears that $T(p, N)/N \to \infty$ as $p \to \infty$. In comparison, computation time for our weighted Birkhoff average is simply proportional to N since it requires a sum of N numbers. The paper gives one figure (Fig. 6) from which the rate of convergence can be computed. It is for a R3BP. Their rotation-number error is proportional to $N^{-3.5}$ and is $\approx 10^{-18}$ at $N = 2^{21} (\approx 2$ million).

Several variants of the Newton's method have been employed to determine

quasiperiodic trajectories in different settings. In [36] the monodromy variant of Newton's method was applied to locate periodic or quasi-periodic relative satellite motion. A PDE-based approach was taken in [37], where the authors defined an invariance equation which involves partial derivatives. The invariant tori are then computed using finite element methods. See also Section 2 in [37] for more references on the numerical computation of invariant tori.

2.2.2 Error in the calculation when the true rotation number is known

In order to test the error in the calculation of rotation number, we present two examples below where we know the exact rotation number. This allow us to determine the actual error in the calculation for the WB_N method as N increases. In both cases the error decreases to less than 10^{-31} and then it grows as N increases, apparently due to accumulated round-off error.

Example 1. Let (θ_n) be an orbit under the pure rotation described in Eq. (1.5) for a rotation by $\rho = \sqrt{2} - 1$. Assume that what we observe is ϕ, a perturbed version of θ, namely,

$$\phi_n = \theta_n + \alpha \cos(2\pi\theta_n) + \beta \sin(2\pi\theta_n), \text{ where } \theta_n = n\rho \pmod 1. \tag{2.6}$$

We use the weighted Birkhoff average as in Eq. (1.2.1) (changing y to ϕ) to obtain an estimate of the rotation number ρ from this orbit. Fig. 2.10 shows the results for $\alpha = 0.1$ and $\beta = 0.2$ in (a) and for the case $\alpha = 0.0$ and $\beta = 0.0$ in (b).

Example 2. Fig. 2.11 shows a geometric version of the problem from the previous example, and again the error in the rotation number is small.

2.2.3 Fourier coefficients and change of coordinates reconstruction

For a quasiperiodic curve as shown in Fig. 2.3(a), there are two approaches to representing the curve. Firstly, we can write the coordinates (X, Y) as a function of $\theta \in S^1$, or secondly, we can reduce the dimension and represent the points on the curve by an angle $\phi \in S^1$, that is, $\phi(X(\theta), Y(\theta))$, which is also $h(\theta) = \theta + g(\theta)$. We have shown g in Fig. 2.3(b) and the exponential decay of the norm of the Fourier coefficients in Fig. 2.3(c). To limit the number of graphs in this paper, we have only created the Fourier series for the periodic part $g(\theta)$.

Given a continuous periodic map $f : S^1 \to \mathbb{R}$,the Fourier series representation of f is the following.

$$\text{For every } t \in S^1,\ f(t) = \frac{b_0}{2} + \sum_{k=1}^{\infty} b_k \cos(2k\pi t) + \sum_{k=0}^{\infty} c_k \sin(2k\pi t), \tag{2.7}$$

where the coefficients b_k and c_k are given by the formulas

$$b_k = 2 \int_{\theta \in S^1} f(\theta) \cos(2k\pi\theta)\ d\theta, \tag{2.8}$$

$$c_k = 2 \int_{\theta \in S^1} f(\theta) \sin(2k\pi\theta)\ d\theta. \tag{2.9}$$

To be able to use the fast Fourier transform, 2^M equally spaced points on the circle are required. If we only have access to an ergodic orbit (x_n) on a curve, then we cannot use the fast Fourier transform as we only have the function values $f(x_n)$ along a quasiperiodic trajectory, and a rotation number ρ. So instead, we obtain these coefficients using a weighted Birkhoff average on a trajectory (x_n) by applying the functional WB_N. For $k = 0$, we find a_0 by applying WB_N to the function 1. For

$k > 0$, we find b_k and c_k as follows.

$$b_k = \mathrm{WB}_N(f(\theta)\cos(2k\pi\theta)) = \sum_{n=0}^{N-1} f(x_n)\cos(2k\pi n\rho)\hat{w}_{n,N}. \tag{2.10}$$

$$c_k = \mathrm{WB}_N(f(\theta)\sin(2k\pi\theta)) = \sum_{n=0}^{N-1} f(x_n)\sin(2k\pi n\rho)\hat{w}_{n,N}. \tag{2.11}$$

By specifying that $\theta_0 = 0$, our computation of rotation number ρ provides all iterates. Namely, $\theta_n = n\rho$. Using the Fourier coefficients, we can thus reconstruct the periodic part of the change of variables function g (see Eq. (3.4)). This is depicted for the R3BP in Fig. 2.3, for the standard map in Fig. 2.5, for the forced van der Pol equation in Fig. 2.6. In all three one-dimensional cases, we depict $\sqrt{b_k^2 + c_k^2}$ as a function of k. Our main observation is that the Fourier coefficients decay exponentially; that is, for some positive numbers α and β, in dimension one, the Fourier coefficients b_k and c_k satisfy

$$\sqrt{|b_k|^2 + |c_k|^2} \leq \alpha e^{-\beta|k|} \text{ for all } k \in \mathbb{Z}. \tag{2.12}$$

This is characteristic of analytic functions. We therefore state that all of the conjugacy functions that we computed in our examples are effectively analytic, "effectively" meaning within the precision of our quadruple precision numerics.

In two dimensions, the computation of Fourier coefficients is similar, but instead of only having one set of cosine and sine functions, for each (j, k), we have two linearly independent sets of complex-valued functions, where $i = \sqrt{-1}$:

$$e^{i(jx+ky)} \text{ and } e^{i(jx-ky)}.$$

We define $a_{j,k}$ and $b_{j,k}$ to be the complex-valued coefficients corresponding to each of these functions.

The reconstructed conjugacy function and decay of coefficients for the two-dimensional torus is depicted in Fig. 2.9(a). The decay of coefficients shown in Fig. 2.9(b) shows $\sqrt{j^2+k^2}$ on the horizontal axis, and $|b_{j,k}|$ and $|c_{j,k}|$ on the vertical axis, where both of these coefficients are complex, meaning that $|\cdot|$ represents the modulus. Again here, the coefficients decay exponentially, though the decay of coefficients is considerably slower in two dimensions due to the added dimension. The data looks quite a lot more crowded in this case, since there are many different values of (j,k) such that the values of $\sqrt{j^2+k^2}$ are identical or very close. In addition, the two sets of coefficients $b_{j,k}$ and $c_{j,k}$ generally converge at different exponential rates. This is why there is a strange looking set consisting of an upper and a lower cloud of data in Fig. 2.9(b). While more information on the difference between these coefficients is gained by interactively viewing the data in three dimensions, we have not been able to find a satisfactory static flat projection of this data. We feel that in a still image, the data cloud shown conveys the maximum information.

We end this section by noting a few sources of error in the computation of Fourier coefficients. If the number of iterates N is too small, then we will not have sufficient coverage to get a good approximation of the coefficients, and the problem becomes more acute as the coefficient number $|k|$ grows. If our approximation of the rotation number is not good, then we cannot expect the approximations of our Fourier coefficients to be good either, and given an error in the rotation number, there will be an $k_{\max}$ such that the Fourier coefficients a_k with $|k| > k_{\max}$ cannot be approximated with any reasonable accuracy. A more subtle form of a

error comes from the fact that if the frequency we are trying to estimate is close to being comensurate with the rotation number, then we will get unexpectedly insufficient coverage of the space when performing iteration. This last type of error is present in both weighted and unweighted averaging techniques and is related to problems of small divisors. Rather than bog down our discussion here, we comment that this is an inherent problem, but it only comes up for the relatively rare and checkable condition of rotation numbers which are close to rational numbers with small denominators, and that does not apply to any of our rotation numbers. We intend to address this last type of error in more detail in another paper.

2.3 Concluding remarks

We have developed a straightforward but effective computational tool for quickly computing a large variety of quantities for quasiperiodic orbits. These quantities include rotation vectors, Fourier reconstruction of conjugacy maps, and in some cases Lyapunov exponents. The methods work well in one and higher dimensions. They are effective using both double and quadruple precision, though we have chosen to do most of our calculations in higher precision to show the full possibilities and quick convergence properties of our method.

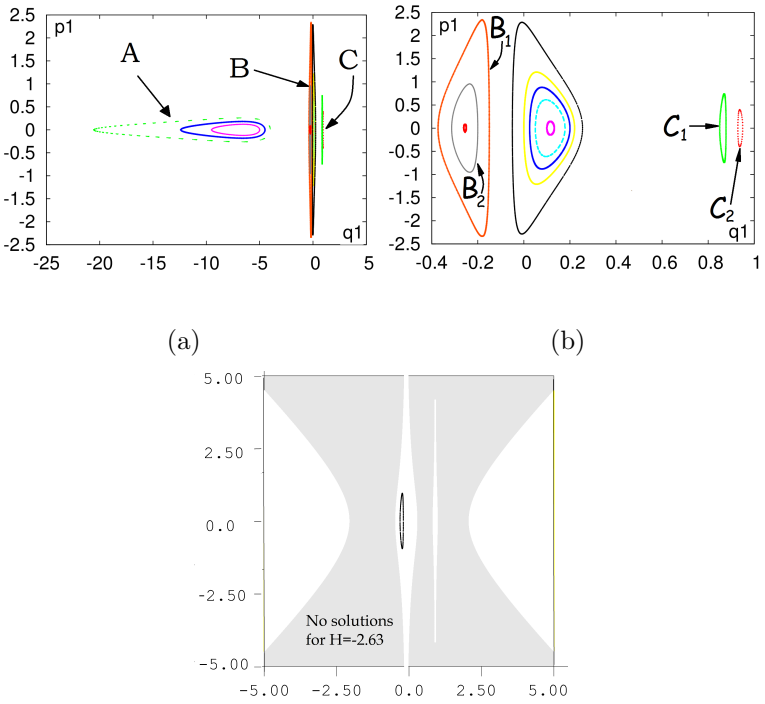

Figure 2.1: **Poincaré-return map for R3BP.** All three parts of this figure show a projection to the $q_1 - p_1$ plane of solutions to the R3BP in Eq. (2.1). The value of the Hamiltonian H for all the curves shown in the figures is the same and $H \approx -2.63$. Parts (a) and (b) show various quasiperiodic trajectories on the Poincaré section $q_2 = 0$. Note that the planet is fixed at the point $(-0.1, 0)$ and the moon at $(0.9, 0)$. Thus some trajectories orbit both the planet-moon system and some only orbit the planet or the moon. Each time the flow hits $q_2 = 0$ and $dq_2/dt > 0$, we plot (q_1, p_1). Each trajectory shown is a quasiperiodic curve. Part (c) shows in white all the initial points (q_1, p_1) on the Poincaré surface for which there exists a p_2 so that the Hamiltonian H at $(q_1, q_2 = 0, p_1, p_2)$ is the same as the one in parts (a) and (b). Part (c) also shows the trajectory which corresponds to the curve B_1 in (a) and (b).

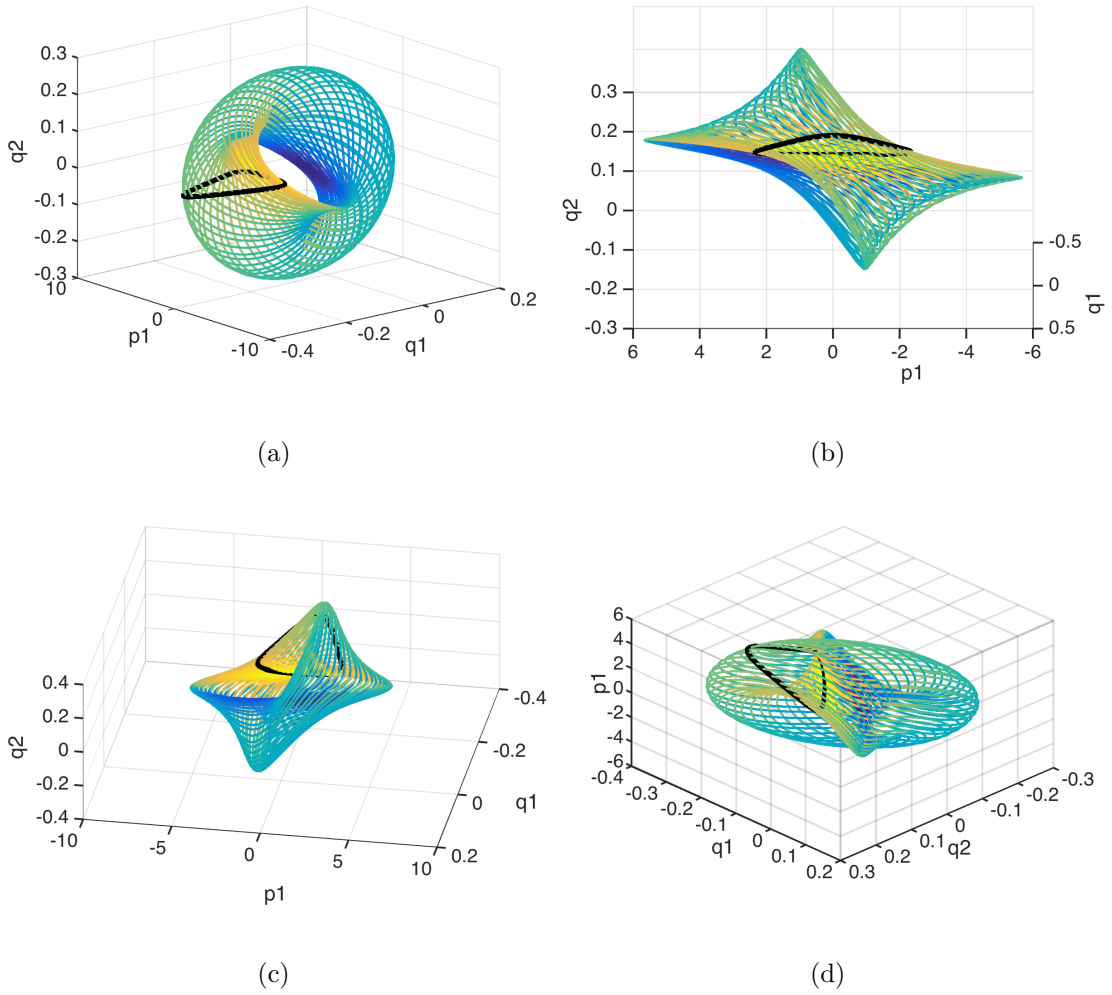

Figure 2.2: **Torus flow for the R3BP.** This trajectory is the solution of Eq. (2.1), shown as curve B_1 in Fig. 2.1. All four views are of the same two-dimensional quasiperiodic torus lying in $\mathbb{R}^4$. Each picture consists of the same trajectory spiraling densely on this torus. We require four different views of this torus because the embedding into three dimensions gives a highly non-intuitive images. The black curve is the set of values of the Poincaré return map with $q_2 = 0$ for this flow torus.

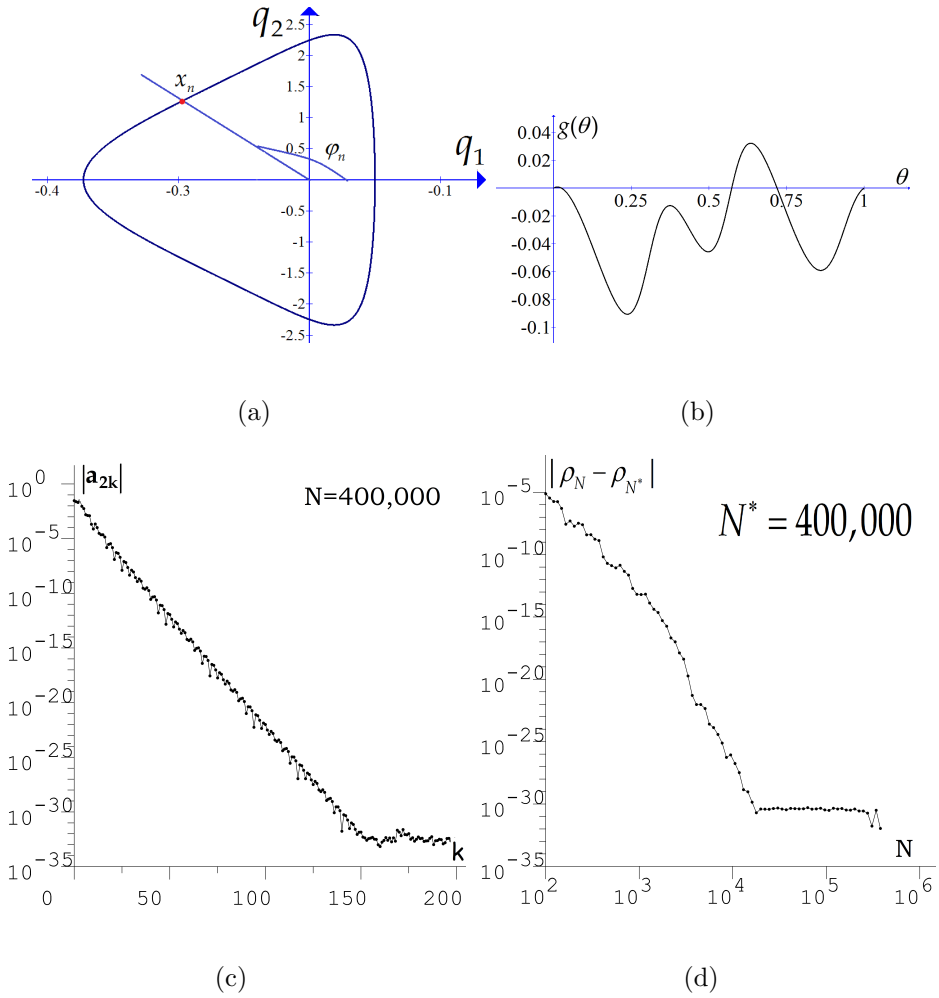

Figure 2.3: **Quasiperiodicity for the R3BP.** For the quasiperiodic curve B_1 in Fig. 2.1, part (a) shows how the invariant curve is parameterized by coordinates $\phi \in S^1 \equiv [0, 1)$. Part (b) depicts the periodic part $g(\theta)$ of the conjugacy between the quasiperiodic behavior and pure rotation by ρ. See Eq. (3.4) for a description of $g(\theta)$. Part (c) shows the norm of the Fourier coefficients of the conjugacy as a function of index. This exponential decay indicates that the conjugacy function is analytic, up to numerical precision. Part (d) shows the convergence rate of the error in the rotation number ρ_N as a function of the number of iterates N. The "error" is the difference $|\rho_N - \rho_{N^*}|$, where $N^* = 400,000$ is large enough so that ρ_N appears to have converged. The step size used for the 8^{th} order Runge-Kutta scheme is 10^{-5}.

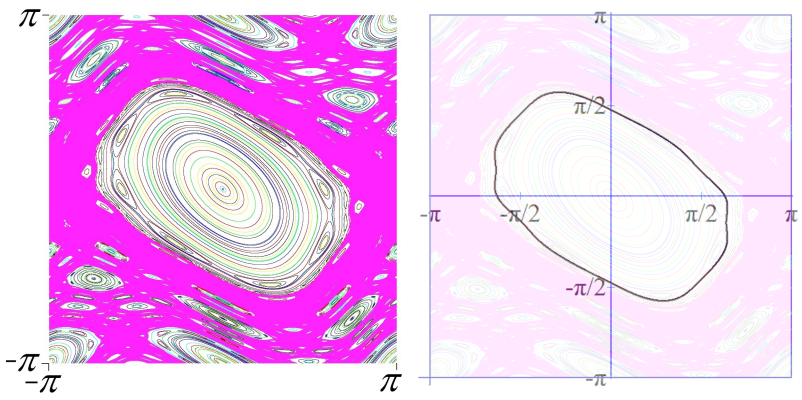

(a) (b)

Figure 2.4: **The standard map.** Part (a) shows a variety of orbits from different initial conditions in the standard map S_1 defined in Eq. (2.3) are plotted on the left. We can see both chaos (shaded area) and quasiperiodic orbits under this map. A single curve with quasiperiodic behavior is plotted in part (b). The orbit has initial conditions $(x, y) \approx (-0.607, 2.01)$. That is, if we restrict the map to this invariant curve, then it is topologically conjugate to a pure irrational rotation.

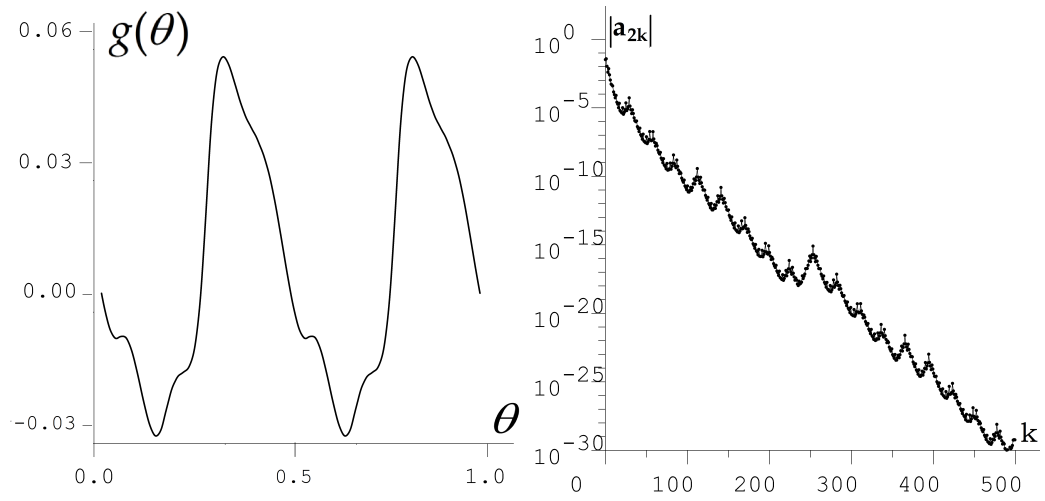

(a) (b)

Figure 2.5: **The standard map conjugacy.** This figure shown the analysis of the quasiperiodic trajectory in Fig. 2.4. Part (a) depicts the periodic part $g(\theta)$ of the conjugacy between the quasiperiodic behavior and pure rotation by ρ. See Eq. (3.4) for a description of $g(\theta)$. Part (b) shows the decay of the Fourier coefficients. Since the conjugacy is an odd function, the odd-numbered Fourier sine and cosine terms are zero and therefore have been omitted from the picture. The decay of the Fourier terms can be bounded from above be an exponential decay, which suggests that the conjugacy is analytic. An orbit of length $N = 10^7$ is used for these computations. A smaller orbit of length $N = 10^6$ does not lead to any significant changes.

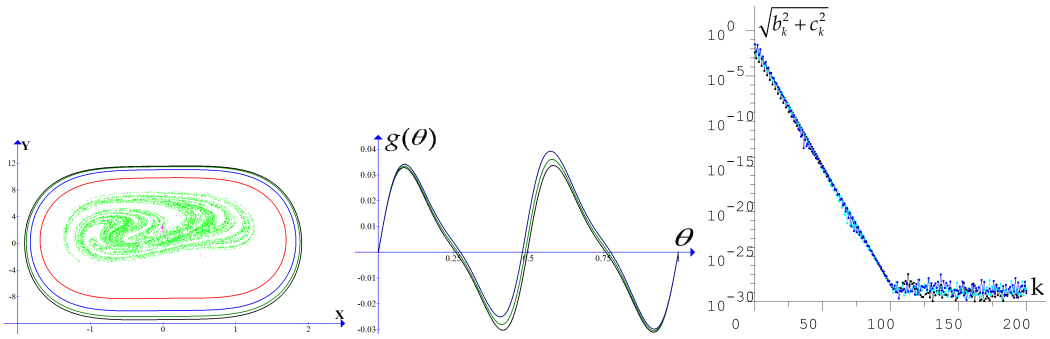

(a) (b) (c)

Figure 2.6: **Forced van der Pol oscillator.** Part (a) shows attracting orbits for a number of different forcing values F for the stroboscopic map of the van der Pol flow given in Eq. (2.4). The plot depicts points $(X, Y) = (x(t_k), x'(t_k))$, where $t_k = 2k\pi/0.83, k = 0, 1, 2, \ldots$. The chaotic orbit lying inside the cycles corresponds to $F = 45.0$. There are stable quasiperiodic orbits shown as curves, which from outermost to innermost correspond to $F = 5.0$, 15.0, 25.0 and 35.0 respectively. Part (b) is the periodic part $g(\theta)$ of the conjugacy (Equation (3.4)) to a pure rotation, for $F = 5.0, 15.0$ and 25.0. Part (c) gives a strong indication of the analyticity of the conjugacy to a pure rotation by studying the decay of the norm of the k^{th} Fourier coefficients with respect to k. The decay is exponentially fast up to the resolution of the numerics.

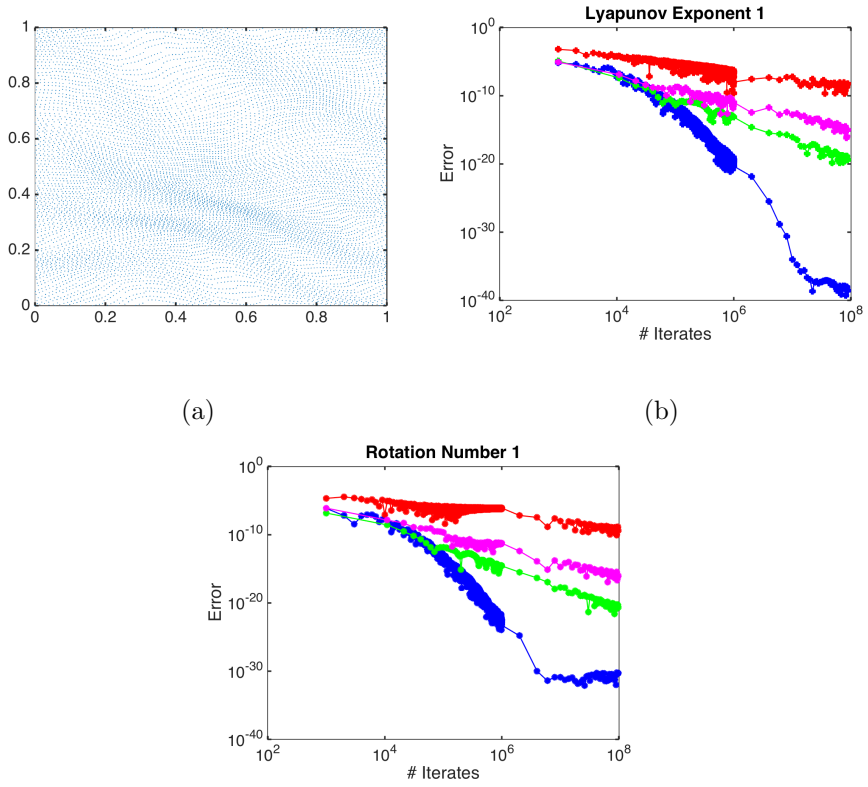

Figure 2.7: **Different choices of w for WB_N.** Part (a) shows an orbit of length 10^4 for the two-dimensional quasiperiodic torus map. The orbit appears to be dense, which is consistent with quasiperiodicity. The two Lyapunov exponents of the orbit are computed using WB_N and we find them to be 0 up to our numerical accuracy. The convergence of this computation for one of the two Lyapunov exponents is shown in blue in (b). The highest to lowest curves show the convergence rates resp. for the first three weighting functions given in Eq. (2.5), resp. in red, magenta, green, and blue. Part (c) shows the convergence rate for the first rotation number for the four different weighting functions, with the same color scheme.

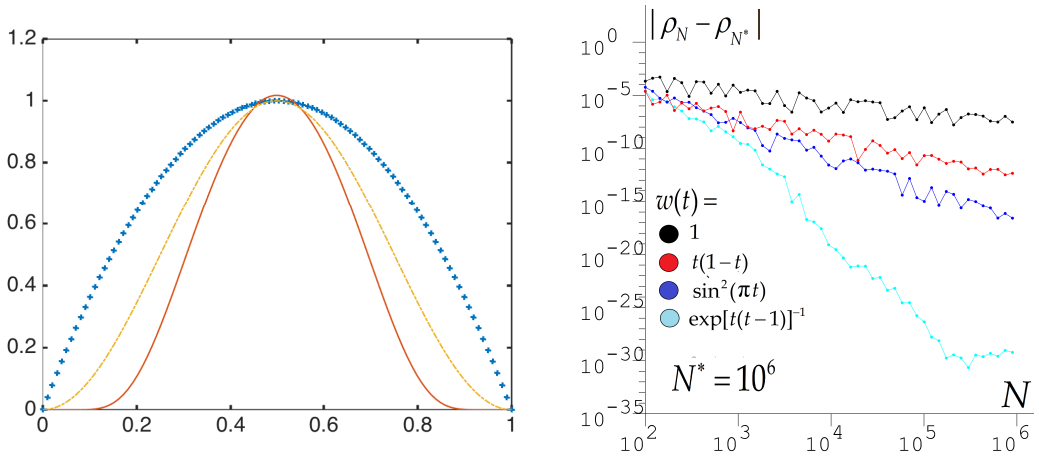

(a) (b)

Figure 2.8: **Rate of convergence for different weight functions**. Part (a) is a plot of three non-constant weighting functions from Eq. (2.5) and below w_{quad} (top), $w_{\sin^2}$ (second), $w_{\exp}$ (lowest). Since only the shape matters, they have been rescaled so that each has a peak of approximately 1.0. For a given w and a given number of iterates N, the rotation number $\hat{\rho}$ approximation is calculated for B_1 of the R3BP, the error of the calculation is the difference $|\rho - \hat{\rho}|$. Part (b) shows the convergence rate of this error as a function of N. The exponential weight function w_{exp} allows WB_N to reach a limit by $N = 50,000$ after which it fluctuates by approximately 10^{-30}.

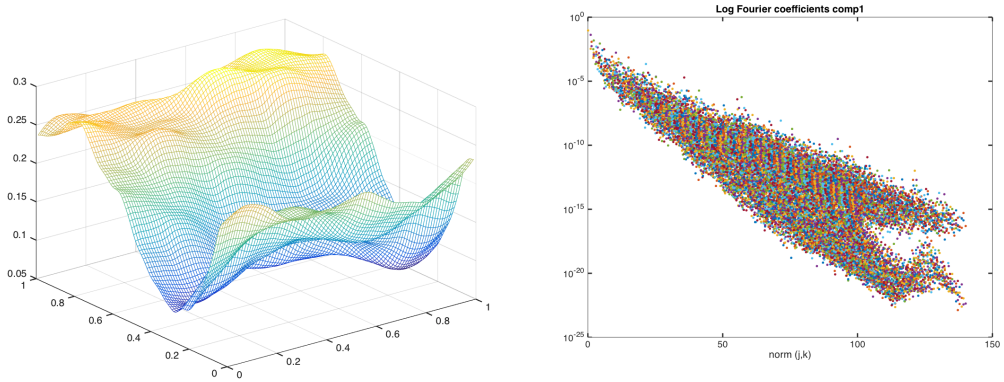

(a) (b)

Figure 2.9: **Conjugacy for the torus.** Part (a) depicts the reconstruction of the periodic part g (see Equation 3.4) of the first component of the conjugacy function for the torus map. The surface is colored by height. The second conjugacy function is similar but not depicted here. Part (b) shows the decay of the Fourier coefficients for this component of the conjugacy function on the log-linear scale.

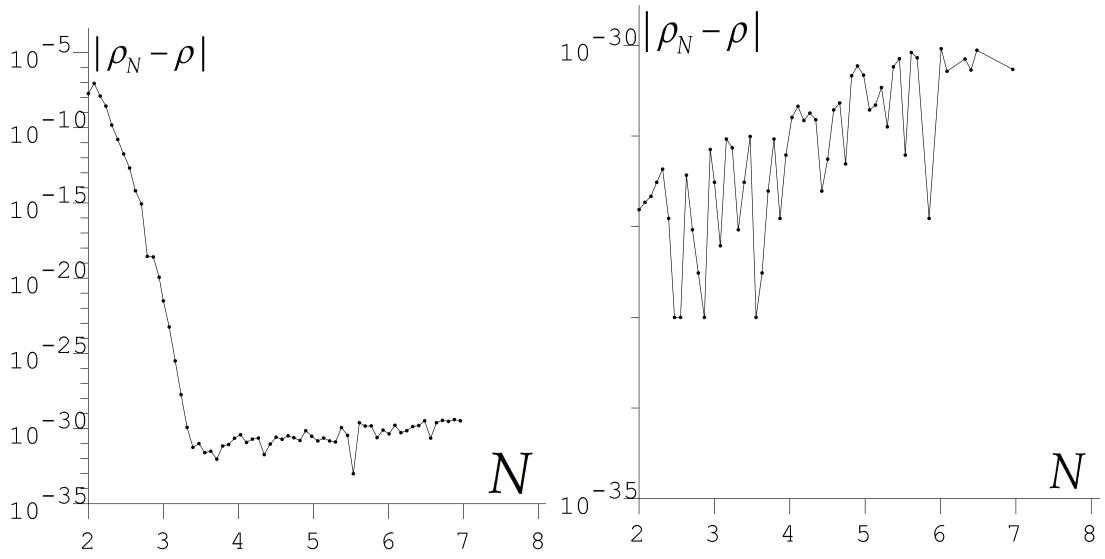

(a) (b)

Figure 2.10: **Testing how well the $\mathbf{WB}_N$ method can determine the rotation number.** Part (a) shows the convergence in the calculation of a known rotation number $\rho = \sqrt{2}-1$, for the trajectory $(\phi_n) = (n\rho \mod 1)$ in Eq. (2.6), with $\alpha = 0.1$, $\beta = 0.2$, and $\rho = \sqrt{2}-1$. The error quickly drops to the limit of numerical precision and then increases slowly as N increases. This increase in the error is apparently due to accumulated round-off error. Part (b) shows the increasing round-off error in the rotation number for the trivial case ($\alpha = \beta = 0$), and again the error grows after passing a minimum as N increases.

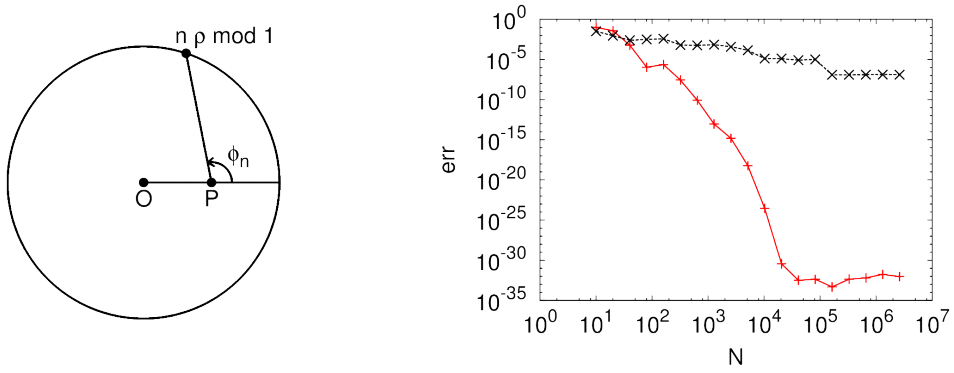

(a) (b)

Figure 2.11: **The error in the computed value of rotation number when the rotation number is known.** Part (a) shows the geometric configuration of the problem, with a constant rotation vector $\rho = \sqrt{2} - 1$ about the origin. The trajectory is $(n\rho \pmod 1)$, but the observer measures the angle ϕ as seen from its perspective at P, which is midway between the center of the circle, O, and the circle itself. Part (b) shows the convergence in the rotation number calculation using the simple Birkhoff average (upper graph) and the weighted Birkhoff average WB_N (lower graph), for the trajectory (ϕ_n) described in (a). The error from the rigorous value $\sqrt{2} - 1$ is calculated for several values of number N. The weighted Birkhoff average $\mathrm{WB}_n(\phi_{n+1} - \phi_n)$ reaches 32-digit precision by $N = 30,000$.

Chapter 3: An open set of torus-maps conjugate to skew products

Abstract. Skew-product maps on the torus, which are of the form

$$(x_{n+1}, y_{n+1}) = (mx_n, g(x_n, y_n)) \mod 1,$$

are relatively easy to analyze and include a variety of interesting dynamical systems. Notice that the dynamics in the X coordinate is $x_{n+1} = mx_n \mod 1$. We present sufficient conditions for a torus map to be conjugate to a skew-product map. The set of maps which satisfy these conditions are open in the C^1 topology.

3.1 Introduction

Recall that the torus $\mathbb{T}^2$ be the product $S^1 \times S^1$. In this paper, we are primarily interested in a class of maps on the torus, called "skew product maps", which are of the form

$$F_0(x, y) = (mx,\ cx + dy + G_0(x, y)) \mod 1 \text{ (in each coordinate).} \tag{3.1}$$

where m, c, d are integers, with $|m| > 1$, and $G_0 : \mathbb{R}^2 \to \mathbb{R}$ is continuous and $\mathbb{Z}$-*periodic* in x and y. [A map $h : \mathbb{R}^2 \to \mathbb{R}$ is said to be $\mathbb{Z}$ **-periodic** in x and y if for every pair of integers n_1 and n_2, $h(x + n_1, y + n_2) = h(x, y)$].

Note that the dynamics in the X coordinate is an expanding circle map

$$x_{n+1} = mx_n \mod 1. \tag{3.2}$$

In other words, skew-product maps have the this circle map as a "factor" map. See [38] for a nice overview of skew-product maps and their treatment as random maps or non-autonomous differential equations. In [39], Kleptsyn and Nalskii, using the setting of stochastic circle diffeomorphisms, prove the important result that the orbits of almost every (with respect to a certain measure) pair of initial conditions on a fiber are asymptotic. [40] looks at skew products with expanding circle maps and proved the occurrence of topological mixing for an open set of maps. The authors of [41] studied the mechanism by which chaos occurs on a certain class of skew-product maps. Other features, like the measure of the non-wandering set, and perturbation of skew product systems, has been in investigated in [42] and [43] respectively. Our main theorem describes a large family of torus maps which are topologically conjugate to maps of the form (3.1) and hence, have many of the properties of skew-product maps.

Lifts of torus maps. For any continuous torus map $F : \mathbb{T}^2 \to \mathbb{T}^2$, there is a **lift**, a map $\hat{F} : \mathbb{R}^2 \to \mathbb{R}^2$ for which

$$F(z) = \hat{F}(z) \mod 1 \tag{3.3}$$

It follows that there is a 2×2 integer-valued matrix M that we call the **homology matrix** of F and a bounded function $G : \mathbb{R}^2 \to \mathbb{R}^2$ such that

$$\hat{F}(z) = Mz + G(z). \tag{3.4}$$

Note that G is $\mathbb{Z}$-periodic. We call G the **periodic part** of F. Because of the $\mathbb{Z}$-periodicity, $G \mod 1$ can also be viewed as a map from $\mathbb{T}^2 \to \mathbb{T}^2$. Note that if for all $z \in \mathbb{T}^2, |\det M(z)| = m > 0$ and if $|\det dF| > 0$, then F is an m-to-1 of the torus, so every point has exactly m pre-images under F.

The following theorem shows that there is a set of torus-maps, open in the C^1 topology, that are conjugate to skew product maps.

Theorem 3.1.1 *Let M be a 2×2 integer-entried matrix satisfying the following assumption.*

$(A1)$ M has a eigenvalue m for which $|m| = |\det M| > 1$. (Hence the other eigenvalue has absolute value 1.)

Then there is a constant $\delta = \delta(M) > 0$ such that if $G : \mathbb{R}^2 \to \mathbb{R}^2$ is a C^1, $\mathbb{Z}$-periodic map satisfying $\|G\|_{C^1} < \delta$, then the torus map given by $F(z) = Mz + G(z) \mod 1$ is conjugate to a map of the form (3.1).

For example if M is symmetric, setting $\delta = 0.5(|m| - 1)$ suffices. **From here onward, we will assume m is positive** – to simplify the notation. The case where m is negative takes only minor modifications.

Our discovery of this theorem began when we observed a striking fact, that if a the homology matrix of continuous map $F : \mathbb{T}^2 \to \mathbb{T}^2$ satisfies $(A1)$, then F has $x \mapsto mx \mod 1$ as a factor map. That is, there is a continuous function Φ that maps $\mathbb{T}^2$ onto S^1 and for all integers $k \geq 0$

$$\Phi(F^k(z)) = m^k \Phi(z).$$

We will prove Theorem 3.1.1 as a corollary to the more general Proposition

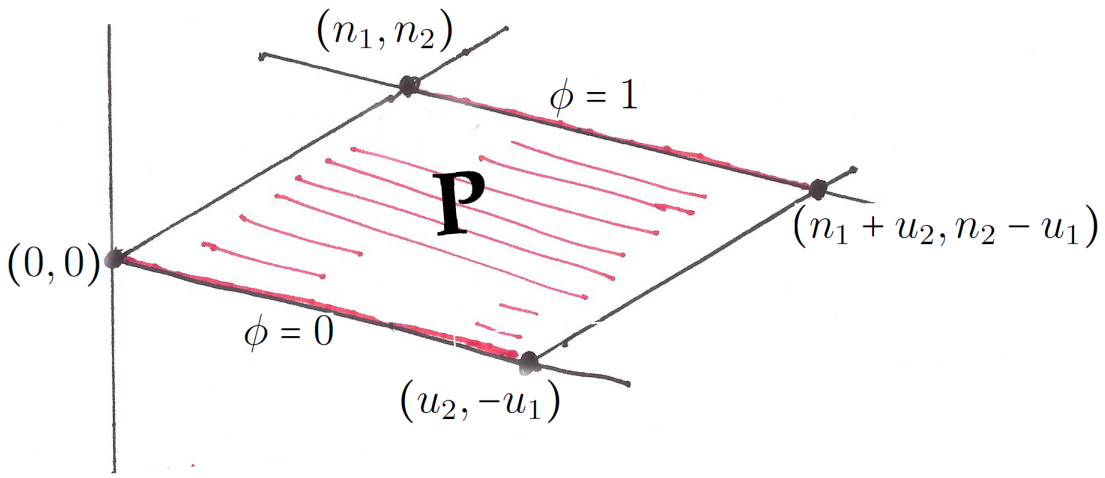

Figure 3.1: **A tiling of the plane.** The vectors (n_1, n_2) and v_m^L, the left eigenvector of the homology matrix M corresponding to eigenvalue m, are chosen with integer coordinates in such a way that $n_1u_1 + n_2u_2 = 1$ where $(u_1, u_2) = v_m^L$, another vector with integer coordinates. The region $P/\mathbb{Z}^2$ is a one-to-one representation of $\mathbb{T}^2$. Note that $\phi(z) := v_m^L \cdot z$ attains a value of 0 on vectors on the line $\{tv_1 = t(u_2, -u_1) : t \in \mathbb{R}\}$ and a value of 1 on the line $\{(n_1, n_2) + t(u_2, -u_1) : t \in \mathbb{R}\}$. These two lines are parallel to the eigenvector v_1 and form two opposite edge of P. ϕ is constant along every line parallel to v_1.

3.1.2 stated later in this section. To state that result, we will first introduce a notion called "invariant, expanding cones".

Invariant, expanding cones. Much of what we do can be immediately extended to higher dimensions, but here we stay with $\mathbb{T}^2$. The property of "dominating expansion" for example can be defined on any manifold, but here, we will define it on $\mathbb{T}^2$. Let e^1, e^2 be two nowhere parallel vector fields on $\mathbb{T}^2$. A tangent vector v at a point $z \in \mathbb{T}^2$ can be represented as $v = (a, b)_e := ae^1(z) + be^2(z)$. Let $v' = dF(z)v$ and let the representation of v' in terms of the vector fields $e^1(F(z)), e^2(F(z))$ be $(a', b')_e$. We say (e_1, e_2) is an **expanding cone structure** if there are constants $K > 1$ and $\alpha > 0$ such that the following are satisfied for every point z:

(i) If $|b| \leq \alpha|a|$, then $|b'| \leq \alpha|a'|$, and

(ii) if $|b| \leq \alpha|a|$, then $|a'| \geq K|a|$.

We can rephrase that as follows. At every point $z \in \mathbb{T}^2$, the $\boldsymbol{\alpha}$**-cone**, denoted $\mathcal{C}_\alpha(z)$ is the set of vectors $(a, b)_e$ (writing in (e_1, e_2) coordinates) in the tangent space at z such that $|b| \leq \alpha|a|$. We say F has an **expanding cone-structure** with respect to (e^1, e^2) if e^1 and e^2 are nowhere zero or parallel, and for some $\alpha > 0$ and some $K > 1$, $\mathcal{C}_\alpha(F(z)) \subset DF(z)(\mathcal{C}_\alpha(z))$ and if $(a', b')_e = DF(z)(a, b)_e$, then $|a'| > K||a|$. Note that by rescaling the vector field e_1, we can make $\alpha = 1$ so without loss of generality, we assume $\alpha = 1$ and omit it from our notation. See Figure 3.2 for a schematic diagram.

Invariant cone systems are in particular, present in hyperbolic systems, as also

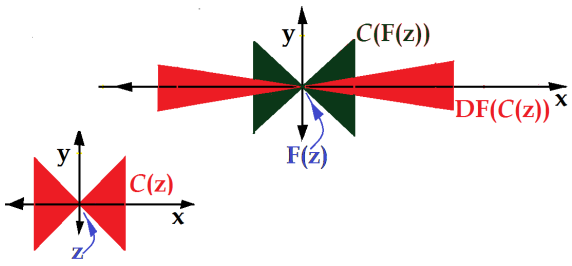

Figure 3.2: **Invariant, expanding cones.** This figure illustrates an invariant, expanding cone structure for a torus map $F : \mathbb{T}^2 \to \mathbb{T}^2$. For the sake of simplicity, e^1 and e^2 have been taken to be the unit vector fields along the X and Y directions of the torus respectively, and $\alpha = 1$. The triangles drawn in red and green lie in the tangent spaces at z and $F(z)$ respectively, and pictorially represent part of the cones containing the vectors $\{(u, v) \mid \|v\| \leq \|u\| \leq 1\}$ in their respective spaces. Any vector within the red cone $\mathcal{C}(z)$ at z is mapped into the green cone $\mathcal{C}(F(z))$ at $F(z)$ under the action of $DF(z)$ and also stretched by a factor of at least $K > 1$.

in various weaker forms of hyperbolicity like dominated cones [44] and dominated splittings [45]. Note that in non-hyperbolic systems, the tangent subspaces spanned by e^1 and e^2 are not invariant. Most of techniques used to prove properties in these different versions of hyperbolicity cannot be extended to the broader class of maps we are interested in, like maps which are either not diffeomorphisms or without a continuous invariant splitting of the tangent space.

Recall that two dynamical systems are said to be **conjugate** if there is a change of coordinates that is continuous and with a continuous inverse, transforming one dynamical system to the other. This change of variables is called a **conjugacy**. Our main results assume that the map F has a non-singular Jacobian at every point.

Such a map is called **local diffeomorphism**, i.e., every point has a neighborhood in which the map is a diffeomorphism. Proposition 3.1.2 below establishes some easily verifiable and satisfiable conditions under which a torus map is conjugate to F_0 in (3.1). Notice that F in Proposition 3.1.2 is not invertible but an m-fold covering map.

Theorem 3.1.2 *Let $F : \mathbb{T}^2 \to \mathbb{T}^2$ be C^1 that satisfies the following.*

(A1) The homology matrix M has a eigenvalue m for which $|m| = |\det M| > 1$. (Hence the other eigenvalue has absolute value 1.); and

(A2) there is an expanding cone-structure [with respect to a pair of vector fields denoted e^1, e^2].

(A3)Assume DF is invertible,

Then F is conjugate to a map of the form (3.1).

Proposition 3.1.2 is proved in Section 3.3. Theorem 3.1.1 is proved in Section 3.3.2.

3.2 Construction of the factor map

Outline of the proof of the Proposition 3.1.2 To construct the conjugacy claimed in Proposition 3.1.2, in Section 3.2.1, we will first construct a factor map $\hat{\Phi} : \mathbb{R}^2 \to \mathbb{R}$ satisfying $\hat{\Phi}(\hat{F}(z)) = m\hat{\Phi}(z)$, where $\hat{\boldsymbol{F}} : \mathbb{R}^{\mathbf{2}} \to \mathbb{R}^{\mathbf{2}}$ is the lift of F and is given by Eq. 3.4 without taking mod 1 in each coordinate. Finally, in Lemma 3.3.2 we will complete the construction of the conjugacy H. It turns out that H is a continuous map but not differentiable. In Section 3.3.1 we will prove that however,

$H \circ F \circ H^{-1}$ is differentiable with respect to the Y-variable. Before the construction, we will make use of the assumptions made on the homology matrix M of F.

3.2.1 The map $\hat{\Phi}$.

The heart of the proof of Proposition 3.1.2 is the following proposition, which says that the torus can be factored into the expanding circle map (3.2).

Proposition 3.2.1 (Existence of a factor map) *Given the assumptions and notation of Proposition 3.1.2, there exists a continuous map* $\hat{\Phi} : \mathbb{R}^2 \to \mathbb{R}$ *such that*

(i) for each $z \in \mathbb{R}^2$ *and each* $k \in \mathbb{N}$, $\hat{\Phi}(\hat{F}^k(z)) = m^k \hat{\Phi}(z)$,

(ii) for each $z \in \mathbb{R}^2$ *and each pair* n_1, n_2 *of integers,* $\hat{\Phi}(z + (n_1, n_2)) - \hat{\Phi}(z)$ *is an integer;*

(iii) there exist integers n_1, n_2 *such that* $\hat{\Phi}((n_1, n_2)) - \hat{\Phi}((0, 0)) = 1$.

A map $\hat{\Phi} : \mathbb{R}^2 \to \mathbb{R}$ will be called an **m-factor map** is it satisfies the properties (i) and (ii) concluded in Proposition 3.2.1. Proposition 3.2.1 therefore states that there is an m-factor map $\hat{\Phi}$.

Proof Write $M = \begin{pmatrix} a & b \\ c & d \end{pmatrix}$, where a, b, c and d integers. By assumption, one of the eigenvalues is 1. Since the product of the eigenvalues is $\det M$, the other eigenvalue is $ad - bc = m > 1$. Let v_1 and v_m be the respective eigenvectors, scaled so that their coordinates are integers that as small as possible; hence, the entries of each of the vectors v_1, and v_2, are "**reduced**" to lowest terms so that the only common factor of its coordinates is 1; that is, they are relatively prime.

If one coordinate is 0, the other has absolute value 1. The sign of the vector is of no importance. Let $v_1 = (u_2, -u_1)$ be a reduced vectors. Then $v_m^L = (u_1, u_2)$ is a (reduced) integer-coordinate vector that is orthogonal to v_1 and also a left eigenvector of M with eigenvalue m, i.e.,

$$(v_m^L)^T M = m(v_m^L)^T. \tag{3.5}$$

It follows from an application of the Euclidean division algorithm that there are integers n_1, n_2 such that

$$n_1 u_1 + n_2 u_2 = 1.$$

Let $\phi : \mathbb{R}^2 \to \mathbb{R}$ be defined as $\phi(z) = v_m^L \cdot z$. Note that ϕ is a linear map and

$$|\phi(z)| \leq \|v_m^L\| \|z\| \tag{3.6}$$

For example, if $a, d \neq 1$, then $v_1 = (b,\ 1-a)$, $v_m = (b,\ m-a)$, $v_m^L = (a-1, b)$, $\phi(x, y) = (a-1)x + by$. $\|\phi\| = \|v_m^L\| = \sqrt{(a-1)^2 + b^2}$.

$\hat{\Phi}$ is defined as follows.

$$\hat{\Phi}(x, y) = \lim_{n \to \infty} m^{-n} \phi(\hat{F}^n(x, y)). \tag{3.7}$$

$\hat{\Phi}$ is continuous and well defined. To prove that (3.7) converges, we will use the following equation which is a consequence of Eq. 3.5.

$$m^{-n} \phi \circ \hat{F}^n(z) = v_m^L \cdot z + \sum_{k=1,\ldots,n} m^{-k} v_m^L \cdot G \circ \hat{F}^{k-1}(z) \tag{3.8}$$

Equations 3.7 and 3.8 enable us to express $\hat{\Phi}$ as an infinite series of operators.

$$\hat{\Phi}(z) = \lim_{n \in \mathbb{N}} m^{-n} \phi \circ \hat{F}^n(z) = v_m^L \cdot z + \sum_{k=1,2,\ldots,} m^{-k} v_m^L \cdot G \circ \hat{F}^{k-1}(z) \tag{3.9}$$

Since G is $\mathbb{Z}$-periodic, it is uniformly bounded. Since $m > 1$ and each of the terms $v_m^L \cdot G \circ \hat{F}^{k-1}(z)$ are bounded by Eq. 3.6, the limit $\hat{\Phi}(z)$ exists as an uniform limit, by the Weierstrass M-test (see [46]). Since each finite sum is a continuous function, by the Uniform Limit Theorem (see [46]), $\hat{\Phi}(z)$ is also continuous.

Let $\|G\|_{C^0}$ denote the C^0-norm of G, defined as $\sup_{z\in\mathbb{R}^2}\|G(z)\|$. The following inequalities follows from the definition of $\hat{\Phi}$ and will be important for making conclusions about the fibers of $\hat{\Phi}$.

$$\text{For every } z \in \mathbb{R}^2, \quad |\hat{\Phi}(z) - \phi(z)| \leq \frac{1}{m-1}\|v_m^L\|\|G\|_{C^0} \tag{3.10}$$

$$\text{For every } z_1, z_2 \in \mathbb{R}^2, \ ||\hat{\Phi}(z_1) - \hat{\Phi}(z_2)| - |\phi(z_1) - \phi(z_2)|| \leq \frac{2}{m-1}\|v_m^L\|\|G\|_{C^0} \tag{3.11}$$

$\hat{\Phi}$ is onto. We will now prove that for every $x_0 \in \mathbb{R}$ and every line $\boldsymbol{L}$ in $\mathbb{R}^2$ parallel to v_m^L, there exists a point (x, y) on the line for which $\hat{\Phi}(x, y) = x_0$. In particular, $\hat{\Phi}$ is onto .

To see this, let the contrary to this statement be true. Since $\hat{\Phi}$ is continuous, the image under $\hat{\Phi}$ of this line is some half open interval, which without loss of generality, is of the form $(x_{\inf}, \infty)$, where $x_0 < x_{\inf}$. Now chose some point on the line z_0 on the line for which $\hat{\Phi}(z_0) = x_{\inf} + 1$. By Equation 3.10,

$$\phi(z_0) < \hat{\Phi}(z_0) + \frac{1}{m-1}\|v_m^L\|\|G\|_{C^0} = x_{\inf} + 1 + \frac{1}{m-1}\|v_m^L\|\|G\|_{C^0}.$$

For every $l > 0$, $z_0 - lv_m^L \in L$. Note that

$$\phi(z_0 - lv_m^L) = \phi(z_0) - l\|v_m^L\|^2 < x_{\inf} + 1 + \frac{1}{m-1}\|v_m^L\|\|G\|_{C^0} - l\|v_m^L\|^2.$$

By assumption, $\hat{\Phi}(z_0 - lv_m^L) > x_{\inf}$. Therefore, we must have,

$$\hat{\Phi}(z_0 - Lv_m^L) - \phi(z_0 - Lv_m^L) > x_{\inf} - [x_{\inf} + 1 + \frac{1}{m-1}\|v_m^L\|\|G\|_{C^0} - l\|v_m^L\|^2] = -1 - \frac{1}{m-1}\|v_m^L\|\|G\|_{C^0} + l\|$$

This equation is true for every $l > 0$. If l is chosen large enough to satisfy $l\|v_m^L\|^2 > 1 + \frac{2}{m-1}\|v_m^L\|\|G\|_{C^0}$, it leads to a contradiction of Equation 3.10. Therefore, our assumption of the contrary was false. ∎

$\hat{\mathbf{\Phi}}$ is a factor map. Note that $\hat{\Phi} \circ \hat{F}(z) = \lim_{n\to\infty} \frac{\phi(\hat{F}^{n+1}(z))}{m^n} = \lim_{n\to\infty} \frac{m\phi(\hat{F}^{n+1}(z))}{m^{n+1}} = m \lim_{n\to\infty} \frac{\phi(\hat{F}^{n+1}(z)}{m^{n+1}} = m\hat{\Phi}(x,y)$. Therefore, we have proved the following.

$$\text{For every } z \in \mathbb{R}^2, \hat{\Phi} \circ \hat{F}(z) = m \times \hat{\Phi}(z) \ (\mod 1) \tag{3.12}$$

We will now prove that $\hat{\Phi} : \mathbb{R}^2 \to \mathbb{R}$ factors into a map $\mathbf{\Phi}$: $\mathbb{T}^2 \to S^1$. To see this first recall that G defined in Equation 3.4 is $\mathbb{Z}$-periodic, therefore for every $\vec{k} \in \mathbb{Z}^2$, every $z \in \mathbb{R}^2$,

$$\hat{F}(z + \vec{k}) = M(z + \vec{k}) + G(z + \vec{k}) = Mz + M\vec{k} + G(z) = M\vec{k} + G(z)$$

Therefore, since G is $\mathbb{Z}$-periodic, for every $j = 0, 1, 2, \ldots$,

$$G(\hat{F}^j(z + \vec{k})) = G(M^j\vec{k} + \hat{F}^j(z)) = G(\hat{F}^j(z)).$$

Therefore, by Equation 3.9

$$\begin{aligned}
\hat{\Phi}(z + \vec{k}) &= \phi(z + \vec{k}) + \sum_{j=1,2,\ldots,} m^{-j}\phi(f(\hat{F}^{j-1}(z + \vec{k}))) \\
&= \phi(z) + \phi(\vec{k}) + \sum_{j=1,2,\ldots,} m^{-j}\phi(f(\hat{F}^{j-1}(z))) \\
&= \hat{\Phi}(z) + \phi(\vec{k})
\end{aligned}$$

Note that $\phi(\vec{k}) \in \mathbb{Z}$. Therefore, $\hat{\Phi}(z + \vec{k}) = \hat{\Phi}(z) \mod 1$. This proves the claim.

The map on $\mathbb{R}$ sending x to mx factors via the map $proj : \mathbb{R} \to S^1$ into the map $x \mapsto mx \mod 1$ on the circle S^1, i.e.,

$$\text{For every } x \in \mathbb{R},\ m \times proj(x) = proj(mx) \ (\mod 1) \tag{3.13}$$

Equations (3.12) and (3.13) combine together to give the following.

$$\text{For every } z \in \mathbb{T}^2,\ \Phi(F(z)) = m\Phi(z) \mod 1. \quad \blacksquare \tag{3.14}$$

3.3 Proof of Proposition 3.1.2

Definition [conic curve]. A differentiable curve in $\mathbb{R}^2$ or in $\mathbb{T}^2$ is said to be a **conic curve** if its tangent at every point lies inside the expanding cone at that point on the manifold. Note that the image of a conic-curve under the map is again a conic curve, with an expansion in length by a factor of at least K.

Proposition 3.3.1 *The fibers of Φ, which are the sets $\Phi^{-1}(\theta_0)$ for some $\theta_0 \in S^1$, are topological circles.*

Proof To prove this, we will first prove the analogous statement for $\hat{\Phi}$, i.e., for every $x_0 \in \mathbb{R}$, $\hat{\Phi}^{-1}(x_0)$ is an open curve. We will then use the fact that Φ is a factor of $\hat{\Phi}$ to prove the claim of the theorem. The direction E^u on $\mathbb{T}^2$ lifts uniquely under the quotient map $q : \mathbb{R}^2 \to \mathbb{T}^2$ to a direction which will also be denoted as E^u. E^u partitions $\mathbb{R}^2$ into a collection of parallel lines.

Claim. Two distinct points in $\hat{\Phi}^{-1}(x_0)$ cannot be connected by a conic curve. To see this, first assume the contrary. So there are distinct points $z_1, z_2 \in \hat{\Phi}^{-1}(x_0)$ and γ is a conic curve joining z_1 and z_2. Then for every $n \in \mathbb{N}$, $F^n(\gamma)$ is again a conic curve whose endpoints are $F^n(z_1)$ and $F^n(z_2)$, both lying in the fiber $\hat{\Phi}^{-1}(m^n x_0)$ by Equation 3.14. By Equation 3.11, we can conclude that $|\phi(F^n z_1 - F^n z_2)| \leq \frac{2}{m-1}\|v_m^L\|\|G\|_{C^0}$. Let l be the length of γ. Then the length of $F^n(\gamma)$ is at least

$K^n\gamma$. Note that the unit eigen direction v_1 cannot lie inside the expanding cone. Therefore, there is a uniform constant $\tau > 0$ such that for any conic curve of length l joining two points A and B,

$$|\phi(A - B)| = v_m^L \cdot (A - B) \geq \|v_m^L\|\tau l.$$

Therefore,

$$\frac{2}{m-1}\|v_m^L\|\|G\|_{C^0} \geq \phi(F^n z_1 - F^n z_2)| \geq \|v_m^L\| l k^n \tau.$$

This inequality holds for every $n = 1, 2, \ldots$. But while the left hand side remains bounded, the right hand side diverges to ∞ as $n \to \infty$. This leads to a contradiction, so our assumption of the contrary was false.

claim $\hat{\Phi}^{-1}(x_0)$ is a curve. To see this, first note that any straight line parallel to v_m^L is a conic curve. Therefore $\hat{\Phi}^{-1}(x_0)$ intersect every line parallel to v_m^L. This combined with the above claim implies that $\hat{\Phi}^{-1}(x_0)$ intersect every line parallel to v_m^L at a unique point. Since $\hat{\Phi}$ is continuous, $\hat{\Phi}^{-1}(x_0)$ is a closed set. Therefore, $\hat{\Phi}^{-1}(x_0)$ is a continuous curve.

Let $P \subset \mathbb{R}^2$ be the parallelogram with vertices $(0, 0)$, $(u_2, -u_1)$, (n_1, n_2) and $(n_1 + u_2, n_2 - u_1)$. Moreover, the area of P is 1 and contains no point with integral coordinates in its interior. See Figure 3.1 for an illustration. Note that $P/\mathbb{Z}^2$ is a one-to-one representation of $\mathbb{T}^2$.

claim $\Phi^{-1}(\theta_0)$ is a closed curve. Let $x_0 \in \mathbb{R}$ be some lift of θ_0 under the projection map $proj$. Then $\Phi^{-1}(\theta_0)$ is the image under $proj$ of the sets $\hat{\Phi}^{-1}(x_0 + n)$, where n ranges over all integers. However, only one of these curves intersect the interior of the region P, which is mapped homeomorphically under $proj$ onto $\mathbb{T}^2$, so

the image is also a curve. Using the dominated cone structure and the periodicity of $\hat{\Phi}$, it can be proved that the images under *proj* of all the curves $\hat{\Phi}^{-1}(x_0 + n)$ is this single closed curve. ∎

We are now ready to construct the conjugacy.

Lemma 3.3.2 *Let $H : \mathbb{T}^2 \to \mathbb{T}^2$ be defined as $H(x, y) = (\Phi(x, y), (n_2, -n_1) \cdot (x, y))$. Then H is a homeomorphism and $H \circ F \circ H^{-1}$ is of the form given in Equation 3.1.*

Proof Since Φ is continuous, H is continuous. We will first prove that H is invertible and then show that, in fact it is a homeomorphism. Finally, we will show that H gives the desired conjugacy. We begin with the observation that $\phi(z) := v_m^L \cdot z$ attains a value of 0 on vectors on the line $\{tv_1 = t(u_2, -u_1) : t \in \mathbb{R}\}$ and a value of 1 on the line $\{(n_1, n_2) + t(u_2, -u_1) : t \in \mathbb{R}\}$. These two lines are parallel to the vector v_1 and form two opposite edge of P. ϕ is constant along every line parallel to v_1. Also, for every $x_0 \in \mathbb{R}$, the interior of the region P intersects exactly one of the curves $\hat{\Phi}^{-1}(x_0 + n)$ for $n \in \mathbb{N}$.

Since $\mathbb{T}^2$ is a compact set and H is continuous, to prove invertibility, it is enough to show that the map is both one-to-one and onto. Let $(x_0, y_0) \in \mathbb{T}^2$. Then $\Phi^{-1}(x_0)$ is a topological circle uniformly transverse to all lines parallel to (n_1, n_2), there is at least one point $z = (x, y)$ on $\Phi^{-1}(x_0)$ such $(n_2, -n_1) \cdot (x, y) = y_0$. Therefore, $H(z) = (x_0, y_0)$. Therefore, H is onto. Consider any two inverse images $z' = (x', y')$ and $z'' = (x'', y'')$ of (x_0, y_0). So both (x', y') and (x'', y'') lie on $H^{-1}(x_0)$. Then by the definition of H, $(n_2, -n_1) \cdot (y'' - y') = 0$, so z', z'' can be joined by a line parallel to (n_2, n_1) axis, which is a conic curve. If $x'' \neq x'$, this would contradict

the fact that different points on $\Phi^{-1}(x_0)$ cannot be joined by a conic curve. This forces x'' to be equal to x'. Therefore, the map is also one-to-one.

For any $(x_0, y_0) \in \mathbb{T}^2$, let $(x_1, y_1) := H^{-1}(x, y)$, $(x_2, y_2) := F(x_1, y_1)$ and $(x_3, y_3) := H(x_2, y_2)$. To show that H is the desired conjugacy have to show that $x_3 = mx_0 \pmod 1$. Note that $x_3 = \Phi(x_2, y_2) = \Phi \circ F(x_1, y_1)$. By Equation 3.14, $x_3 = m \times \Phi(x_1, y_1)$. But since $(x_1, y_1) = H^{-1}(x_0, y_0)$, $\Phi(x_1, y_1)$ must be equal to x_0. Therefore, $x_3 = mx_0 \pmod 1$. ∎

3.3.1 The fibers of $\hat{\Phi}$

In this section, we will prove that the fibers of ϕ, which are the sets $\phi^{-1}(x)$ for $x \in \mathbb{R}$ are differentiable curves. Before proving that, we will describe a generalized notion of tangent vectors which is applicable to continuous curves.

Let $\lambda : (0, 1) \to \mathbb{R}^d$ be a continuous curve. Let $t_0 \in (0, 1)$ and $z_0 = \lambda(t_0)$. For every non-zero vector $v \in \mathbb{R}^d$, let $\hat{v}$ denote the normalized vector $\frac{v}{\|v\|}$, where $\|v\|$ is the Euclidean norm of v. A unit vector $\hat{v}_0$ will be called a **generalized tangent direction** to λ at z_0 is there is a sequence $(t_n)_{n\in\mathbb{N}}$ such that $t_n \to t_0$, and if v_n denotes the vector $\lambda(t_n) - \lambda(t_0)$, then $\hat{v}_n \to \hat{v}_0$.

Properties of generalized tangent directions. The following properties of generalized tangent directions follow immediately from their definition.

1. Since the definition of a generalized tangent direction is a local property, the definition can be extended to continuous curves in manifolds, like $\mathbb{T}^2$.

2. Every curve has at least one generalized tangent direction at each of its points.

This is because, the vectors $\hat{u}_n$ all lie in the unit sphere S^{d-1} of the tangent space at z_0. Since this unit circle is compact, for any sequence $t_n \to t_0$ and $u_n := \lambda(t_n) - \lambda(t_0)$, the vectors $\hat{u}_n$ will have at least one limit point.

3. Note that a curve is C^1 iff there is a unique generalized tangent direction (upto change of sign), at each of its points.

Lemma 3.3.3 *Let $\lambda : S^1 \to M$ be a continuous curve in a d dimensional manifold M. Let $F : M \to M$ be a local diffeomorphism. Then DF maps generalized tangent directions of λ into generalized tangent directions of $F(\lambda)$.*

Proof Let $\hat{v}$ be a generalized tangent direction to λ at a point $z_0 = \lambda(t_0)$ for some $t_0 \in S^1$. We will prove that $DF(z_0)(v)$ is along a generalized tangent direction to $F(\lambda)$ at $F(z_0)$. By definition, there is a sequence $t_n \to t_0$ such that if $v_n := \lambda(t_n) - \lambda(t_0)$, then $\hat{v}_n \to \hat{v}_0$. Let z_n denote the point $\lambda(t_n)$. So $z_n = z_0 + v_n$.

Let $\lambda(r_0)$ correspond to the point $F(z_0)$, and similarly, $\lambda(r_n) = F(\lambda(t_n))$, where $r_0, r_1, r_2, \ldots \in S^1$. Then note that $r_n \to r_0$. By the definition of the derivative of a function F, $\lim_{n\to\infty} \frac{\|F(z_0+v_n)-(F(z_0)+Df(z_0)v_n)\|}{\|v_n\|} = 0$.

Therefore, $F(z_n) = F(z_0 + u_n) \to F(z_0) + DF(z_0)v_n$ or $F(z_n) - F(z_0) \to DF(z_0)v_n$.

Therefore, $\frac{F(z_n)-F(z_0)}{\|F(z_n)-F(z_0)\|} \to \frac{DF(z_0)v_n}{\|DF(z_0)v_n\|}$.

But since $v_n \to v_0$, we must have that $DF(z_0)v_n \to DF(z_0)v_0$ or $\frac{DF(z_0)v_n}{\|DF(z_0)v_n\|} \to \frac{DF(z_0)v_0}{\|DF(z_0)v_0\|}$.

Therefore, $\frac{F(z_n)-F(z_0)}{\|F(z_n)-F(z_0)\|} \to \frac{DF(z_0)v_0}{\|DF(z_0)v_0\|}$.

Therefore, $DF(z_0)v_0$ must be a generalized tangent direction to the curve $F(\lambda)$ at the point $F(z_0)$. ∎

Proposition 3.3.4 *Under the same assumptions as Proposition 3.1.2 and with* $\hat{\Phi}$ *as in Eq. 3.7, the fibers of* $\hat{\Phi}$ *in* $\mathbb{R}^2$ *are* C^1 *curves.*

Proof Before proving this proposition we make two important observations. Firstly, the fiber $\hat{\Phi}^{-1}(x_0)$ is mapped under F^n into the fiber $\hat{\Phi}^{-1}(m^n x_0)$, by Eqn. 3.12. Secondly, a fiber $\hat{\Phi}^{-1}(x_0)$ cannot have a generalized tangent direction lying inside the α-cone, because of Proposition 3.3.1.

By Proposition 3.3.1, $\hat{\Phi}^{-1}(x_0)$ is the graph of some continuous map $\lambda : S^1 \to \mathbb{R}$ and is parameterized as $\{(\lambda(t), t) | t \in S^1\}$. Suppose λ is not differentiable at some $t_0 \in S^1$. So it has at least two distinct non-zero tangent vectors at $z_0 := \lambda(t_0)$, namely, u and v. Let v be written as the direct sum $u' \oplus e_x$, where u' is parallel to u. Then since e_x lies within the α-cone, it expands faster than u under the action of DF. Therefore, for n sufficiently large, the vector $DF^n(z_0)v = DF^n(z_0)u' + DF^n(z_0)e_x$ is a generalized tangent direction to $\hat{\Phi}^{-1}(m^n x_0)$ at the point $F^n(z_0)$ and must lie in $\mathcal{C}(F^n(z_0))$, contradicting the second observation we had made in the beginning of this proof. Therefore, there does not exist two such vectors u and v and so $\hat{\Phi}^{-1}(x_0)$ must be a C^1 curve. ∎

Corollary 3.3.5 *Let it be assumed Without loss of generality that the X direction is contained within the expanding cones. Every fiber* $S_\theta := \Phi^{-1}\theta$ *is a* C^1 *closed curve, expressible as a the graph of a* C^1 *function* $\{(\lambda(y), y) : y \in S^1,\}$ *with the slope of* λ *bounded above by* α*.*

Proof Note that the fibers of Φ are the images of the fibers of $\hat{\Phi}$ under the map $proj \times Id$. By Prop. 3.3.1 and 3.3.4, the former are C^1 curves which intersect every

line Y = constant at a unique point. Therefore, the fibers of $\hat{\Phi}$ are also are also graphs of C^1 maps from X coordinate into Y coordinate. Two distinct points in $\hat{\Phi}^{-1}(x_0)$ cannot be connected by a conic curve, the slope of λ is bounded above by α. Since $proj$ is C^2, the images themselves must be C^1 closed curves with the same properties. ∎

3.3.2 Proof of Theorem 3.1.1

The proof of this corollary starts with two observations,

(i)the existence of an expanding cone structure is an open condition in the C^1-topology of maps.

(ii) the homology matrix of a torus map is independent of the periodic part G of the map. [See Eq. 3.4]. Secondly, for the linear torus map given by the homology matrix, namely, $M : \mathbb{T}^2 \to \mathbb{T}^2$, there is an expanding cone structure with $K = m$, $\alpha = \infty$, $e^1 = v_m$, $e^2 = v_1$. Therefore, there is a bound $\delta > 0$ such that if $\|G(y)\|_{C^1} < \delta$, then the map still retains the same homology matrix and an expanding cone structure.

∎

Chapter 4: The occurrence of Multi-chaos

Abstract. In the most frequently studied dynamical systems all the periodic orbits in a chaotic set have the same number of unstable dimensions, but this property seems to fail in high dimensional systems. In this paper, we define a property called "multi-chaos", in which there are dense periodic orbits of more than one unstable dimension, along with the usual properties of chaos. We will construct a family of toral maps which happen to be the first examples of multi-chaos. These maps are non-hyperbolic and non-invertible and cannot be studied using the approach of invariant splittings of the tangent space. Our technique is to construct a continuous change of variables for these systems so that one of the new variables satisfies $x \to mx \mod 1$; in particular the dynamics in X are independent of the other variable.

4.1 Introduction

Chaos and Multi-chaos. A variety of definitionsof chaos are available depending on the tools at hand and whether the investigation is computational (where there is a well defined system on which computational experiments can be made), experimental (where data is collected from a physical experiment), or theoretical

(where the goal is a rigorous investigation, for example in [12]). A new definition by Hunt and Ott [47] that includes situations in which there are no periodic orbits. Here we will define a closed uncountable set $X \subset M$ to be **chaotic** if it satisfies the following.

(M_i) X is an invariant set of F.

(M_{ii}) X has a dense trajectory.

(M_{iii}) X has a dense set of periodic orbits.

In many simple systems, a chaotic set has a fixed number of unstable dimensions in the sense that all periodic orbits in the set have the same unstable dimension. We will say a set X is **k-chaotic** if all of its periodic orbits have k-dimensional unstable manifolds and the set X is at least k-dimensional. We will say X is **multi-chaotic** if

(M_{iv}) X is k-chaotic for two or more values of k.

In the theory of blow-out bifurcations and riddled basins, one often sees chaotic sets that contain a piece of an invariant plane of dimension k_1 in which there are periodic orbits of different unstable dimensions, some of which are larger than k_1. Hence, at least part of their unstable manifolds are transverse to the plane. Often there is a larger chaotic set that contains that piece of invariant plane. Such sets have the potential of being multi-chaotic, but no examples have been shown to have that property. In fact this paper contains the first rigorous demonstration of the existence of a multi-chaotic set. Experiments on higher dimensional chaotic sets have shown that the periodic orbits frequently have different numbers of unstable

dimensions. Our paper is a part of a larger investigation in which we look for various means by which we can have multi-chaos. In [48], Glendining examined a system of coupled dynamical systems and proved the existence repellor periodic orbits that are dense in the two-dimensional chaotic attractor X. Our numerical investigations seem to suggest that the chaotic saddles are dense i the other properties of multi-chaos are also present.

The multi unstable dimension problem. Consider a dynamical system with two hyperbolic periodic points P and Q. If they have the same unstable dimension and in addition, the stable manifold of each intersects the unstable manifold of the other, the configuration is called a **heteroclinic cycle**. Then there is an invariant Cantor set with a dense trajectory that contains both P and Q. Hence the dense trajectory comes arbitrarily close to both P and Q. If the unstable dimension of Q is more than that of P, then generically, the stable and unstable manifolds of P and Q respectively will not intersect since the sum of their dimensions is less than the dimension of the ambient space. Therefore, in such a case, the mechanism of heteroclinic intersections by which trajectories can be dense near Q is lost. So we are faced with the problem of determining why should there be trajectories arbitrarily near P which pass arbitrarily close to Q and return close to P, etc., in chaotic sets with varying unstable dimensions. We are interested in explaining the geometry that leads to chaos and in particular, dense trajectories in such systems. Figure 4.1 illustrates this case in a 3-dimensional setting.

There are several examples of maps in which saddles of different unstable dimensions co-exist. In [49], Smale and Abraham investigated a 4-dimensional system

which is a Cartesian product of the cat map on the torus and the horseshoe map on the 2-sphere. In [50], the authors discussed the property of "non-shadowability" for a family of maps with saddles of varying dimensions. The presence of two saddles of different unstable dimensions was used in [51] to prove the existence of a set of ergodic, non-hyperbolic maps residual in $\mathrm{Diff}^1(M)$.

The simplest maps that could exhibit varying unstable dimensions are in 2 dimensional systems, where a repellor and saddle can co-exist. Of course, the stable manifold of a repellor P is the set of points x such that $F^n(x) = P$ for some non-negative integer n. The presence of a dense trajectory requires that the map is not one-to-one. In this paper, we study a certain class of maps on the 2-torus $\mathbb{T}^2$, that have both repellors and saddles. Such a map on the 2-torus was studied in [41]. We will assume that the dynamics has a dominant expanding direction, which leads to the presence of an invariant structure in the tangent space called an *invariant cone system.*

Chaos from quasiperiodicity. In [52], it was shown that dynamical systems with three-period quasiperiodicity on the 3-torus $\mathbb{T}^3$ could be given arbitrarily small perturbations and be made chaotic. This proved that chaotic systems are topologically dense near three-period quasiperiodicity. In [34], the authors considered the measure-theoretic density of these chaotic configurations near the quasiperiodic state and found numerically that they were not prevalent. It was also conjectured here that the route to chaos proposed by Ruelle and Takens in [53] was not typical. The latter's idea involves the destabilization of a third incommensurate frequency of a two-period quasiperiodic attractor. The quasiperiodic route to chaos was also

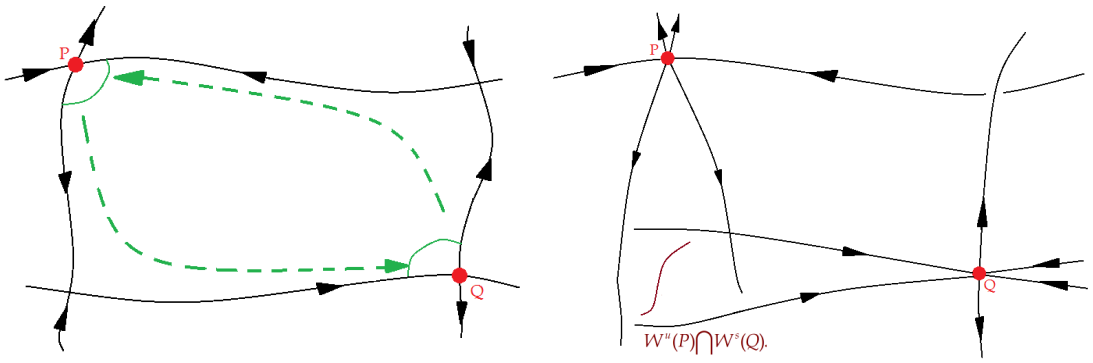

(a) (b)

Figure 4.1: A Heteroclinic cycle is created when stable and unstable manifolds of a saddle P intersect the unstable and stable manifolds respectively of another saddle Q. Part (a) displays such a case for two saddles in a 2-dimensional setting. Since the unstable dimensions of P and Q are the same, the two intersections persist under small perturbations of the dynamical system. The regions marked in green are portions of neighborhoods of P and Q and each of these regions have a Cantor set of points which keep coming close to P and Q infinitely many times in their trajectories. Part (b) shows a configuration in a 3-dimensional setting in which the unstable dimensions of P and Q are 2 and 1 respectively. As a result, for almost every perturbation of the system, $W^s(Q)$ and $W^u(P)$ will not intersect. Thus, the configuration of a heteroclinic cycle is absent and we have to look for some other mechanism by which points near P land close to Q and vice versa.

reportedly observed in quasiperiodically driven systems, in [54]. In [55], Glendinning constructed an open family of 2D-flows such that the return maps on a suitable chosen Poincare section undergo transition to chaos. At the boundary of chaos, there is a single stable periodic orbit and countably infinitely many periodic points.

Vertical circles A *vertical circle* is a set of the form $\{X = x\} = \{x\} \times S^1 \subset \mathbb{T}^2$, where $x \in S^1$. It will be denoted as $\boldsymbol{S_x}$. Then the map (3.1) maps vertical circles into vertical circles, that is,

$$\text{For every } x \in S^1,\ F(S_x) = S_{F(x)} \tag{4.1}$$

All the vertical circles S_x with x of the form

$$x_0 = \frac{k}{m^n - 1} \mod 1 \tag{4.2}$$

are invariant under F^n. These will be called the **periodic circles** of the map. So if $z_0 = (x_0, y_0)$ is a periodic point, then x_0 must be of the form (4.2) and z_0 is a fixed point of the circle map $F^n|_{S_{x_0}}$. Depending upon whether this fixed point is attracting, neutrally stable or repelling for $F^n|_{S_{x_0}}$, z_0 is a saddle, non-hyperbolic periodic point or repellor for F.

Our first result, Theorem 4.1.1, proves the occurrence of multi-chaos. Here we use maps that have an expanding cone structure containing the X direction. In general for a maps given by Eq. 3.1, such a structure will be present if the following condition holds.

$$\|g\|_{C^1} \leq 0.5m$$

Theorem 4.1.1 (Theorem A) *Assume that a torus map $F : \mathbb{T}^2 \to \mathbb{T}^2$ is given by Equation 3.1, has a periodic saddle $\mathcal{S}$ and an expanding cone structure containing*

the X direction. Then if there exists a periodic circle S_x such that $F^p|S_x$ is conjugate to an irrational rotation. Then the map (3.1) has multi-chaos.

Theorem 4.1.2 given below is a consequence of Theorems 4.1.1 and 3.1.2. It is in effect, a generalization of Theorem 4.1.1 .

Theorem 4.1.2 (Theorem B) *Let $F : \mathbb{T}^2 \to \mathbb{T}^2$ be a C^1 map of the torus such that* $\det DF$ *is invertible everywhere and satisfies the following.*

(i) Its winding matrix M has a unit eigenvalue and a determinant greater than 1.

(ii) There is an expanding cone system containing either the X-direction $(1, 0)$ *or the Y-direction* $(0, 1)$.

(iii) F has a periodic saddle and an invariant quasiperiodic circle.

Then F is conjugate to a map of the form (3.1) and has multi-chaos.

Corollary 4.1.3 *Let M be a matrix with integer entries with a unit eigenvalue and determinant more than 1. Then there is a $\delta > 0$ such that for every $\mathbb{Z}$-periodic $f : \mathbb{R}^2 \to \mathbb{R}^2$ such that $\|f\|_{C^1} < \delta$, the map $F : \mathbb{T}^2 \to \mathbb{T}^2$ whose lift is $\bar{F} = M + f$ is conjugate to a map of the form (3.1) and has multi-chaos.*

Section 4.2 has some definitions and properties needed to prove the two theorems. Section 4.3 contains the proof to Theorem 4.1.1.

4.2 Some definitions and lemmas

4.2.1 Stable and unstable manifolds.

Let M be a closed d-manifold, $F : M \to M$ be a C^1 map and let P be a hyperbolic periodic point of period p. This means that the matrix $DF^p(P)$ is a hyperbolic matrix. In particular, this means that F is a diffeomorphism when restricted to some small neighborhood of P. Within a suitably chosen small neighborhood of P of radius ϵ, the map F^p is conjugate to the hyperbolic linear map in $DF^p(P) : \mathbb{R}^d \to \mathbb{R}^d$ which has the origin as its fixed point. Such a linear map has stable and unstable subspaces, which correspond to the local stable and unstable manifolds of P, which are defined below.

$\boldsymbol{W^s_\epsilon(P)} := \{y \in M : \text{for every integer } n \geq 0,\ d(f^{pn}(y), P) < \epsilon\}$.

$\boldsymbol{W^u_\epsilon(P)} := \{y \in M : \text{for every integer } n \geq 0,\ d(f^{-pn}(y), P) < \epsilon\}$.

The global stable and unstable manifolds for P can now be defined as

$\boldsymbol{W^s(x)} := \{y \in M \ : \ \lim_{n\in\mathbb{N}} d(f^n(y), f^n(x)) = 0\}$.

$\boldsymbol{W^u(x)} := \{y \in M \ : \ \lim_{n\in\mathbb{N}} d(f^{-n}(y), f^{-n}(x)) = 0\}$.

Let $z_0 = (x_0, y_0)$ be a periodic saddle of period p for the map given by Equation 3.1. Let $W^s = W^s(z_0)$ be the stable manifold of this saddle. Then $B(z_0) = W^s \cap S_{x_0}$ is an open sub-interval of the vertical circle S_{x_0} containing z_0. Then W^s is given by

$$W^s(z_0) = \bigcup_{n=0,1,2,\ldots} F^{pn}(B(z_0)), \text{ where } B(z_0) = W^s(z_0) \cap S_{x_0}.$$

Remark. If P is a periodic repellor of period p, then $W^u_\epsilon(P) = B_\epsilon(P)$, the open ϵ-ball around P. Therefore, $W^u(P)$ is the open set $\bigcup_{n\in\mathbb{N}} F^{pn} B_\epsilon(P)$. It is therefore

a d-dimensional manifold. Similarly, $W^s(P)$ is the 0-dimensional manifold which is the countable union of points $\underset{n\in\mathbb{N}}{\cup} F^{-pn}(P)$.

4.2.2 Snap-back repellors

Dense set of repellors F.R. Marotto introduced the notion of snapback repellor in 1978 [56], based on Li-Yorkes theorem on chaos. He redefined snapback repellors in 2005 as follows.

Definition [56]. Let R be a periodic repellor of F. Suppose that there exists a point $Q \neq R$ such that $Q \in W^u(R)$, $F^n(Q) = R$ for some $n \in \mathbb{N}$ and $det(DF(\cdot)) \neq 0$. Then R is called a snapback repellor of F. Note that Q is a homoclinic intersection point for P and any periodic repellor with homoclinic intersection point(s) are snap-back repellors. Snap-back repellors provide a powerful tool for proving various aspects of chaos. For example, in [57], the authors present an estimate of the radius of the repelling neighborhood of a snap-back repellor and used it to search for homoclinic orbits.

The situation we will analyze is simpler than Marotto's, and we will state a simplified version of a lemma by Marotto which we will also prove for the sake of completion.

Lemma 4.2.1 (Snap-back repellor lemma) *Let F be a C^1 map on a manifold M Let R be a snapback repellor and Q a homoclinic point of R. Then Q is a limit point of periodic repellors.*

Proof Let U be a neighbourhood of R. It will be proved that exists a periodic re-

pellor in U. Let W be a neighbourhood of R about which the map can be linearized. Since $\partial_2(g) > 1$ at R, by taking small enough, it can be assumed without loss of generality that $\partial_2(g) > K > 1$ in W. Since $Q \in W^u(R)$, exists $M \in \mathbb{N} \ni$ exists $Q_M \in F^{-M}(Q) \cap W$. Hence for every $n \in \mathbb{N}$, exists $Q_{M+n} \in F^{-(M+n)}(Q) \cap W$. Let $V \subseteq U$ be a neighborhood of Q such that $F^N(V) \subseteq W$. Let V_M be a neighbourhood of Q_M in W which maps onto V under F^M. Let for every $n \in \mathbb{N}$, V_{M+n} denote the n-th inverse image of V_M that lies within W. Since W is a linearizable neighbourhood of the repellor R, $diam(V_{M+n}) \to 0$ implies that for all large n, $V_{M+n} \subset F^N(V)$.

However, $F^{N+M+n}(V_{M+n}) = F^N(V) \supset V_{M+n}$,

$\Rightarrow$ by the Brower fixed point theorem, exists a point P of periodicity $M + N + n$ in V_{M+n}. Since $P \in V_{M+n}$, the first n iterates of P lie within W and atmost $M + N$ iterates lie outside W. By the choice of W, for large n, P is a repelling periodic point.

Now $F^{M+n} \in V \subset U$, hence U has a repelling periodic point as claimed. ∎

4.3 Proof of Theorem 4.1.1

By the hypothesis of the theorem, there is a periodic saddle $\mathcal{S}$ of period p_1 and a periodic circle S_{x_0} [see Eq. 4.2 for definition] of period p_2 such that $F^{p_2}|S_{x_0}$ is an irrational rotation. By the definition of quasiperiodicity, the restriction $F^{p_2}|S_{x_0}$ must be conjugate to an irrational rotation. Let $N = p_1 p_2$. Then $\mathcal{S}$ and S_{x_0} are fixed under F^N and $F^N|S_{x_0}$ is conjugate to an irrational rotation. Given the assumptions of Theorem 1.1., we will assume without loss of generality,

(H1) $p_1 = p_2 = 1$, $\mathcal{S} = (0, 0)$ and $x_0 = 0.5$, which we shall call "the middle circle" and denote as $\mathbf{\Gamma}$.

Outline of the proof. We will first prove two necessary properties of the map, which will be used to establish the various features of multi-chaos for the map. Specifically, in Lemma 4.3.1, we prove that the map in Theorem 4.1.1is topologically transitive and in Section 4.3.1 we prove that the saddle has a dense unstable manifold. Finally, in Section 4.3.2, we use these two properties of F to prove properties (i)-(iv) of multi-chaos.

A map $F : M \to M$ on a manifold M is said to be **strongly transitive** if for every open $D \subset M$, there is $n \in \mathbb{N}$ such that $\underset{1 \le k \le n}{\cup} F^k(D) = M$.

Lemma 4.3.1 *Under the hypothesis of Theorem 4.1.1, F is strongly transitive.*

Proof Let us assume the simplifying assumption (H1). Since F is uniformly expanding in the x-direction by factor $m > 1$, for sufficiently large $n_1 \in \mathbb{N}$, $F^n(D)$ stretches across all x-coordinates and in particular, intersects Γ in an open interval I. Since $F|\Gamma$ is a quasiperiodic map, for sufficiently large $n_2 \in \mathbb{N}$, $\underset{k \in [n_2]}{\cup} F^k(I) = \Gamma$. Therefore, $\underset{k \in [n_2]}{\cup} F^{n_1+k}(I)$ contains a neighborhood V of Γ. By the compactness of Γ and the expanding nature of F in the x-direction, for sufficiently large $n_3 \in \mathbb{N}$, $F^{n_3}(V) = \mathbb{T}^2$. Hence, the union of the first $n = n_1 + n_2 + n_3$ iterates of D cover $\mathbb{T}^2$.

∎

4.3.1 Density of W^u.

Proof that W^u is dense. The proof of the density of W^u will be by contradiction. Suppose W^u is not dense in $\mathbb{T}^2$, i.e., there exists an open, non-empty set $\boldsymbol{U}$ such that $U \cap W^u = \Phi$. Since W^u is forward invariant, it may be assumed without loss of generality that U is backward-invariant. By Lemma 4.3.1, U must be an open, dense set disjoint from W^u. Let $\boldsymbol{K}$ be the closure of W^u. Then every point on K lies on the boundary of U. Note that W^u is a conic-curve and therefore, must intersect Γ at least one point z. Since $F|\Gamma$ is conjugate to an irrational rotation, the orbit of z must be dense in Γ. However, the orbit of z is also a part of W^u. Therefore, $\Gamma \subset K$.

A vertical curve is a curve on the torus with a constant X-coordinate. The following lemma establishes that of a vertical curve contained in the open sets U and at distance δ from Γ has a length l bounded by $\alpha\delta$, where α comes from the definition of expanding cones. However, we will also show that the ratio $l\delta$ is unbounded for vertical curves contained in U. This contradiction will complete the proof of W^u being dense.

Lemma 4.3.2 (An upper bound) *Assume the hypothesis of Theorem 4.1.1 and also (H1). Let λ be a vertical curve in $\mathbb{T}^2$ of length $l > 0$ and at a distance δ from Γ ($0 < \delta \leq 0.5$). Then we must have $\frac{l}{\delta} \leq 2\alpha$.*

Proof Let x_1 be the X coordinate of the curve λ. without loss of generality, we may assume that $x_1 = 0.5 - \delta$. Let $(0.5-\delta, y_0)$ and $(0.5-\delta, y_2)$ be the two endpoints of λ,

with $y_0 < y_1$. Let the vertical mid-point be $(0.5-\delta, y_1)$, where $y_1 = 0.5(y_0+y_2)$. Then by assumption, the point $0.5, y_1)$ is a point on Γ. Since W^u has dense intersections with Γ, for every $\epsilon > 0$, there is a point $(0.5, y_1') \in \Gamma \cap W^u$ at a distance less than ϵ from $(0.5, y_1)$. Let the segment of W^u starting at $(0.5, y_1')$ intersect $S_{x_1} = S_{0.5-\delta}$ at $(0.5-\delta, y_3)$. Without loss of generality, let $y_3 \leq y_0$.

Then since W^u is a conic-curve with slope bounded by α, $|y_3 - y_1| \leq |y_3 - y_1'| + |y_1 - y_1'| \leq \alpha\delta + \epsilon$.

But $l = 2|y_0 - y_1| \leq 2|y_3 - y_1| \leq 2\alpha|\delta| + 2\epsilon$. Since this inequality holds for every $\epsilon > 0$, it must hold for $\epsilon = 0$. This gives the inequality $\frac{l}{\delta} \leq 2\alpha$. ∎

Contradiction of Lemma 4.3.2. Let $\delta \in (-0.1, 0.1)$ be fixed. The intersection of the open set U with the topological circle $\{\delta\} \times S^1$ is a disjoint collection of maximal, open arcs. Let I_0 be such a component interval with Y-span $l > 0$. For every integer $n \geq 1$, there is a continuous arc I_n which lies in the interior of $(-\delta, \delta) \times S_{x_0}$ such that $F^n(I_n) = I_0$. Let $m_x := z \underset{\min}{\in} \mathbb{T}^2 |\partial_x F_1|$ and $m_y := z \underset{\max}{\in} \mathbb{T}^2 |\partial_y F_2|$. Since $m_x > m_y$. So I_n lies within the annulus $(-\frac{\delta}{m_x^n}, \frac{\delta}{m_x^n}) \times S^1$ and has a Y-span of atleast $\frac{l}{m_y^n}$. Note that I_n is still a C^1-curve with slope bounded below by $\alpha' > \alpha$. Also, I_n lies in U, since U is backward invariant. However, the ratio of the Y-span to the distance from its mid-point is $l\left(\frac{m_x}{m_y}\right)^n$ which tends to ∞ as $n \to \infty$. This is a contradiction of Lemma 4.3.2.

Therefore, the assumption that W^u is not dense has lead to a contradiction and must be false. Hence W^u must be dense in $\mathbb{T}^2$. ∎

4.3.2 Density of periodic saddles and repellors

Proof of density of periodic saddles. We had assumed without loss of generality that the point $(0,0)$ is a saddle. The circle S_0 is fixed under F, so let $S_1, \ldots, S_k$ be the saddles on this circle, S_1 being equal to $(0,0)$. Then the union of the stable manifolds of these saddle contains all the points on S_0 other than the repellors and so is dense in S_0. The set of pre-images of this circle is the set of vertical circles $\{x = \frac{2k\pi}{3^n-1}$ with $k \geq 0$ and $n > 1$ integers $\}$, which is dense in $\mathbb{T}^2$. Since the unstable manifolds of these saddles are also dense, the set of homoclinic intersections of W^u with W^s for the saddles are dense. However, any homoclinic intersection point is a limit point of periodic saddles. Therefore, the set of periodic saddles must be dense in the whole torus. ∎

In this section, the following useful result will be proved which will be used to show that repellors are dense in the torus.

Proposition 4.3.3 *For every $z \in \mathbb{T}^2$, the set of pre-images of z, given by $\bigcup_{n\in\mathbb{N}} F^{-n}(z)$, is dense in $\mathbb{T}^2$.*

Proof Let I denote the set $\bigcup_{n\in\mathbb{N}} F^{-n}(z)$. Since I is backward invariant, so is $\bar{I}$, its closure. Since F is expanding uniformly in the X-direction, and $F|\Gamma$ is quasiperiodic, $\Gamma \subset \bar{I}$. Let $U = \mathbb{T}^2 - \bar{I}$. Then U is an open set and forward invariant. The proof of Lemma 4.3.1 shows that if U is nonempty, then U must contain Γ, a contradiction. Hence U is empty, $\bar{I} = \mathbb{T}^2$ and therefore I is dense in $\mathbb{T}^2$. ∎

Proof of existence of a repellor. By assumption, there is a saddle $\mathcal{S}$ in

the torus. Let it lie on the circle S_x. Then $\mathcal{S}$ is a fixed point of $F|S_x$. Moreover, it must be an attracting fixed point as the unstable manifold of $\mathcal{S}$ is transverse to the Y-direction. Therefore, $F|S_x$ must also have a repellor $\mathcal{R}$ on S_x. Then $\mathcal{R}$ is a repellor for F. ∎

Proof of density of periodic repellors. Since $\mathcal{R}$ is a repellor, it has a repelling neighbourhood W, hence $W \subset W^u(\mathcal{R})$. Since W^u is closed under forward iterates, $\bigcup_{n=0,1,2,\ldots} F^n W \subseteq W^u$. By Lemma 4.3.1, $\bigcup_{n=0,1,2,\ldots} F^n W] = \mathbb{T}^2$. Therefore, $W^u(\mathcal{R}) = \mathbb{T}^2$. Also, the set of inverse images of $\mathcal{R}$ is dense in $\mathbb{T}^2$. Each of these pre-images are snap-back repellors, as they lie in $\mathbb{T}^2$, the unstable manifold of $\mathcal{R}$. By the Snap-back repellor lemma, Appendix 4.2.1, every snap-back repellor is a limit point of periodic repellors, hence, the set of periodic repellors too must be dense. ∎

Proof of existence of a dense trajectory A dense trajectory is equivalent to transitivity of the map. Recall that a map is called **transitive** if for any pair of non-empty open sets A and B, there exists some $n \in \mathbb{N}$ such that $F^{-n}(A) \cap B$ is non empty. Transitivity is however implied by Lemma 4.3.1. Therefore, F has multi-chaos and Theorem 4.1.1 is proved. ∎

4.3.3 Topological mixing.

In fact, we can add a stronger property of the map F, that of being topologically mixing. Recall that a map is called **topologically mixing** if for any pair of non-empty open sets A and B, there exists some $N \in \mathbb{N}$ such that for every $n \in \mathbb{N}$

such that $n > N$, $F^{-n}(A) \cap B$ is non empty. The topological mixing property of the map is proved by the following proposition.

Proposition 4.3.4 *Assume that the unstable manifold of every saddle is dense for the map (3.1). Then F is topologically mixing.*

Proof Let A, B be two non-empty, open subsets. Since F_0 is uniformly expanding in the X-direction, for some integer $k > 0$, $F^k(A)$ will intersect the stable manifold of some periodic saddle P of period p. By assumption, the unstable manifold W^u of P is dense in $\mathbb{T}^2$, it passes through B. Let $z \in W^u \cap B$. Then there is a $\delta > 0$ such that B contains a δ neighborhood of z. By the lambda lemma, there is an integer $N > 0$ such that for every integer $n > N$, $F^n(F^k(A))$ contains points within distance δ of $z \in W^u$ and therefore, lying within B. Therefore, for every integer $n > k+N$, $F^{k+N}(A) \cap B$ is non-empty, which implies that F is topologically mixing.

∎

Appendix A: Dense saddles in skew product maps

Abstract In this chapter, we look at a specific class of maps in the torus and explore the consequences of this map having a dense set of periodic saddles. The main result states that under these assumptions, the torus splits into a countable number of invariant cylinders with disjoint interiors and the map is transitive on each cylinder.

Our main result states that a map on the torus with dense saddles may not be transitive, but there will be a decomposition of the torus into a finite number of cylinders with disjoint interiors with the map transitive on each component. Let $z_0 = (x_0, y_0) \in \mathbb{T}^2$ be a periodic point of period $p \in \mathbb{N}$. Then one of the eigenvalues of $dF^p(z_0)$ is m^p. Therefore, depending upon whether the other eigenvalue, which equals $|\partial_2(g \circ F^{p-1})(z_0))|$, is lesser than, equal to or greater than 1, z_0 is a saddle, non-hyperbolic or a repellor. Our main result will carry the additional assumption that the expansion in the X-direction by m dominates any expansion in the Y-direction. This can be stated as

$$|\partial_2 g(x, y)| < m \text{ for } \forall (x, y) \in \mathbb{T}^2. \tag{A.1}$$

We will also find use for a stronger condition on the expansion, which is

$$|\partial_2 g(x, y)| < 0.5m \text{ for } \forall (x, y) \in \mathbb{T}^2. \tag{A.2}$$

So if $z_0 = (x_0, y_0)$ is a periodic point, then x_0 must be of the form (4.2) and z_0 is a fixed point of the circle map $F^n|S_{x_0}$. Depending upon whether this fixed point is attracting, neutrally stable or repelling for $F^n|S_{x_0}$, z_0 is a saddle, non-hyperbolic periodic point or repellor for F.

A *cylinder* is a set diffeomorphic to $S^1 \times [0, 1]$. Recall that a map is *transitive* if it has a dense trajectory or equivalently, for every pair of open sets U and V, there is some $n \in \mathbb{N}$ for which $F^{-n}(U) \cap V \neq \Phi$. A set X is called *forward-invariant* wrt F if $F(X) \subseteq X$. It is called *strongly forward-inavariant* if $F(X) = X$. *Backward-invariance* and *invariance* is similarly defined.

Theorem A.0.5 (Main result) *Let (3.1) be a local diffeomorphism that has dense periodic saddles and satisfies (A.2). Then either the map is transitive or there exists some $p \in \mathbb{N}$ such that the torus is a union of finitely many cylinders with disjoint interiors such that F^p acts transitively on each cylinder and the action of F on the set of cylinders is a permutation whose cycles are of order p.*

The following two corollaries are immediate consequences of the main theorem. They show that the splitting of the torus into invariant cylinders can be refuted by easily satisfiable conditions.

Corollary A.0.6 *Let (3.1) be a local diffeomorphism with dense periodic saddles , satisfies (A.2), such that there is a periodic circle $\Gamma_{k,n}$ of the form (4.2) on which F^n is transitive. Then the map F is transitive on $\mathbb{T}^2$.*

Corollary A.0.7 *Let (3.1) be a local diffeomorphism that has dense periodic saddles*

and satisfies (A.2). Moreover, suppose that there are two periodic points whose periods are coprime. Then the map F is transitive on $\mathbb{T}^2$.

Section A.1 has some definitions and properties needed to prove Theorem A.0.5. Finally, section A.2 presents the proof to Theorem A.0.5.

A non-transitive torus map with dense periodic saddles. Consider the cylinder $C = S^1 \times [0,1]$. We will first construct a map on this cylinder which has a dense set of periodic saddles and leaves the boundaries $S^1 \times \{0\}$ and $S^1 \times \{1\}$ invariant. Then the map on the torus can be constructed by gluing corresponding boundaries of each cylinder together. We will continue to use the notation S_x to denote the vertical line segments $\{x\} \times [0,1]$.

The following map on the cylinder is a modification of a torus map studied in [41].

$$F(x,y) = (3x \pmod{()1},\ y + 0.01\sin(2\pi y) + 0.2g(y)\sin^2(\pi x)), \tag{A.3}$$

where $(x,y) \in S^1 \times [0,1]$. Here $g : [0,1] \to [0,1]$ is a smooth map which equals 0 in a small neighborhood of 0 and 1 and equals 1 for $y \in [0.01, 0.99]$. The map has a fixed saddle point z at $(0, 0.5)$. Let R be the set bounded by the circle $S^1 \times [0.4]$ and from the bottom by portions of the unstable manifold of z. Using a bit of arithmetic, it was shown in [41] that $R \subset S^1 \times [0, 0.4]$ and that $R \subset F(R)$. Therefore, every point in R has a preimage in R. Also note that $\frac{\partial F_y}{\partial y} > 1$ in R. From this it follows that the unstable manifold W_u of z is dense in R. This region also has a periodic repellor, so the forward iterates of R covers the interior of the cylinder C. Therefore, W^u is everywhere dense.

Now note that the stable manifold W^s of z contains $S_0 - \{z\}$ and all of its inverse images. The inverse images of S_0 are the vertical lines $\{S_x \mid x = \frac{k}{3^n} \pmod 1,\ k, n \in \mathbb{N}\}$. W^s is dense on each such vertical line and these lines are dense in C. Therefore W^s is dense in C.

Therefore, the intersections of W^u with W^s are transverse homoclinic points and dense in C. Each of them are limit points of periodic points, hence, the set of periodic points is dense in C.

A.1 Definitions and properties

A.1.1 Stable and unstable manifolds.

In this section, the definitions of local and global, stable and unstable manifolds are reviewed.

Local stable and unstable manifolds for hyperbolic maps. Let M be a closed n-manifold, $F : M \to M$ be a C^1 diffeomorphism, $\Lambda \subseteq M$ is a compact hyperbolic set. Then for $\forall x \in \Lambda$, $\forall \epsilon > 0$:

$\boldsymbol{W^s_\epsilon(x)} := \{y \in M \mid \forall n \in \mathbb{N}_0,\ d(f^n(y), f^n(x)) < \epsilon\}$.

$\boldsymbol{W^u_\epsilon(x)} := \{y \in M \mid \forall n \in \mathbb{N}_0,\ d(f^{-n}(y), f^{-n}(x)) < \epsilon\}$.

Global stable and unstable manifolds for hyperbolic maps. Let M be a closed n-manifold, $F : M \to M$ be a C^1 diffeomorphism, $\Lambda \subseteq M$ is a compact hyperbolic set. Then for $\forall x \in \Lambda$, $\forall \epsilon > 0$:

$\boldsymbol{W^s(x)} := \{y \in M \mid \lim_{n\to\infty} d(f^n(y), f^n(x)) = 0\}$.

$\boldsymbol{W^u(x)} := \{y \in M \mid \lim_{n\to\infty} d(f^{-n}(y), f^{-n}(x)) = 0\}$.

It follows from hyperbolic systems' theory and proved in various sources, such as [58], that $\exists \epsilon_0 > 0$ such that for $\forall 0 < \epsilon < \epsilon_0$,

$W^s_\epsilon(x)$ is a manifold and $W^s(x) = \bigcup_{n\in\mathbb{N}_0} F^{-n}(W^s_\epsilon(x))$.

$W^u_\epsilon(x)$ is an embedded manifold and $W^u(x) = \bigcup_{n\in\mathbb{N}_0} F^{n}(W^u_\epsilon(x))$.

Stable and unstable manifolds of hyperbolic periodic points. Let a point P on a n-dimensional manifold M be a hyperbolic periodic point of period p, of a map F. Then P must be a hyperbolic fixed point of the map F^p. By the Hartman-Grobman theorem [59], there is a neighbourhood W of P in which F^p is C^1 conjugate to the linear map $dF^p(P)$. The local stable and unstable manifolds of P exists in this neighborhood. The global stable and unstable manifolds can then be described as above.

A.1.2 Invariant cone systems.

Invariant system of cones : Let M be a manifold, $F : M \to M$ a C^1 map. Let $T(M) = E^u + E^s$ be a splitting of the tangent bundle and for $\forall x \in M$, $\forall \alpha > 0$, the α-unstable cone at x, denoted as $\mathcal{C}^u_\alpha(x)$, is defined to be $\{(v^u, v^s) \in T(x, M) || v^s| \leq \alpha |v^u|\}$. Then (M, F) is said to have a system of invariant cones wrt the splitting $E^u \oplus E^s$ if $\exists \alpha > 0$ such that for $\forall x \in M$, $\forall v \in \mathcal{C}^u_\alpha(x)$, $v' = dF(x)(v) \in \mathcal{C}^u_\alpha(F(x))$.

Invariant, expanding system of cones : Let M be a manifold, $F : M \to M$ a C^1 map. Let $T(M) = E^u + E^s$ be a splitting of the tangent bundle. Then (M, F) is said to have a an invariant expanding cone system if $\exists \alpha > 0$, $k > 1$ such that for

$\forall x \in M$, $\forall v \in \mathcal{C}^u_\alpha(x)$, $v' = dF(x)(v) \in \mathcal{C}^u_\alpha(F(x))$ and $|v'| > k|v|$.

If the splitting $E^u \oplus E^s$ and constants $\alpha > 0$ and $K > 0$ are clear from the context, then they will be dropped from the notation and the invariant, expanding cone system $\mathcal{C}^u_\alpha$ will be simply denoted as $\{ \boldsymbol{\mathcal{C}(x)} \mid x \in M\}$ or $\{ \boldsymbol{\mathcal{C}_\alpha(x)} \mid x \in M\}$.

We will now describe curves whose tangent bundle is contained in the cone system. Borrowing from a similar idea in physics, we will call such curves *causal*.

Differentiable causal curves A C^1 curve $\lambda : \mathbb{R} \to M$ is said to be a causal curve if its tangent vector at every point lies inside the cone associated with that point. In other words, for $\forall t \in \mathbb{R}$, $\lambda'(t) \in \mathcal{C}_\alpha(\lambda(t))$.

This definition of causality can be extended from differentiable curves to continuous curves

Causal curves A C^0 curve $\lambda : \mathbb{R} \to M$ is said to be a causal curve if at every point z_0 on λ and any neighborhood U of z_0, any point z on U can be joined to z_0 by a differentiable, causal curve γ lying inside U.

Causal curves are therefore Lipschitz curves. By Rademacher's theorem (see [60], Theorem 3.1.6), they are differentiable at Lebesgue almost every point. In particular, they are rectifiable and their length can be obtained by integrating their slopes.

Lemma A.1.1 (Properties of an expanding system of unstable cones) *Let M be a manifold, $F : M \to M$ a C^1 map with an invariant, expanding cone system*

wrt the splitting $E^s \bigoplus E^u$ *and constants* K *and* α*. Let* $\lambda : \mathbb{R} \to M$ *be a causal curve. Then*

1. *The image* $F(\lambda)$ *under the map of the causal curve* λ *is also a causal curve.*

2. $length(F(\lambda)) > K\ length(\lambda)$*.*

3. $length(F^n(\lambda)) > K^n\ length(\lambda)$*, which* $\to \infty$ *as* $n \to \infty$*.*

Proof 1. For $\forall t \in \mathbb{R}$, $(F \circ \lambda)'(t) = dF(\lambda(t))\lambda'(t)$. Since the cone system is forward invariant, this vector $\in K^u_\alpha(\lambda(t))$, hence $F(\lambda)$ is a causal curve too.

2. $length(F(\lambda)) = \int\limits_{\mathbb{R}} |(F \circ \lambda)'(t)|dt \leq \int\limits_{\mathbb{R}} k|(\lambda)'(t)|dt = K\ length(\lambda)$.

3. This follows from (i) and (ii) above.

Cone system for (3.1). Let e_x and e_y denote the vector fields along the X and Y directions respectively. Take E^u to be e_x and E^s to be e_y. Then the map (3.1) has an invariant cone system wrt the splitting $e_x \oplus e_y$ if it satisfies (A.1). The cone system will be expanding if the stronger condition (A.2) is satisfied.

In an invariant cone system, the cone $\mathcal{C}(x)$ at a point x is mapped under $DF(x)$ into the cone at $F(x)$. The following quantities a_n track how thin the images $DF^n(x)(\mathcal{C}(x))$ get with the iteration number n.

$$\text{For } \forall n \in \mathbb{N},\ \forall z \in M,\ \alpha_n(z) := \sup\{\frac{\|v\|}{\|u\|} \mid (u, v) \in DF^n(\mathcal{C}_\alpha(z))\}. \tag{A.4}$$

$$\text{For } \forall z \in M,\ \bar{\alpha}(z) := \inf_{n \in \mathbb{N}} \alpha_n(z). \tag{A.5}$$

If $\bar{\alpha}(z) > 0$, then all of the images $DF^n(\mathcal{C}(z))$ will contain the $\bar{\alpha}$-cone wrt the splitting $E^u \oplus E^s$. Note that the $E^u(DF^n(z))$ always lies inside $DF^n(\mathcal{C}(z))$. This can be summarized as follows.

$$\text{For } \forall z \in M,\ \forall n \in \mathbb{N},\ E^u(F^n(z)) \subseteq \mathcal{C}_{\bar{\alpha}}(F^n(z)) \subseteq dF^n(\mathcal{C}_\alpha(z)) \subseteq \mathcal{C}_\alpha(F^n(z)) \quad \text{(A.6)}$$

So if $\bar{\alpha}(z) = 0$, E^u must be invariant under DF along the orbit of z. Conversely, if E^u is not an invariant sub-bundle, then $\bar{\alpha} > 0$.

Stable and unstable manifolds. It turns out that in dynamical systems with an expanding, invariant cone system, the stable and unstable manifolds, W^s and W^u , have a nice behavior which have been described in the following two propositions.

Proposition A.1.2 *In a 2-manifold M with an invariant, expanding cone system, the unstable manifold of a saddle is an embedded, causal curve.*

Proof Let z be a saddle, W^u its unstable manifold. By Lemma A.3.1, $\mathcal{C}(z) \cap T_z(W^u)$ contains a subspace of dimension 1. Since W^u is 1-dimensional, $T_z(W^u)$ must be contained in the interior of $\mathcal{C}(z)$. By continuity of the tangent space along W^u and of the cone system $\mathcal{C}$, $\exists \epsilon > 0$ such that for $\forall z' \in W^u_\epsilon(z)$, $T_{z'}(W^u) \in \mathcal{C}(z')$. Therefore, since the curve $W^u_\epsilon(z)$ is causal and since $W^u(x) = \bigcup_{n \in \mathbb{N}_0} F^n(W^u_\epsilon(z))$, by Lemma A.1.1, it is an embedded, causal curve.

Proposition A.1.3 *In a manifold M with an invariant, expanding cone system, the stable manifold of a saddle is everywhere transverse to the invariant cones.*

Proof Let W^s be the stable manifold of a saddle z. The proof has two parts. First we will prove that W^s_ϵ is transverse to the cone system for some $\epsilon > 0$. Secondly, we will show this implies that the entire stable manifold is transverse to the cone system.

Since $T_z(W^s)$ is a contracting eigenspace and vectors in $\mathcal{C}(z)$ expand by at least $k > 1$, $T_z(W^s)$ must be disjoint from $\mathcal{C}(z)$. Since both $\mathcal{C}$ and W^s are C^1 structures and $\mathcal{C}(z)$ is a closed set, for sufficiently small $\epsilon > 0$, W^s_ϵ is transverse to the cone system.

Suppose at some $z_0 \in W^s$, $\exists w \in T_{z_0}(W^s) \cap \mathcal{C}(z_0)$. By the definition of the stable manifold, $z_n := F^n(z_0) \to z$, so for every large $n \in \mathbb{N}$, $z_n \in W^s_\epsilon$. By the invariance of the cone structure, $dF^n(w) \in \mathcal{C}(z_n)$, a contradiction of the previous conclusion. So no such z_0 exists and W^s is everywhere transverse to the cone system.

A.2 Proof of Theorem A.0.5

In this section it will be assumed that F in (3.1) is a local diffeomorphism and its periodic saddles are dense in $\mathbb{T}^2$. If F is transitive, then the theorem is already proved, so we will proceed with the assumption that F is not transitive. So there exists an open subset U of $\mathbb{T}^2$ whose images are not dense in $\mathbb{T}^2$.

By assumption, there exists a periodic point of period $p \in \mathbb{N}$ in U. Hence, $\forall n \in \mathbb{N}$, $F^{pn}(U)$ intersects U. Since U, is connected, so is $F^{pn}(U)$, therefore, for $\forall N \in \mathbb{N}$, $U_n := \bigcup_{0 \le n \le N} F^{pn}(U)$ is a connected set. $U_\infty := \bigcup_{n \in \mathbb{N}_0} F^{pn}(U)$ is open and $K := \bar{U_\infty}$ is closed and hence compact. Both K and U_∞ are forward invariant under

F^p.

Given any subset A of a topological space X, $\boldsymbol{Int(A)}$ will denote the interior of the set A.

By Lemma A.3.3, $U_\infty = Int(K)$, $\partial(K)$ and K^C are strongly forward and backward invariant under F^p. As a consequence, we can conclude that,

Lemma A.2.1 *Unstable manifolds of periodic saddles do not cross ∂K. Moreover, if a saddle lies on ∂K, then its unstable manifold lies in ∂K.*

Claim 1. The connected component of the boundary of K are C^1, causal, closed curves. Thence, we will conclude that K is homeomorphic to a cylinder. This is proved in Section A.2.1.

Claim 2. $\mathbb{T}^2$ decomposes into a finite number of such cylinders with disjoint interiors and each cylinder is mapped into and onto another cylinder. This is proved in Section A.2.1.

A.2.1 The proof of Claim 1

The boundary of K. By making U smaller if necessary, we may assume without loss of generality that U is homeomorphic to an open rectangle and that its boundary has four C^1 components, the top and the bottom boundary are tangent to E^u and its left and right boundaries are tangent to E^s. For $\forall x \in S^1$, $\boldsymbol{K_x}$ is the 1-dimensional set $S_x \cap K$. This is a compact set and hence a union of compact intervals. Therefore, a point $z_0 = (x_0, y_0) \in \partial K$ is either the boundary of a proper component interval of K_{x_0} or a singleton component of K_{x_0}. We will first prove

that each connected component of ∂K is an embedded curve. To prove this, we will show that there is a unique C^0 curve embedded in ∂K that passes through z_0. The claim will be proved separately for both the possibilities for z_0 in Lemmas A.2.2 and A.2.3.

Lemma A.2.2 *For $\forall z_0 = (x_0, y_0) \in \partial K$ which are boundary points of proper component intervals of K_{x_0}, $\exists$ a unique C^0 curve embedded in ∂K that passes through z_0.*

Proof If S_{x_0} is given the usual orientation, then every proper component interval of K_{x_0} has an upper boundary and a lower boundary. Without loss of generality, the point $z_0 = (x_0, y_0)$, which lies on the boundary of a proper component interval of K_{x_0}, is an upper boundary. We will first demonstrate the existence of a continuous curve embedded in ∂K and passing through z_0.

Since $z_0 \in \partial K$, $\exists z_n \in U$ and $k_n \in \mathbb{N}$ such that $F^{pk_n}(z_n) \to z$ and $F^{pk_n}(z_n) \in S_{x_0}$. Since z is the upper boundary of a component interval, this convergence is from below. Let γ be the upper boundary of U. Let z'_n be the point in γ with the same X-coordinate as z_n. Since F is orientation preserving, $F^{pk_n}(z'_n) \to z$ and $F^{pk_n}(z'_n) \in S_{x_0}$.

Let I be a small open interval in S^1 around x_0. For all $x \in I$, let $y_n(x)$ be the y coordinate of the point where the curve $\gamma_n := F^{pk_n}(\gamma)$ first hits S_x after passing through $F^{pk_n}(z'_n)$. Since γ is a causal curve, so are its images γ_n under F^{pk_n}. Then it follows that $\Gamma(x) := \sup_{n \in \mathbb{N}} y_n(x)$ is a continuous, causal curve passing through z and lying in ∂K.

We will now prove that this embedded curve is unique. Suppose $\exists$ two different curves Γ_1 and Γ_2 in ∂K passing through z_0. Let Q be a periodic saddle close to z_0 such that one of these curves lies above it and the other below it. Then since the unstable manifold of Q is causal, it must intersect one of these curves, which contradicts Lemma A.2.1.

Lemma A.2.3 *For $\forall z_0 = (x_0, y_0) \in \partial K$ which are singleton components of K_{x_0}, $\exists$ a unique C^0 curve embedded in ∂K that passes through z_0.*

Proof Let $z_0 = (x_0, y_0)$ be a singleton component of S_{x_0}. Since it lies on ∂K, it is a limit point of points z_n in the interior of K.

We will first show that these points z_n can be chosen to lie on S_{x_0}. Suppose not, then let $z_n = (x_n, y_n)$. Then without loss of generality, $x_n \to x_0^-$. Let $I(x_n) = [\Gamma_1(x_n), \Gamma_2(x_n)]$ be the component of K_{x_n} that contains z_n. By Lemma A.2.2, Γ_1 and Γ_2 can be extended to C^0 curves in a left neighborhood of x_0. Since there are no points in the interior of K in a neighborhood of z_0 in S_{x_0}, Γ_1, Γ_2 intersect S_{x_0} at z_0. Let Q be a periodic saddle close to z_0 such that one of these curves lies above it and the other below it. Then since the unstable manifold of Q is causal, it must intersect one of these curves, which contradicts Lemma A.2.1. So the assumption was false and hence, z_0 is a limit of proper component intervals of K_{x_0}.

Let these component intervals be $I_n = [a_n, b_n]$. Without loss of generality, I_n-s converge to z_0 from below. By Lemma A.2.1, there exists C^0 curves Γ_n embedded in ∂K and passing through b_n. For $\forall x$ in a neighborhood of x_0, $\Gamma(x) := \bar{\lim}_{n\to\infty} \Gamma_n(x)$. This Γ lies in ∂K and is C^0 and causal. It is also the unique curve in ∂K passing

through z_0.

Lemma A.2.4 *No point $z_0 = (x_0, y_0)$ on a boundary curve of ∂K passing through an upper/lower boundary point can be a singleton component of K_{x_0}.*

Proof Let Γ_1 be a boundary curve of ∂K passing through an upper boundary point z_1. Without loss of generality, z_0 is the closest point to z_1 lying on Γ_1, so the segment of the curve Γ_1 from z_1 to z_0 must have only upper boundary points and consequently, has an adjacent lower boundary curve Γ_2. Since Γ_1, Γ_2 are C^0 and z_0 is an isolated point of K_{x_0}., they must intersect at z_0. This contradicts the uniqueness of embedded curves in ∂K passing through z_0.

Lemma A.2.5 *A boundary curve of ∂K passing through an upper boundary point, cannot intersect a boundary curve of ∂K passing through a lower boundary point.*

Proof Let the contrary be true, so there exists a boundary curve Γ_1 of ∂K passing through an upper boundary point z_1 and intersecting a boundary curve Γ_2 of ∂K passing through a lower boundary point z_2. Let the point of intersection be $z_0 = (x_0, y_0)$. Then since Γ_1, Γ_2 are continuous, z is a singleton component of K_{x_0}. However, this is not possible by Lemma A.2.4

Lemma A.2.6 *Let $z \in \partial K$ be a lower boundary point. Then $F^p(z)$ is also a lower boundary point and the connected component of ∂K containing z has only lower boundary points. Analogous statements hold true for upper boundary points.*

Proof Since F is orientation preserving and by Lemma A.2.1, lower boundary points are mapped into lower boundary points. Since $\mathbb{T}^2$ itself is orientable, an em-

bedded curve, which is a co-dimension 1 embedded submanifold, is also orientable and hence, if a boundary has a lower boundary point, then all of its points are lower boundaries.

Now consider an adjacent upper boundary and lower boundary Γ_1 and Γ_2 respectively. These two curves do not intersect each other. Hence, the region R enclosed by them is either homeomorphic to a cylinder or an infinite tape. If it is a cylinder, then the Claim 1 is proved. So we will demonstrate that it cannot be an infinite tape.

The proof will by contradiction, so we will assume that R is an infinite tape. Therefore, Γ_1, Γ_2 must be open curves of infinite length. We will first show that none of them can have more than one periodic saddle using the following lemma.

Lemma A.2.7 *Let Γ be an causal, open curve in $\mathbb{T}^2$ invariant under F^p. Then at most one periodic point can lie on Γ.*

Proof Since Γ is causal and is invariant under F^p, it must have infinite length.

The proof will be by contradiction. So let Q_1, Q_2 be two periodic points on Γ with periods p_1, p_2 respectively. Let $N = pp_1p_2$. Then Q_1, Q_2 are fixed points of F^N and Γ is invariant under F^N.

Γ must be the unstable manifold of both with Q_1 and Q_2. Let L be the section of the curve joining with Q_1 and Q_2. Then for $\forall n \in \mathbb{N}$, $F^{nN}(L)$ is a sub-segment of Γ with Q_1 and Q_2 as its endpoints. Since Γ is an open curve and since F is a local diffeomorphism, L is the only such curve-segment, hence $F^N(L) = L$. This contradicts the expansion property of the map F on causal curves.

However, the next lemma proves that periodic points on the Γ_i-s are dense. This leads to a contradiction and consequently, proves Claim 1.

Lemma A.2.8 *Every point z_0 in an upper boundary curve is a limit point of periodic points lying on that curve.*

Proof Suppose $z_0 = (x_0, y_0)$ is a point on an upper boundary of K. Let Γ_1 be the upper boundary passing through z_0 and let Γ_2 be the adjacent lower boundary. Let I be a small neighborhood of x_0 in S^1. Then the region $R := \{z = (x, y) \in \mathbb{T}^2 \mid x \in I,\ \Gamma_2(x) \leq y \leq \Gamma_1(x)\}$ is homeomorphic to a rectangle. Since periodic saddles are dense, $\exists$ a periodic saddle $z_1 = (x_1, y_1)$ in R of period $q \in \mathbb{N}$. Then the circle S_{x_1} must be invariant under $F^p q$ and for a sufficiently large $N \in \mathbb{N}$, all the periodic points on S_{x_1} are fixed under F^{pqN}. Let L be the line segment $S_{x_1} \cap R$. L contains the periodic point Q.

Note that Q is an attracting fixed point for the map $F^{NP}|S_{x_1}$. By Lemma A.3.3, the end-points of L must be fixed points.

A.2.2 The proof of Claim 2

As a result of the lemmas in the previous section, we can conclude that the invariant set K is diffeomorphic to a cylinder $S^1 \times [0, 1]$ and $Int(K)$, K^C and ∂K are invariant under F^p. Now instead of considering the iterated map F^p, we wil examine the action of F on K.

Lemma A.2.9 *Suppose for some $m \in \mathbb{N}$, $F^m(K) \cap K \neq \Phi$. Then $F^m(K) = K$.*

Proof Let the contrary be assumed, i.e., $F^m(K) \cap K \neq \Phi$ for some $m \in \mathbb{N}$. Since $F^p(K) = K$, it may be assumed without loss of generality that $0 < m < p$. Since F is a local diffeomorphism and $F^{p-m}(F^m(K) = K$, we must have,

$$F^m(\partial K) = \partial(F^m(K)),\ F^m(Int(K)) = Int(F^m(K) \tag{A.7}$$

The boundary of K is composed of two disjoint, closed, causal curves which are the upper and lower boundaries respectively. Since F is orientation preserving, F maps upper(lower) boundaries to upper(lower) boundaries, so $F^m(K)$ is also a cylinder. The only way by which the upper/lower boundary of K intersects the upper/lower boundary of $F^m(K)$ and satisfy (A.7) is if they coincide. Therfore, $F^m(K) = K$.

Lemma A.2.10 *The images of K under F form a disjoint collection of cylinders.*

Proof Suppose for some $0 \leq m < n < p$, $F^m(K) \cap F^n(K) \neq \Phi$. Then $F^{p-n}(F^m(K) \cap F^n(K)) \neq \Phi$. But $F^{p-n}(F^m(K) \cap F^n(K)) \subseteq F^{p-n+m}(K) \cap F^p(K) = F^{p-n+m}(K) \cap K$. Therefore, $\exists p' := p - (n - m)$ which is less than p and for which $F^{p'}(K) \cap K \neq \Phi$. Without loss of generality, p' is the minimum such integer > 0.

Then by Lemma A.2.9, this implies that $F^{p'}(K) = K$. From this it follows that the images $K = F^0(K), \ldots, F^{p'-1}(K)$ are all distinct cylinders.

Lemma A.2.11 *The number periodic cylinders is finite.*

Proof Henceforth, K and its images $F^1(K), F^2(K), \ldots$ will be called *periodic cylinders*. Since by assumption, F is not transitive, it does not have dense trajectories. Therefore, every point is in a periodic cylinder. We will show that there are only

a finite number of periodic cylinders, whence, $\mathbb{T}^2$ can be decomposed into a finite "stack" of cylinders with disjoint interiors.

Let K be a periodic cylinder. For $\forall k, n \in \mathbb{N}$, the intersection $\Gamma_{k,n} \cap \partial K$ has a periodic point, where $\Gamma_{k,n}$ is described in (4.2). Since (3.1) is C^1, each $\Gamma_{k,n}$ can have a finite number of periodic points on it wrt the map F^n. Therefore, the set of such periodic cylinders K must be finite in number.

Lemma A.2.12 *All the periodic cylinders have the same period.*

Proof Let p be the minimum period of a periodic cylinder K_1. Therefore, if Γ is its upper boundary, then $F^p(\Gamma) = \Gamma$. But Γ is the lower boundary of the cylinder K_2 stacked above K_1. Therefore, the period of K_2 must be a divisor of p and because of the minimality of p, must be p itself. A repetition of this argument a finite number of times establishes that all the cylinders have the same period p.

Therefore, we have proved our main result Theorem A.0.5.

A.3 Appendix : Some lemmas

Lemma A.3.1 *Let z be a saddle and W^u its unstable manifold. If $dim(W^u) = 1$, then W^u is an embedded causal curve.*

Proof Suppose that M is an n-manifold. Let S^{n-1} be the unit sphere in $T_z(M)$. Then the intersection $Q := \mathcal{C}(z) \cap S^{n-1}$ is compact. If the dimension of E^u is k for some $0 < k < n$, and $\alpha = tan(\theta)$ for some $\theta \in (0, \frac{\pi}{2}$, then Q is diffeomorphic to $S^{k-1} \times D^{n-k-1} \times [-\theta, \theta]$ via the map $\phi : (u, v, t) \mapsto \cos(t)u + \sin(t)v$.

If $k = 1$, then $Q \cong S^0 \times D^{n-1}$. Now consider the map $G : S^{n-1} \to S^{n-1}$ defined as $G(w) = \frac{dF(z)(w)}{\|w\|}$. This map is well defined and smooth because $dF(z)$ is invertible and linear. Since $\mathcal{C}(z)$ is invariant under $dF(z)$, $G : K \to K$. Therefore, by the Brower fixed point theorem, G has a fixed point w in K. But w is a fixed point of G iff $\exists \lambda > 0$ such that $dF(z)(w) = \lambda w$. Since dF is an expanding map on $\mathcal{C}$, λ must be > 1.

Since $dF(z)$ is hyperbolic, all subspaces of $T_z(M)$ invariant under $dF(z)$ must be subspaces of either $T_z(W^u)$ or $T_z(W^s)$. In particular, the eigenvector w must be in one of these subspaces. Since its eigenvalue λ is > 1, w must $\in T_z(W^u)$. Then the span of w is the 1-dimensional subspace contained in the intersection $\mathcal{C}(z) \cap T_z(W^u)$.

Lemma A.3.2 *Let $F : M \to M$ be a local diffeomorphism on a compact manifold M. Let the periodic points of F be dense in M and let $U \subset M$ be open and forward-invariant under F. Suppose that $K := \bar{U}$ is a proper subset of M. Then $F^p(K) = K$, $F(\partial K) = \partial K$ and $F(K^C) = K^C$.*

Proof Since K is forward invariant under F, $F(K) \subseteq K$. Suppose it is a strict subset, i.e., $F(K) \subset K$. Since K is compact, $F(K)$ is compact and hence closed. Therefore, $K - F(K)$ has non-empty interior V. Let $Q \in V$ be a periodic point of period q. Then $F^q(Q) = Q$. However, $Q = F^q(Q) \in F^q(K)$ which is disjoint from V which contains Q, leading to a contradiction. Hence the assumption was wrong and $F(K) = K$.

We will first prove that $F(\partial K) \subseteq \partial K$. Let the contrary be assumed, hence $\exists x \in \partial K$ such that $F(x) \in Int(K)$. Since F is a local diffeomorphism, it is an

open mapping too. Hence, $\exists$ a neighborhood V of x such that $F(V)$ is an open set contained in the interior $Int(K)$ of K. Since x is a boundary point, V contains an open set in the exterior of K. Let Q be a periodic point of period q lying in $V - K$. Then $F^q(Q) = Q$. But $F(Q) \in F(V) \subset K$, and by the forward invariance of K under F, $F^n(Q)$ never exits K and hence is never equal to Q which lies outside K, leading to a contradiction.

We will next prove that in fact, strict equality holds. Let the contrary be assumed, i.e., $F(\partial K) \subset \partial K$. Then $\exists x \in \partial K$ such that $F(x)$ is disjoint from ∂K. However, since $F(K) = K$, x must have an inverse image y in $Int(K)$. Take a neighborhood V of y in K. Then $F(V)$ is a neighborhood of x. Since x is a boundary point, $F(V)$ intersects K^C. this contradicts the forward invariance of K. Hence the initial assumption was untrue and $F(\partial K)$ must equal ∂K.

The last equality follows from the previous two.

Lemma A.3.3 *Let F be a a C^1 map on S^1 with a non-zero derivative. Let $J \subset S^1$ be an compact set such that both J and ∂J are forward invariant. Let a component interval L of J contain an attractor. Then the endpoints of L are periodic points.*

Proof For $N \in \mathbb{N}$ sufficiently large, all the periodic points of F^N are fixed points. J and ∂J remain invariant under F^N. Consider an endpoint A of L. The proof will be by contradiction, so suppose that A is not a fixed point of F^N.

Let Q be the fixed point on L closest to A. By assumption, $Q \neq A$. Q must be an attractor or repellor. We will prove that both cases lead to contradictions and hence, the assumption about A not being a fixed point will be proved false.

If Q is an attractor, then A is in the basin of attraction of Q and F^N maps A closer to Q. In other words, $F^N(A) \in Int(L) \subseteq Int(J)$, violating the invariance of ∂J.

If Q is a repellor, then A lies in the basin of repulsion of Q and hence, A has an inverse image under F^N in the interior of the line segment QA. Since F has non-zero derivative, $F^N(QA)$ must contain a neighborhood of A. Since $A \in \partial J$, $F^N(QA)$ intersects the exterior of J. This contradicts the invariance of J.

Bibliography

[1] M Brin and G Stuck. *Introduction to Dynamical Systems*. Cambridge University Press, October 14, 2002.

[2] U Krengel. On the speed of convergence in the ergodic theorem. *Monatshefte fr Mathematik*, 86 (1):3–6, 1978.

[3] S Das, E Sander, Y Saiki, and J A Yorke. Quantitative quasiperiodicity. *Preprint : arXiv:1508.00062 [math.DS]*, 2015.

[4] M R Herman. Sur la conjugaison diffrentiable des diffomorphismes du cercle des rotations. *Publications Mathmatiques de l'Institut des Hautes tudes Scientifiques*, 49 (1):5–233, 1979.

[5] C Simó. *Averaging under fast quasiperiodic forcing*. Springer US, 1994.

[6] C Simó, P Sousa-Silva, and M Terra. Practical stability domains near $L_{4,5}$ in the restricted three-body problem: Some preliminary facts. *Progress and Challenges in Dynamical Systems*, 54:367–382, 2013.

[7] A Luque and J Villanueva. Quasi-periodic frequency analysis using averaging-extrapolation methods. *SIAM J. Appl. Dyn. Syst.*, 13(1):1–46, 2014.

[8] M Lin and M Weber. Weighted ergodic theorems and strong laws of large numbers. *Ergodic Theory and Dynamical Systems*, 27 (02):511–543, 2007.

[9] A Bellow, R Jones, and J Rosenblatt. *Almost everywhere convergence of weighted ergodic averages*. ProQuest, 2009.

[10] A Bellow and V Losert. The weighted pointwise ergodic theorem and the individual ergodic theorem along subsequences. *Transactions of the American Mathematical Society*, 288 (1):307–345, March, 1985.

[11] F Durand and D Shneider. Ergodic averages with deterministic weights. *Annales de l'Institut Fourier*, 52 (2):561–583, 2002.

[12] E Sander and J A Yorke. The many facets of chaos. *International Journal of Bifurcation and Chaos*, 25(4):15300, 2015.

[13] Y Katznelson and D Ornstein. The absolute continuity of the conjugation of certain diffeomorphisms of the circle. *Ergodic Theory and Dynamical Systems*, 9:681–690, 1989.

[14] Y Katznelson and D Ornstein. The differentiability of the conjugation of certain diffeomorphisms of the circle. *Ergodic Theory and Dynamical Systems*, 9:643–680, 1989.

[15] J C Yoccoz. Conjugaison differentiable des diffeomorphismes du cercle dont le nombre de rotation verifie une condition diophantine. *Annales scientifiques de l'cole Normale Suprieure*, 17 (3):333–359, 1984.

[16] V Arnold. Small denominators. i. mapping of the circumference onto itself. *Amer. Math. Soc. Transl. (2)*, 46:213–284, 1965.

[17] Milne-Thomson and Louis Melville. *The calculus of finite differences*. American Mathematical Soc., 2000.

[18] S Bochner and K Chandrasekharan. *Fourier Transforms*. Princeton University Press, 1949.

[19] S Newhouse, D Ruelle, and F Takens. Occurrence of strange axioma attractors near quasi periodic flows on tm, m3. *Comm. Math. Phys.*, 64(1):35–40, 1978/79.

[20] S Das and J A Yorke. Super convergence of ergodic averages for quasiperiodic orbits. *Preprint : arXiv:1506.06810 [math.DS]*, 2015.

[21] T M Seara and J Villanueva. On the numerical computation of Diophantine rotation numbers of analytic circle maps. *Phys. D*, 217(2):107–120, 2006.

[22] C Baesens, J Guckenheimer, S Kim, and R S MacKay. Three coupled oscillators : mode-locking, global bifurcations and toroidal chaos, 1991.

[23] H W Broer and G B Huitema. Unfoldings of quasi-periodic tori in reversible systems, 1995.

[24] R Vitolo, H Broer, and C Simó. Quasi-periodic bifurcations of invariant circles in low-dimensional dissipative dynamical systems. *Regular And Chaotic Dynamics*, 16(1-2):154–184, February 2011.

[25] H Hanßmann and C Simó. Dynamical stability of quasi-periodic response solutions in planar conservative systems. *Indagationes Mathematicae*, 23(3):151–166, September 2012.

[26] M B Sevryuk. Quasi-periodic perturbations within the reversible context 2 in kam theory. *Indagationes Mathematicae*, 23(3):137–150, September 2012.

[27] H W Broer, G B Huitema, F Takens, and B L J Braaksma. Unfoldings and bifurcations of quasi-periodic tori. *Memoirs of the American Mathematical Society*, 83(421):viii–175, 1990.

[28] A P Kuznetsov, N A Migunova, I R Sataev, Y V Sedova, and L V Turukina. From chaos to quasi-periodicity. *Regular And Chaotic Dynamics*, 20(2):189–204, May 2015.

[29] H Poincaré. *Leons de mécanique céleste : professées à la Sorbonne.* Paris : Gauthier-Villars, 1905.

[30] J B Greene. *Poincaré and the Three Body Problem.* American Mathematical Society, October 29, 1996.

[31] Y Yamaguchi and K Tanikawa. A remark on the smoothness of critical KAM curves in the standard mapping. *Progress of Theoretical Physics*, 101 (1), January, 1999.

[32] S N Chow, M van Noort, and Y Yi. Quasiperiodic dynamics in Hamiltonian 1.5 degree of freedom systems far from integrability. *Journal of Differential Equations*, 212:366–393, 2005.

[33] B van der Pol. A theory of the amplitude of free and forced triode vibrations. *Radio Review*, 1:701–710, 1920.

[34] Celso Grebogi, Edward Ott, and James A Yorke. Are three-frequency quasiperiodic orbits to be expected in typical nonlinear dynamical systems ? *Physical Review Letters*, 51 (5):339, August 1, 1983.

[35] C Grebogi, E Ott, and J A Yorke. Attractors on an n-torus: Quasiperiodicity versus chaos. *Physica D. Nonlinear Phenomena*, 15(3):354–373, April 1985.

[36] V M Becerra, J D Biggs, S J Nasuto, V F Ruiz, W Holderbaum, and D Izzo. Using Newton's method to search for quasi-periodic relative satellite motion based on nonlinear Hamiltonian models. *7th International Conference On Dynamics and Control of Systems and Structures in Space*, 7, 2006.

[37] F Schilder, H M Osinga, and W Vogt. Continuation of quasi-periodic invariant tori. *SIAM Journal on Applied Dynamical Systems*, 4 (3):459–488, 2005.

[38] A Berger and S Siegmund. On the gap between random dynamical systems and continuous skew products. *Journal of Dynamics and Differential Equations*, 15 (2-3), 2003.

[39] V Kleptsyn and M B Nalskii. Contraction of orbits in random dynamical systems on the circle. *Functional Analysis and Its Applications*, 38 (4):267282, 2004.

[40] A J Homburg. Circle diffeomorphisms forced by expanding circle maps. *Ergod. Th. and Dynam. Sys.*, 32:20112024, 2012.

[41] E J Kostelich, C Grebogi I Kan, E Ott, and J A Yorke. Unstable dimension variability: A source of nonhyperbolicity in chaotic systems. *Physica D*, 109, (1-2):8190, 1 November 1997.

[42] Victor Kleptsyn and Denis Volk. Nonwandering sets of interval skew products. *Nonlinearity*, 27 (7), 2014.

[43] Y Ilyashenko and A Negut. Holder properties of perturbed skew products and fubini. *Nonlinearity*, 25 (8):2377–2411, 2012.

[44] Richard Ma. A proof of the c^1-stability conjecture. *Publications Mathmatiques de l'Institut des Hautes tudes Scientifiques*, 66, (1):161–210, 1987.

[45] E Pujals and M Sambarino. On the dynamics of dominated splitting. *Annals of Mathematics*, 169:675–740, 2009.

[46] Walter Rudin. *Principles of mathematical analysis*. McGraw-Hill Science/Engineering/Math., 1976.

[47] B Hunt and E Ott. Defining chaos. *arXiv:1501.07896v3 [nlin.CD]*, 2015.

[48] P Glendinning. Milnor attractors and topological attractors of a piecewise linear map. *Nonlinearity*, 14 (2):239, March, 2001.

[49] R Abraham and S Smale. *Non-genericity of Omega-stability*. American Mathematical Society, 1970.

[50] G C Yuan and J Yorke. An open set of maps for which every point is absolutely nonshadowable. *Proceedings of the American Mathematical Society*, 128 (3):909–918, 2000.

[51] L J Diaz and A Gorodetski. Non-hyperbolic ergodic measures for non-hyperbolic homoclinic classes. *Ergod. Th. and Dynam. Sys.*, 29:14791513, 2009.

[52] S Newhouse, D Ruelle, and F Takens. Occurrence of strange axiom a attractors near quasiperiodic flows on tm, m3. *Communications in Mathematical Physics*, 64 (1):35–40, 1978.

[53] D Ruelle and F Takens. On the nature of turbulence. *Communications in Mathematical Physics*, 20 (3):167–192, 1971.

[54] T E Ponce Kapitaniak and J Wojewoda. Route to chaos via strange non-chaotic attractors. *Journal of Physics A: Mathematical and General*, 23 (8):383–387, 1990.

[55] P Glendinning. Robust new routes to chaos in differential equations. *Physics Letters A*, 168 (1):40–46, 1992.

[56] F R Marotto. Snap-back repellers imply chaos in rn. *J. Math. Anal. Appl*, 63, 1978.

[57] Kang-Ling Liao and Chih-Wen Shih. Snapback repellers and homoclinic orbits for multi-dimensional maps. *J. Math. Anal. Appl*, 386, 2012.

[58] Stephen Smale. Differentiable dynamical systems. *Bull. Amer. Math. Soc.*, 73:747–817, 1967.

[59] P Hartman. On local homeomorphisms of euclidean spaces. *Boletn de la Sociedad Matemtica Mexicana*, 5:220–241, 1960.

[60] Herbert Federer. *Geometric measure theory*. BerlinHeidelbergNew York: Springer-Verlag, 1969.